Antibody Responses to SARS-CoV-2 in a large university setting and in context of *Mycobacterium tuberculosis* infected animals

Dissertation

Presented in Partial Fulfillment of the Requirements for the Degree Doctor of Philosophy in the Graduate School of The Ohio State University

By

Marlena Rae Merling, B.S.

Biomedical Sciences Graduate Program

The Ohio State University

2024

Dissertation Committee

Dr. Richard Robinson, Advisor

Dr. Fernanda Novais, Advisor

Dr. Amy Lovett-Racke

Dr. Ian Davis

Dr. Adriana Forero

Abstract

Severe acute respiratory syndrome associated coronavirus 2 (SARS-CoV-2) infected, asymptomatic individuals are an important contributor to Coronavirus Disease 2019 (COVID-19) transmission. SARS-CoV-2-specific immunoglobulin (Ig)—as generated by the immune system following infection or vaccination—has helped limit SARS-CoV-2 transmission from asymptomatic individuals to susceptible populations (e.g. elderly). Here, we describe the relationships between COVID-19 incidence and SARS-CoV-2 lineage, viral load, saliva Ig levels (SARS-CoV-2-specific IgM, IgA and IgG), and ACE2 binding inhibition capacity in asymptomatic individuals between January 2021 and May 2022. These data were generated as part of a large university COVID-19 monitoring program in Ohio, United States of America, and demonstrate that COVID-19 incidence among asymptomatic individuals occurred in waves which mirrored those in surrounding regions, with saliva SARS-CoV-2 viral loads becoming progressively higher in our community until vaccine mandates were established. Among the unvaccinated, infection with each SARS-CoV-2 lineage (pre-Omicron) resulted in saliva Spike-specific IgM, IgA, and IgG responses, the latter increasing significantly post-infection and being more pronounced than Nucleocapsid-specific IgG responses. Vaccination resulted in significantly higher Spike-specific IgG levels compared to unvaccinated infected individuals, and uninfected vaccinees' saliva was more capable of inhibiting Spike

function. Vaccinees with breakthrough Delta infections had Spike-specific IgG levels

comparable to those of uninfected vaccinees; however, their ability to inhibit Spike

binding was diminished. These data are consistent with COVID-19 vaccines having

achieved hoped-for effects in our community, including the generation of mucosal

antibodies that inhibit Spike and lower community viral loads, and suggest breakthrough

Delta infections were not due to an absence of vaccine-elicited Ig, but instead limited

Spike binding activity in the face of high community viral loads.

Due to latent tuberculosis infection (LTBI) being widespread and SARS-CoV-2

remaining a major infectious agent, understanding the interaction of *Mycobacterium

tuberculosis* (Mtb) and SARS-CoV-2 is crucial in diagnosis and treatment. This study

sought to examine how the immune response to Mtb affects subsequent SARS-CoV-2

challenge. Specifically, we wanted to know if TB infected mice had cross-reactive

antibodies and adaptive immune cells to SARS-CoV-2 proteins, which may explain why

mice infected with Mtb had better outcomes and lower viral loads than naïve mice when

subsequently infected with SARS-CoV-2 in other studies. C57BL/6J mice were infected

with Mtb via aerosol and after forty days, challenged with human SARS-CoV-2

intraperitoneally which does not replicate in C57BL/6J mice, and sacrificed days 1, 3,

and 7 after SARS-CoV-2 challenge. Flow cytometry of spleen cells indicated no

differences in frequency of activated T cell or antigen-experienced B cells in response to

stimulation with SARS-CoV-2 peptide libraries. Quantitative PCR of lung RNA

demonstrated an increase in inflammatory cytokines and T cells in mice infected with

Mtb. SARS-CoV-2 specific IgG measurements in lung homogenate and serum showed no cross-reactivity of Mtb antibodies, but an increase in SARS-CoV-2 specific IgG in mice infected with Mtb and challenged with SARS-CoV-2 in a lung specific manner. These data suggest the following: (1) TB antibodies and spleen immune cells are not cross-reactive to SARS-CoV-2, and (2) TB accelerates the production of SARS-CoV-2 specific IgG within the lungs, with no change detected in T cell associated RNA transcripts. This research offers a mechanism for how prior TB is protective against subsequent SARS-CoV-2 infection.

Dedication

This dissertation is dedicated to my parents and siblings, John, Mary Ann, Everett, Weston, Carly, Conrad, Nathaniel, Leland, Harrison, and Coretta. Their love, teasing, and willingness to listen to my complaints kept me motivated throughout my graduate school journey. Thank you, I love you guys.

Acknowledgments

I would like to acknowledge the many people at The Ohio State University who have helped me throughout my years as a graduate student, whether they shared a protocol or reagents, taught me how to use equipment, collaborated on a paper, or were a friend. The MI&I community has provided me with much support. Specifically, I want to thank Dr. Sahar Mahfooz who has not only taught me countless things and always helped me in the lab, but is also a great friend. I will miss her delicious food. I would also like to thank Dr. Fernanda Novais for adopting me into her lab and mentoring me with kindness.

Most of all, I would like to acknowledge Dr. Richard Robinson for his mentorship and support. He has guided me to become the best scientist and person that I could be. I am extremely appreciative of his patience, teachings, and sense of humor. We have shared many laughs and some tears, and I am grateful for the time we spent together. Thank you.

Vita

2015……………………………………………Carroll High School

2015–2019……………………………………….B.S. in Biology, University of Dayton

2019–2024…………………………………….Graduate Research Associate,

Department of Microbial Infection and Immunity, The Ohio State University

Publications

1. Faris, R., **Merling, M.**, Andersen, S.E., Dooley, C.A., Hackstadt, T., and Weber, M.M. (2019). Chlamydia trachomatis CT229 Subverts Rab GTPase-Dependent CCV Trafficking Pathways to Promote Chlamydial Infection. Cell Rep *26*, 3380-3390.e5. 10.1016/j.celrep.2019.02.079.

2. Mahfooz, N.S., **Merling, M.R.**, Claeys, T.A., Dowling, J.W., Forero, A., and Robinson, R.T. (2023). Human IL-35 Inhibits the Bioactivity of IL-12 and Its Interaction with IL-12Rβ2. Immunohorizons *7*, 431–441. 10.4049/immunohorizons.2300039.

3. Liu, Z., Ma, A., Mathé, E., **Merling, M.**, Ma, Q., and Liu, B. (2021). Network analyses in microbiome based on high-throughput multi-omics data. Brief Bioinform *22*, 1639–1655. 10.1093/bib/bbaa005.

4. **Merling, M.R.**, Williams, A., Mahfooz, N.S., Ruane-Foster, M., Smith, J., Jahnes, J., Ayers, L.W., Bazan, J.A., Norris, A., Norris Turner, A., et al. (2023). The emergence of SARS-CoV-2 lineages and associated saliva antibody responses among asymptomatic individuals in a large university community. PLoS Pathog *19*, e1011596. 10.1371/journal.ppat.1011596.

5. Klever A.M., Alexander K.A., Almeida D., Anderson M.Z., Ball R.L., Beamer G., Boggiatto P., Buikstra J.E., Chandler B., Claeys T.A., Concha A.E., Converse P.J., Derbyshire K.M., Dobos K.M., Dupnik K.M., Endsley J.J., Endsley M.A., Fennelly K., Franco-Paredes C., Hagge D.A., Hall-Stoodley L., Hayes D. Jr, Hirschfeld K., Hofman C.A., Honda J.R., Hull N.M., Kramnik I., Lacourciere K., Lahiri R., Lamont E.A., Larsen M.H., Lemaire T., Lesellier S., Lee N.R., Lowry C.A., Mahfooz N.S., McMichael T.M., **Merling M.R.**, Miller M.A., Nagajyothi J.F., Nelson E., Nuermberger E.L., Pena M.T., Perea C., Podell B.K., Pyle C.J., Quinn F.D., Rajaram M.V.S., Mejia O.R., Rothoff M., Sago S.A., Salvador L.C.M., Simonson A.W., Spencer J.S., Sreevatsan S., Subbian S., Sunstrum J., Tobin D.M., Vijayan K.K.V., Wright C.T.O., Robinson R.T. (2023). The Many

Hosts of Mycobacteria 9 (MHM9): A conference report. Tuberculosis (Edinb) *142*, 102377. 10.1016/j.tube.2023.102377.

6. Hayes, D., Shukla, R.K., Cheng, Y., Gecili, E., **Merling, M.R.**, Szczesniak, R.D., Ziady, A.G., Woods, J.C., Hall-Stoodley, L., Liyanage, N.P., et al. (2022). Tissue-localized immune responses in people with cystic fibrosis and respiratory nontuberculous mycobacteria infection. JCI Insight *7*, e157865. 10.1172/jci.insight.157865.

Fields of Study

Major Field: Biomedical Sciences Graduate Program

Table of Contents

List of Tables

List of Figures

<center>**Chapter 1: Introduction**</center>

1.1 SARS-CoV-2

Pathogenesis of SARS-CoV-2

Coronaviruses are single-stranded RNA (ssRNA) viruses that cause respiratory disease in a range of mammalian hosts[1]. The Coronavirus Disease 2019 (COVID-19) pandemic began in December 2019, after transmission of a novel coronavirus to individuals living in China[2,3]. The sequence homology of this novel coronavirus to severe acute respiratory syndrome associated coronavirus (SARS-CoV) led to its being named SARS-CoV-2 (CoV2)[4]. International spread of SARS-CoV-2 was rapid, and by February 2020 it had spread to nearly every country in the world[1]. Now, over 4 years after its emergence, SARS-CoV-2 is estimated to have infected ~774 million individuals and killed >7 million individuals worldwide[5]. The United States of America (US) has reported more deaths than any other country[5], but did not have the highest proportion of deaths per population as of March 2023[6].

SARS-CoV-2 spreads via aerosol and respiratory droplets[7], causing either an asymptomatic infection or a flu-like illness that affects multiple organ systems and presents as fever, cough, new loss of taste or smell, diarrhea, dyspnea, malaise, delirium, and death[8,9]. Although people of all ages and health conditions have contracted COVID,

<center>1</center>

those with the worse outcomes often have comorbidities. COVID-19 patients who had

hypertension, obesity, cardiovascular disease, diabetes, and chronic lung disease have the

worst prognosis[10]. Those at higher risk of death include elderly people from long-term

care facilities, people with chronic kidney disease, and cancer patients[10]. The spread of

SARS-CoV-2 by asymptomatic people to those who are more vulnerable makes studying

asymptomatic people with SARS-CoV-2 important.

SARS-CoV-2 Proteins

The SARS-CoV-2 genome encodes 16 non-structural proteins, 9 accessory proteins, and

4 structural proteins which are visualized in this review by Bai et al[11]. The non-structural

proteins (nsps) are required for RNA synthesis, whereas the accessory proteins provide

an immune evasion and reproductive advantage through host interactions[11]. The

structural proteins are Spike, Nucleocapsid, Envelope, and Membrane which are required

for viral assembly. The Spike protein is essential for SARS-CoV-2 infection of target

cells and contains a receptor-binding domain (RBD) which recognizes and binds the main

host receptor, angiotensin-converting enzyme 2 (ACE2)[12–14]. In humans, ACE2 is

expressed in all major organs including the lungs, but highest expression is in the

gastrointestinal tract[15]. The SARS-CoV-2 genome has been detected in many human

tissues after infection including lungs, kidneys, heart, brain, blood, and stomach, with the

highest levels in the respiratory tract[16,17]. The Spike protein is made up of two subunits—

S1 and S2—S1 containing the receptor-binding domain (RBD)[18]. The Nucleocapsid

packages and protects the viral RNA[18]. The Envelope protein is involved in viral

localization within host cells and regulates viral lysis[18]. The Membrane protein is crucial for viral assembly through protein-protein interactions and determines viral shape[11,19].

SARS-CoV-2 Replication

SARS-CoV-2 replication begins with viral attachment to the host cell via the Spike protein binding to its receptor ACE2 on the host cell membrane[13]. The Spike protein is cleaved by the host transmembrane serine protease 2 which allows for membrane fusion and entry into the host cell[20]. Because SARS-CoV-2 is a positive-sense RNA virus, direct translation of the nsps encoding portion of the genome proceeds in the host cell cytoplasm after the genome is unpacked from the Nucleocapsid proteins via cellular proteases[21]. The nsps, including an RNA-dependent RNA polymerase, form a replication and transcription complex that uses the genomic RNA as a template for genome transcription and subgenomic RNA that is used to translate viral structural and accessory proteins[21]. The newly synthesized genomic RNA is packaged with Nucleocapsid proteins, enclosed within an envelope, and released from the host cell[21].

Immune Response to SARS-CoV-2

The early response to SARS-CoV-2 infection in non-severe cases involves robust IFN type I and III and T cell specific responses, prior to antibody detection[22,23]. During viral RNA replication, there is the formation of double-stranded RNA (dsRNA) intermediates. Both ssRNA and dsRNA are sensed by innate host Toll-like receptors (TLR3 and TLR7) and cytosolic RNA sensors (RIG-I and MDA-5)[24]. These RNA-bound receptors activate a

signaling cascade that then promotes the expression of type I and type III IFNs[24]. Type I and type III IFNs lead to the expression of interferon-stimulated genes (ISGs) which have a variety of functions including inhibition of viral mRNA translation and initiation of inflammation and apoptosis[25].

As the innate responses decrease over time, the adaptive immune response including CD4 and CD8 T cells and memory B cells increases, which in turn the viral load decreases as the adaptive immune responses controls the infection[26]. However, COVID-19 patients with severe disease have a dysregulated inflammatory response. A mild and delayed IFN response leads to prolonged viral replication and prolonged cytokine production which contributes to immune-mediated disease severity[27]. Indeed, patients with severe illness have a higher concentration of IL-1b, IL-6, IL-10, IL-2, TNF and IFN-γ (IFNg) in serum[28,29]. Other immune dysfunctions associated with COVID-19 are abnormal granulocyte and monocyte numbers, an increase in neutrophils, and an increased IgG response[30]. Additionally, many COVID-19 patients, more commonly those with severe cases, are reported to have lymphopenia, specifically with decreased T cell counts[28,29].

B cells and antibodies have a prominent role in protection against SARS-CoV-2. After previous coronavirus disease outbreaks, such as those caused by SARS-CoV and Middle East respiratory syndrome coronavirus (MERS-CoV), animal models and other experimental systems demonstrated that coronavirus-specific antibodies are generated soon after infection[31,32], and can block viral entry by interfering with the Spike:ACE2

interaction[33–38]. In the upper respiratory tract and oral cavity, antibodies are generated by B cells in mucosa-associated lymphoid tissue and regional draining lymph nodes, typically within several days of antigen encounter, and comprise several isotypes (IgM, IgA, and IgG) which differ in their secretion kinetics and effector mechanisms[39,40]. IgM is often the first isotype to appear following antigen exposure, and eliminates viruses by precipitating the membrane attack complex on virus-infected cells (i.e. the classical complement pathway)[40]. In the context of SARS-CoV-2 infection, however, IgA dominates the early neutralizing antibody response at mucosal sites[41]. IgA, a weak inducer of the complement pathway, protects mucosal sites by blocking and sterically hindering antigen interaction with the epithelial surface, trapping it in mucus which is eventually cleared via peristalsis[40]. IgG is often the last isotype to appear following antigen exposure, mostly appears in the oral cavity due to passive leakage from the blood circulation via gingival crevicular epithelium, and is the most versatile in terms of effector mechanisms and durability[40]. IgG confers protection through neutralization as well as opsonization of the virus to increase macrophage phagocytosis in a dose-dependent manner where lower amounts of non-neutralizing IgG is more protective[42]. An overview of the main functions of antibodies is shown in Figure 1.

Vaccination against SARS-CoV-2

The fact that coronavirus-specific Ig is secreted following natural infection, long-lived, and able to disrupt Spike:ACE2 interactions are the foundations on which multiple monitoring, therapeutic, and vaccine strategies against SARS-CoV-2 have been built.

5

Prior to mass PCR testing, SARS-CoV-2-reactive Ig in sera was the only biomarker for monitoring SARS-CoV-2 prevalence at a population level[43]. The discovery that plasma of COVID-convalescent individuals contains polyclonal Ig with SARS-CoV-2-neutralizing activity[44] paved the way for multiple clinical trials testing the efficacy of convalescent plasma therapy against COVID[45]. In the US, the first COVID-19 vaccines available comprised either a two-dose encapsulated mRNA formulation (BNT162b2 or mRNA-1273) or a single-dose adenovirus vector formulation (Ad26.COV2.S). The US Food & Drug Administration (FDA) granted emergency use authorizations (EUA) for BNT162b2 and mRNA-1273 on December 11 2020 and December 18 2020, respectively[46,47]; the FDA EUA for Ad26.COV2.S was granted on February 27 2021[48]. The advent of these and other COVID-19 vaccines led to dramatic declines in COVID-19 morbidity and mortality[49], and—relative to vaccinated individuals—unvaccinated individuals are more likely to need hospitalization or die following SARS-CoV-2 infection[50].

SARS-CoV-2 Evasion of Immune Response

The success of SARS-CoV-2 is due in part to its ability to evade host immune responses. SARS-CoV-2 encodes nsps that inhibits global host mRNA splicing, protein translation, and membrane protein trafficking which all serve to inhibit IFN production and release in a non-specific manner[51,52]. The nsps and accessory proteins of SARS-CoV-2 also specifically antagonize interferon type I production as well as inhibit downstream signaling of type I IFN which then prevents the expression of ISGs[53,54]. One accessory protein (open-reading frame 8 protein) down regulates major histocompability complex

class I which helps to hide infected cells from cytotoxic T cells[55]. Additional strategies include epitope masking of the Spike protein to avoid antibody recognition, avoiding host cell apoptosis by inducing incomplete mitophagy, and evading antibody neutralization by using exosomes to house progeny viruses[56]. SARS-CoV-2 utilizes multiple methods of immune evasion to ensure its survival within the host.

Emergence of SARS-CoV-2 Variants of Concern

Viruses mutate to varying degrees depending on the nature of their genome and the proofreading activity (or lack thereof) of associated polymerases[57]. The exoribonuclease (nsp14) and its cofactor (nsp10) of SARS-CoV-2 ensure high-fidelity of its genome by decreasing the incidence of mismatched nucleotides which counteracts its low-fidelity RNA-dependent RNA polymerase[58]. However, SARS-CoV-2 is not invulnerable to mutations, and within a year of its emergence multiple lineage variants of concern (VOCs) appeared in numerous countries. B.1.1.7 (now called Alpha) and B.1.351 (now called Beta) were the first VOCs to be identified in September 2020 (Alpha, in United Kingdom) and October 2020 (Beta, in South Africa), and contained numerous missense mutations affecting the Spike protein[59,60]. The Alpha and Beta lineage RBD mutations (N501Y [i.e. asparagine at position 501 changed to tyrosine] in Alpha; K417N, E484K, and N501Y in Beta) lead to tighter Spike:ACE2 structural interactions[61,62] and increased the transmissibility of SARS-CoV-2[63–65]. In January 2021, the P.1. (now called Gamma) lineage was reported in Brazil to contain even more missense mutations in more genes, including Nucleocapsid and notably Spike[66]. As with Alpha and Beta, the mutations

inherent to the Gamma lineage RBD (K417T, E484K, and N501Y) increased its transmissibility[62,66]. Two additional lineages emerged in March 2021 and November 2021, respectively, and in time would supplant all prior lineages in the speed with which they spread: the Delta lineage, which was first reported in India[67], and the Omicron lineage, reported in southern Africa[68]. One of Delta's mutations, P681R, enhances Spike cleavage which in turn improves viral entry[69], whereas the success of Omicron lineages is more due to immune evasion[70,71]. Specifically, Omicron's G446S and N460K mutations are responsible for enhanced resistance to neutralizing antibodies[72]. SARS-CoV-2 continues to evolve, and deaths due to COVID-19 continue to cause overall declines in life expectancy for many countries, including the US[73,74].

1.2 Tuberculosis

Pathogenesis of Tuberculosis

Tuberculosis (TB) is the second-leading cause of death by a single infectious agent in the world. Approximately one quarter of the world is infected with TB, with about ten million people falling ill each year and causing an estimated 1.3 million deaths in 2022[75]. TB is caused by the bacillus *Mycobacterium tuberculosis* (Mtb) and is primarily spread by aerosols expelled by infected people. Although typically a pulmonary disease, Mtb can infect any organ. There are two disease types of TB—latent TB infection (LBTI) and active TB. Individuals with LTBI have no or few symptoms and often are unaware of infection. About 5-10% of individuals with LTBI will later develop active TB[76]. Individuals with active TB can experience many symptoms including prolonged cough,

chest pain, fatigue, weight loss, fever, and night sweats. Anti-tuberculosis treatment involves lengthy and often expensive antibiotic regimens, which hinders adherence to treatment.

Immune Response to TB

Infection in the lung begins with alveolar macrophages phagocytoses Mtb, where Mtb prevents fusion of the phagosome and lysosome to allow survival[77]. Once the bacteria gains access to the lung interstitium, the infection is further established and innate immune cells are recruited[77]. Bacilli are brought to the lung draining lymph nodes where priming of the adaptive immune response begins[78]. As primed T and B cells migrate to the site of infection, an organized structure called a granuloma is formed, which consists of a macrophage layer surrounded by lymphocytes, often with a necrotic core surrounded by neutrophils[78]. CD4 T cells, mainly Th1, express IFNg, TNF, and IL-2 which activate macrophages to induce anti-bacterial activity[78]. Both IFNg and TNF have long been shown to be essential for a protective immune response to TB[79,80]. CD8 T cells are less studied but have a cytotoxic role in recognizing and killing infected macrophages[78]. B cells and antibodies are multifunctional—developing optimal anti-tuberculosis immunity, regulating cytokine production, and modulating inflammation[78]. The complex interactions between both innate and adaptive immune cells contribute towards control of Mtb infection.

Coinfection

9

Due to the global prevalence of TB, coinfections with Mtb are not uncommon. Unfortunately, most coinfections with Mtb lead to worse patient outcomes. Patients with coinfection of Mtb and intestinal helminths showed a cytokine profile skewed toward a T helper 2 response with decreased IFNg and a tendency towards more severe pulmonary disease[81]. Other human studies of helminth and Mtb coinfections demonstrate a reduced response to Mtb antigens, and mouse studies show increased Mtb bacterial burdens in mice coinfected with Mtb and helminths[82]. Worse patient outcomes are not limited to Mtb coinfection with extracelluar infections. A review of influenza and TB coinfection literature reported that experimental animal studies and multiple analytical human studies found increased severity of disease and/or death with coinfection[83]. Additionally, TB is the leading cause of death in people who have human immunodeficiency virus (HIV), as HIV depletes CD4 T cells which are crucial for controlling Mtb infection[84]. HIV is also harbored in monocytes and macrophages, reducing their phagocytic activity which in turn increases susceptibility to TB[85]. Overall, coinfections with Mtb seem to negatively affect patient outcomes and the ability to generate an appropriate immune response.

With the advent of the COVID-19 pandemic, there was fear that countries with high TB burden may suffer more than other countries as coinfection with TB is usually detrimental. However, the relationship between TB and SARS-CoV-2 infection is less concrete. Although human studies examining TB and SARS-CoV-2 coinfection have generally found that coinfection exacerbates both TB and SARS-CoV-2 severity, there were some conflicting conclusions and some studies included individuals with additional

co-morbidities[86–90]. It has also been found that individuals with latent TB infection (LTBI) and SARS-CoV-2 had higher levels of inflammatory cytokines including IFNg, TNF, IL-1b, IL-6, IL-2, IL-12, and IL-4 than individuals with LBTI alone or SARS-CoV-2 infection alone[91]. In contrast, mouse studies have shown that mice given intravenous Bacillus Calmette-Guérin (BCG) vaccination or infected with Mtb and then subsequently infected with SARS-CoV-2 had a less severe SARS-CoV-2 infection and lower viral loads than naïve mice[92–97]. A proposed mechanism for this protection is that the increase of IFNg from BCG vaccination leads to upregulation of IFN-stimulated genes that have antiviral activity[98]. Supporting this idea, studies found that COVID-19 severity was correlated with negative or indeterminate Mtb antigen Interferon gamma release assay (IGRA) results, some due to low levels of IFNg in the blood overall[99–101]. These studies suggest that prior Mtb exposure and higher IFNg levels leads to reduced COVID-19 symptoms. Regardless of whether coinfection with Mtb and SARS-CoV-2 has a positive or negative effect on SARS-CoV-2 viral loads and disease severity, understanding how the immune environment is altered in response to coinfection is important for treatment of these diseases, especially considering the high prevalence of TB/SARS-CoV-2 coinfection.

The COVID-19 pandemic has exposed nearly all of humanity to a novel coronavirus that has mutated into different variants. Transmission of SARS-CoV-2 is often through asymptomatic individuals, who are less studied in SARS-CoV-2 literature. The aim of this research was to investigate the relationship between SARS-CoV-2 variants and

antibody response, one of the main protective means against the virus, in asymptomatic individuals in a large university setting. TB is another disease where many people are asymptomatic, where one quarter of the population is latently infected with Mtb. Coinfection of Mtb and SARS-CoV-2 demonstrates an unusual interaction where prior Mtb exposure may be actually beneficial to the host. Continuing to focus on antibody response, along with other aspects of TB immunology, my research aimed to uncover how long-term infection with Mtb positively affects the immune response to a subsequent encounter with SARS-CoV-2 antigens. Together, this work details how antibody responses to SARS-CoV-2 differ under different conditions and how individuals are protected from SARS-CoV-2 disease.
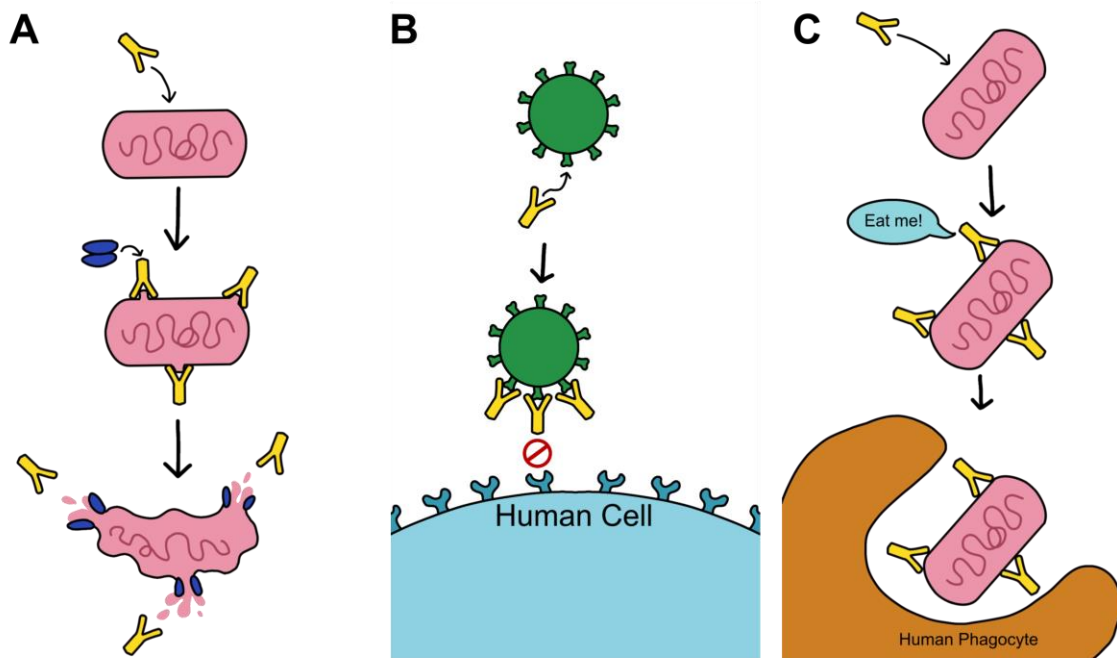
Figure 1: Overview of Antibody Functions. (**A**) Complement System Activation: Antibodies bind to bacteria or infected host cell which recruit complement proteins that disrupt the cell membrane, leading to its death. (**B**) Neutralization: Antibodies bind to virus or bacteria surface proteins and physically prevent the pathogen from binding to its

host cell receptor. (**C**) Opsonization: Antibodies bind to the pathogen which marks it for phagocytosis. Figure drawn by Coretta Merling.

Chapter 2: The emergence of SARS-CoV-2 lineages and associated saliva antibody responses among asymptomatic individuals in a large university community

Chapter 2, along with portions of Chapter 1, were previously published as: **Merling, M.R.**, Williams, A., Mahfooz, N.S., Ruane-Foster, M., Smith, J., Jahnes, J., Ayers, L.W., Bazan, J.A., Norris, A., Norris Turner, A., et al. (2023). The emergence of SARS-CoV-2 lineages and associated saliva antibody responses among asymptomatic individuals in a large university community. PLoS Pathog 19, e1011596. 10.1371/journal.ppat.1011596.[102] This work is reproduced in accordance with the Creative Commons Attribution License (4.0).

Attributions: conceptualization, data curation, formal analysis, investigation, methodology, validation, visualization, writing – original draft, writing – review & editing

2.1 Introduction

Since interrupting the Spike:ACE2 interaction was the goal of now-approved vaccines[103,104], and remains a goal of potential COVID-19 therapies[105,106], the continual emergence of new SARS-CoV-2 lineages with numerous and diverse Spike mutations threatens our ability to prevent and treat future SARS-CoV-2 infections. It is therefore important to understand the relationships between SARS-CoV-2 lineage emergence,

SARS-CoV-2-specific Ig levels—as elicited by either natural infection or vaccination—and their neutralization capacity. This is especially true of asymptomatic individuals who are PCR positive (PCR[POS]), as they are estimated to account for 50–65% of all transmission[107,108]. In this chapter, we describe the relationships between COVID-19 incidence, SARS-CoV-2 lineage, viral load, SARS-CoV-2-specific Ig responses (IgM, IgA, & IgG), and inhibitory capacity in the saliva of asymptomatic PCR[POS] individuals, as the oral cavity and saliva—in addition to being readily accessible—are important sites of SARS-CoV-2 infection and transmission[109] (especially newer Omicron VOCs[110–114]). SARS-CoV-2-specific Ig responses were similarly assessed in PCR[NEG] individuals with a history of SARS-CoV-2 infection and/or COVID-19 vaccination with pre-Omicron vaccines. These data were generated as part of a large university COVID-19 monitoring program which occurred between August 2020 and June 2022.

2.2 Methods

Ethics statement

This work was reviewed and approved by The Ohio State University Biomedical Sciences Institutional Review Board (IRB, ID #2021H0080). This work was also reviewed and approved by the Ohio State Institutional Biosafety Committee (IBC) (ID #2020R00000046). Each participant provided formal, electronic consent to the following *HIPAA AUTHORIZATION TO DISCLOSE PROTECTED HEALTH INFORMATION* statement: "I voluntarily authorize OSUWMC to use and/or disclose my COVID-19 test results to The Ohio State University as part of the ongoing surveillance testing related to

COVID-19 community spread. I understand that my COVID-19 test results are considered Protected Health Information (PHI) and no payment will be exchanged for disclosure of my test results. I further understand that I have the right to revoke this authorization, in writing, by sending written notification to: Office of Compliance and Integrity-Privacy, 650 Ackerman Road, Columbus, Ohio 43202. I understand that PHI used or disclosed pursuant to this authorization may be redisclosed by the recipient and its confidentiality may no longer be protected by federal or state law. I consent to the use of electronic signature and understand that my documenting consent below, I have affirmatively executed this authorization." Per our IRB-approved Waiver of Consent Process, we did not seek additional consent beyond that which participants had already agreed (i.e. the above *HIPAA AUTHORIZATION TO DISCLOSE PROTECTED HEALTH INFORMATION* statement) for the following reasons: (1) our study used leftover human specimens that were not individually identifiable; (2) the use of each sample posed no additional risk to the original donor than that to which they are already aware (i.e. the potential loss of privacy), and the intent of our study also related to surveillance of COVID-19 community spread, to which donors have already consented per the statement above.

Saliva specimen collection and handling

The Ohio State COVID-19 monitoring program was active from August 2020 through June 2022. As part of this program, saliva specimens were collected on a weekly basis from students, staff, and faculty who self-reported as being asymptomatic at the time of

specimen collection. At the time of specimen collection each participant provided formal, electronic consent per our Ethics Statement. On and prior to the day of saliva collection at one of several mass testing sites (Figure 2A), individuals were instructed to define themselves *symptomatic* if they had at least one or more of the following: fever, chills, shortness of breath, difficulty breathing, fatigue, muscle aches, body aches, headache, new loss of taste, new loss of smell, sore throat, congestion, runny nose, nausea, vomiting, or diarrhea. To prevent contagion, symptomatic individuals were instructed not to come to the mass testing site and were instead referred to a healthcare provider for follow-up (e.g. the campus student health clinic). Individuals were defined as *asymptomatic* if they had none of the symptomatic conditions listed above. On the day of testing, individuals were instructed to refrain from food or drink for 30 minutes prior to collection, and to gently eject saliva into the collection tube, swallowing first and keeping saliva free from mucus, until the 1 mL mark on a sterile conical was reached (i.e. passive drool method). Specimens from asymptomatic individuals were collected at each of the six Ohio State campuses in Franklin county (OSU-Columbus), Licking county (OSU-Newark), Richland county (OSU-Mansfield), Allen county (OSU-Lima), Marion county (OSU-Marion) and Wayne county (OSU-Wooster). Specimens were then couriered to the CLIA-approved Applied Microbiology Services Lab (AMSL) of the Ohio State Infectious Disease Institute (IDI) and analyzed in accordance with the SalivaDirect assay, a clinical diagnostic test that is Emergency Use Authorization (EUA) approved by the US Food & Drug Administration (FDA) for SARS-COV-2 detection[115]. While performing the SalivaDirect real time polymerase chain reaction (PCR), saliva samples were stored

in a 4°C cold room until they were deemed either PCR negative (PCR^{NEG}) or PCR

positive (PCR^{POS}) for SARS-CoV-2. Per the SalivaDirect method[116], any sample with a

C$_T$ value $\leq$ 40 was considered PCR^{POS} for SARS-CoV-2. The positive or negative status

of the sample was reported to the individual and regional public health authorities

(Columbus Public Health, Ohio Department of Health, ODH) per state and federal

policies at the time. PCR^{POS} saliva samples and select PCR^{NEG} saliva samples were then

removed from the 4°C cold room, aliquoted into microcentrifuge tubes, frozen (-20°C),

and analyzed for viral genome sequencing and lineage identification, as well as host

antibody response characterization.

Sequencing and lineage identification

PCR^{POS} saliva samples with a C$_T$ $\leq$ 33 had their whole SARS-CoV-2 viral genome

sequenced and lineage assigned per the methods described in our previous work[117]

(samples with a C$_T$> 33 had insufficient viral RNA for sequencing). There was only one

exception to this in September 2021, when a single sample with a C$_T$ of >35 was

sequenced. SARS-CoV-2 genome copy numbers were calculated via linear regression

analysis, by comparison to the C$_T$ values of SalivaDirect reference standards. SARS-

CoV-2 genome sequences were submitted to the Global Initiative on Sharing Avian

Influenza Data (GISAID) database in a manner consistent with ODH expectations and

policies at that time, in as close to real time as possible. The abbreviations we use for

each lineage in this study and associated figures are as follows: CoV2^{Anc}, the ancestral

lineage of SARS-CoV-2 which emerged from Wuhan, China; CoV2^{US}, the B.1.2 lineage

which was among the first detected in our region of the US[117–119]; CoV2[Alpha], the B.1.1.7

lineage or Alpha VOC which was first reported by the UK in December 2020[59];

CoV2[Beta], the B.1.351 lineage or Beta VOC which was first reported in South Africa in

December 2020[60]; CoV2[Gamma], the P.1 lineage or Gamma VOC which was first reported

in Brazil in January 2021[66]; CoV2[Delta], the B.1.617.2 lineage or Delta VOC which was

first reported in India in December 2020[67]; CoV2[Omicron], the B.1.1.529 lineage or

Omicron VOC which was first reported in South Africa in Nov 2021[68]; CoV2[O-BA.1], the

BA.1 subvariant of CoV2[Omicron]; CoV2[O-BA.2], the BA.2 subvariant of CoV2[Omicron]; CoV2[O-BA.4], the BA.4 subvariant of CoV2[Omicron]; CoV2[O-BA.5], the BA.5 subvariant of CoV2[Omicron].

The nonsynonymous Spike mutations which distinguish these lineages are depicted in

Figure 9. Any lineage which was not a VOC or otherwise not mentioned above (e.g.

Epsilon) is labeled "Non-VOC."

COVID-19 wave designations and comparisons

We defined a COVID-19 wave within our university community as when new PCR[POS]

case counts rose above the overall period median for ≥ 3 weeks in a row (the overall

period being January 2021 through June 2022). For comparisons to COVID-19 incidence

in surrounding counties, we accessed publicly available ODH data via their public-facing

dashboard (accessed November 14 2022).

Measuring binding antibody levels in saliva

After PCR results were reported (typically within 24 hours of specimen collection), PCR[POS] and select PCR[NEG] specimens were removed from the 4°C cold room, aliquoted into microcentrifuge tubes containing Triton X-100 to inactivate SARS-CoV-2 (final concentration: 1% Triton X-100)[120]. PCR[NEG] samples were selected based on the donors' having had either a prior SARS-CoV-2 infection (allowing us to measure durability of the antibody response following natural infection) or their having been vaccinated against COVID-19 (allowing us to compare the antibody responses of uninfected vaccinated individuals to those of infected vaccinated individuals, a.k.a. breakthrough infections). All samples were treated identically regardless of whether they were PCR[POS] or PCR[NEG]. Following the addition of Triton X-100, samples were vortexed and allowed to incubate for 1 hour at room temperature[120]. Samples were subsequently stored at -80°C until the antibody levels in all samples could be measured at the same time, thus eliminating batch effects. Meso Scale Diagnostics (MSD) V-Plex platform assays Panel 1 (#K15375U), Panel 5 (#K15383U, #K14384U, #K15385U), Panel 6 (#K15433U) and Panel 13 (#K15463U, #K15464U, #K15465U) were used to measure the concentration of SARS-CoV-2 antigen specific immunoglobulin (IgM, IgA and/or IgG) in PCR[POS] and PCR[NEG] samples. Briefly, the MSD V-Plex assay comprises a 96-well plate which, within each well, contains multiple spots that are coated with defined antigens. For our study, these antigens included recombinant forms of three CoV2[Anc] lineage proteins (Nucleocapsid [N], Spike, and the Spike Receptor Binding Domain [RBD]), as well as CoV2[Alpha] Spike, CoV2[Beta] Spike, CoV2[Gamma] Spike, and CoV2[Delta] Spike (Figure 9). The Spike antigens consisted of the trimerized form of the ectodomain; the N antigen consisted of the full-

length protein. Antibodies in the sample bind to the antigens, and reporter-conjugated secondary antibodies were used for detection. Saliva samples were thawed on ice and diluted by a factor of 10 in the diluent provided in the V-Plex assay kit for each assay. The V-Plex assays were performed according to manufacturer instructions, and plates were read on an MSD instrument which measures light emitted from reporter-conjugated secondary antibodies. Using MSD's analysis software, the light signal measured by the MSD instrument was converted into arbitrary units (AU) representing amount of antibody present relative to the standard curve of the assay. The AU values for IgM, IgA, and IgG binding to $CoV2^{Anc}$ N, Spike, and Spike RBD were transformed to WHO binding antibody units (BAU) via validated WHO standards and conversion factors provided by MSD. The AU values for IgM, IgA, and IgG binding to other forms of N or Spike (i.e., those of VOC) cannot be converted to WHO BAU, as there are no WHO standards for these recombinant proteins. For this reason, the levels of each Ig isotype which bind to $CoV2^{Alpha}$, $CoV2^{Beta}$, $CoV2^{Gamma}$, and $CoV2^{Delta}$ forms of Spike are expressed as AU.

Spike inhibition assay

The capacity of saliva specimens to inhibit Spike activity was quantified using a commercially available ACE2 displacement assay (MSD COVID-19 ACE2 Neutralization Kit method). Plate-bound Spike was incubated with diluted saliva (the same specimens used for Ig measurements) per manufacturer protocols, followed by washing and addition of a luminescent probe-conjugated, recombinant form of human

ACE2. The extent to which luminescence declined relative to non-saliva (i.e., diluent only) treated wells was used to derive a percent inhibition value for each individual sample, using the following formula: % inhibition = 1 –(saliva sample luminescence value / diluent only luminescence value) × 100.

Graphing and statistics

Graphs were generated in RStudio (version 3.6.3) or GraphPad (version 9.5.1). All statistical tests were performed in RStudio. Data was tested for normality using the Kolmogorov-Smirnov test and for equal variance using the Bartlett test of homogeneity of variances. For data that did not have normal distribution, the Kruskal-Wallis rank sum test was used to determine if there were significant differences between groups in unpaired datasets, and the Friedman rank sum test was used in paired datasets. Within those datasets, the significant differences between groups were identified via an unpaired or paired Wilcoxon rank sum test as appropriate with Benjamini-Hochberg p value adjustment method. For the neutralization data which contained several zero values, the Shapiro-Wilk normality test was used, followed by the Bartlett test of homogeneity of variances. The Kruskal-Wallis rank sum test was used to determine if significant differences were present, followed by Dunn's test with Benjamini-Hochberg p value adjustment method to identify which groups were significantly different. Differences between groups were considered significant if $P < 0.05$ and are graphically indicated by 1 or more asterisks (*$P < 0.05$; **$P < 0.005$; ***$P < 0.0005$; ****$P < 0.00005$).

22

Abbreviations

The following abbreviations are used throughout this chapter: **PCR^{POS}**, an individual or saliva specimen that was PCR positive for SARS-CoV-2 (C_T value ≤ 40); **PCR^{NEG}**, an individual or saliva specimen that was PCR negative for SARS-CoV-2; **Spike** and **N,** unless otherwise stated the Spike and N proteins of SARS-CoV-2 (not any other coronavirus); **CoV2-Ig**, immunoglobulin of any isotype that recognizes any SARS-CoV-2 antigen; **IgM^{Spike}**, IgM that recognizes Spike; **IgA^{Spike}**, IgA that recognizes Spike; **IgG^{Spike}**, IgG that recognizes Spike; **IgG^{RBD}**, IgG that recognizes the Spike Receptor Binding Domain; **IgG^{N}**, IgG that recognizes the N protein; **Vax^{POS}**, an individual who was fully vaccinated against COVID-19 prior to saliva specimen collection; **Vax^{NEG}**, an individual who was not fully vaccinated against COVID-19 prior to saliva specimen collection; **New^{POS}**, an individual who at the time of saliva collection was PCR^{POS} for the first time; **Prior^{POS}**, an individual who at the time of saliva collection was PCR^{NEG} but who had a prior CoV2 infection (i.e. the individual had been PCR^{POS} 2–37 weeks prior).

Vaccination status

For the purposes of our study, an individual was defined as "Vax^{POS}" if they had been fully vaccinated against COVID-19 prior to the date of saliva specimen collection, with either of the following vaccines: BNT162b2 (both doses), mRNA-1273 (both doses), Ad26.COV2.2. Among the Vax^{POS} individuals in our study, the aggregate representations of each vaccine are as follows: ~75% were vaccinated with BNT162b2, ~17% with mRNA-1273, and ~8% with Ad26.COV2.2. An individual was defined as "Vax^{NEG}" if

they were not fully vaccinated against COVID-19 prior to saliva specimen collection.

This includes individuals who had only received one dose of either BNT162b2 or

mRNA-1273, without receiving the second dose. All samples were identically treated

regardless of whether they came from someone who was Vax^{POS} or Vax^{NEG}.

2.3 Results

Study overview

The first confirmed cases of COVID-19 in the state of Ohio were reported on March 9

2020[121]. The Ohio State University suspended on campus activities the same day[122] and

subsequently developed a campus wide plan to monitor the incidence of SARS-CoV-2

infection among its students, staff and faculty[123]. Individuals participating in this

monitoring program, which formally began in August 2020, provided saliva on a weekly

basis for COVID-19 testing. Prior to testing, individuals who self-reported as being

symptomatic were not tested and were instead given a clinical referral. Individuals who

self-reported as being asymptomatic provided a saliva specimen via a passive drool

method at each of our six university campuses (Figure 2A). Specimens were assessed by

our CLIA-certified lab for the presence of SARS-CoV-2 using real-time quantitative

reverse transcription PCR (qRT-PCR). Specimens were not pooled prior to testing. qRT-

PCR results were reported to the individual and the regional public health authority per

state and federal policies at the time. If a specimen had a C_T value ≤40 it was considered

positive for SARS-CoV-2 virus (PCR^{POS}). Per our Institutional Review Board (IRB)

approved protocol and workflow (Figure 2B), PCR^{POS} saliva samples were subsequently

used for SARS-CoV-2 lineage identification and SARS-CoV-2-specific immunoglobulin (CoV2-Ig) measurements. In some instances, select saliva samples that were negative for SARS-CoV-2 virus (PCR[NEG]) were also collected, the reasons for which will be made clear in sections below. The relationships between these molecular and immunological readouts to one another, as well as to coded data concerning the prior infection status and vaccination status of the saliva donor, are described below for the period spanning January 2021 (before COVID-19 vaccines were widely available to students in our university community) to June 2022, when the monitoring program ended. See chapter 2.2 for details regarding saliva collection, symptomatic versus asymptomatic designation, qRT-PCR, SARS-CoV-2 lineage identification, CoV2-Ig measurements, and statistical analyses. In total, >850,000 diagnostic PCR tests were performed by our lab during this monitoring program.

The incidence of SARS-CoV-2 positivity in our university community occurred in waves which reflected those occurring in surrounding regions

The incidence of new PCR[POS] cases among asymptomatic individuals in our university community, for the period spanning January 2021 to June 2022, is shown in Figure 3A along with the seven day average PCR positivity rate (Figure 3B). COVID-19 monitoring occurred before January 2021; however, because the bulk of PCR testing at that time was contracted to a commercial entity, our access to the raw PCR data before January 2021 is limited. Above these data are two timelines relevant to data interpretation, indicating when Ohio COVID-19 vaccination policies shifted from prioritizing at risk populations

(e.g. elderly) to anyone ≥16 years of ages well as the deadlines for all our community members (i.e. university students, faculty, and staff) to have received their first and second COVID-19 doses (October 15 2021 and November 15 2021, respectively)[124]. Indicated below the data are corresponding intervals in the academic calendar, which will be referred to in subsequent sections. We identified 11,958 PCR[POS] individuals between January 2021 to June 2022; the median, mean and maximum new PCR[POS] cases per test day were 15, 34 and 523, respectively. There were, however, six time periods when the new case counts rose above the overall period median for ≥ 3 weeks in a row. These six time periods are hereafter referred to as Waves 1–6 and spanned the following dates: *Wave 1*, January 11 2021 to January 29 2021; *Wave 2*, February 22 2021 to March 12 2021; *Wave 3*, March 22 2021 to April 16 2021; *Wave 4*, August 16 2021 to September 24 2021; *Wave 5*, November 15 2021 to February 18 2022; *Wave 6*, April 18 2022 to May 6 2022. The waves of COVID-19 incidence amongst asymptomatic individuals in our university community mirrored (rather than preceded) the waves of COVID-19 incidence in the counties surrounding each university campus[125] (Figure 10).

Prior to community vaccine requirements being established, SARS-CoV-2 was becoming progressively more concentrated in the saliva of asymptomatic individuals
The emergence of SARS-CoV-2 VOCs in multiple Ohio communities[125–131] with potential for greater infectivity and/or transmissibility led us to assess the relationship between SARS-CoV-2 abundance in saliva and VOC identity. We used the qRT-PCR cycle threshold (C_T) value as a readout of SARS-CoV-2 abundance, as the SalivaDirect

C_T value is inversely proportional to SARS-CoV-2 viral load (i.e. a lower C_T value corresponds to higher SARS-CoV-2 RNA levels in the tested sample)[116], and a commonly used as a proxy for probability of transmission (i.e. a lower C_T value correspond to higher transmission probability)[132–136]. VOC identity was determined by next generation sequencing of the entire SARS-CoV-2 genome and subsequent alignment with Global Initiative on Sharing Avian Influenza Data (GISAID) reference sequences. During the entire monitoring period, SARS-CoV-2 genome sequences were submitted to the GISAID database in a manner consistent with ODH expectations and policies at that time, in as close to real time as possible.

The weekly composite C_T values of all PCR[POS] samples, and daily individual C_T values of sequenced samples are shown in Figure 4A and 4B, respectively, with color annotations in Figure 4B indicating the lineage identity. The same data are also presented as wave composites (Figure 4C) in order to best illustrate the following trends: During Wave 1 (Week 2 of January 2021 to Week 4 of January 2021), the mean C_T value of all PCR[POS] saliva samples was 29.8 (Figure 4C). During Wave 2 (Week 4 of February 2021 to Week 2 of March 2021) the mean C_T value was 29.3 (Figure 4C). The mean C_T value lowered to 29.0 during Wave 3 (Week 4 of March 2021 to Week 2 of April 2021) (Figure 4C). The number of tests performed fell precipitously during June 2021 and July 2021, as the campus population is minimal during the summer months; therefore, we are reluctant to draw conclusions from or otherwise compare Summer 2021 C_T value data to the prior semester, when testing volume was higher. Upon resumption of high-volume testing during the later weeks of August 2021, which marked the beginning of the Autumn 2021

semester and Wave 4 (Week 3 of August 2021 to Week 3 of September 2021), we noted the lowest mean C_T value of all waves (27.9) (Figure 4C). The extrapolated SARS-CoV-2 genome copy concentrations (Figure 4D) are consistent with Wave 4 saliva samples having the highest virus concentrations of all waves. Wave 5 was the longest wave (Week 3 of November 2021 to Week 2 of February 2022) with daily PCR[POS] cases reaching a maximum of 523 on January 11, 2022. The mean C_T value of Wave 5, which followed our community deadline for vaccine requirements, was 30.1 and significantly higher than that of Wave 4 (Figure 4C). The last wave before the COVID-19 monitoring program ended, Wave 6 (Week 2 of April 2022 to Week 1 of May 2022), had a lower mean C_T value (28.6) than Wave 5 (Figure 4C). The lowest C_T value we ever observed was on February 18 2021 ($C_T = 14.2$).

Each wave of SARS-CoV-2 positivity corresponded to the emergence of a new SARS-CoV-2 lineage within our community

The SARS-CoV-2 lineages present in each individual PCR[POS] sample during the same time periods as above are shown in Figure 4B, exceptions being samples with a C_T value of >33 as these could not be sequenced due to the viral RNA levels being too low. Males were more likely to meet sequencing criteria (i.e. a $C_T \leq 33$) than females during Waves 1–3 (Figure 11A); this was not true of later Waves, however, and female representation was higher during the entire monitoring period overall (Figure 11A). Among sequenced samples, the median and mean ages of individuals were 21 and 23, respectively, and varied minimally during the monitoring period (Figure 11B). During the period spanning

January 2021 to mid-February 2021, the predominant lineage was B.1.2, which we hereafter refer to as CoV2[US] since it was among the first detected in our region of the US[117–119]. The period of CoV2[US] lineage predominance corresponds to Wave 1 in our community (Figures 3 and 4B). Beginning mid-February 2021 and extending to mid-March 2021 was a period of time when an array of lineages which we collectively refer to as "non-VOC" were predominant, as they were more diverse compared to earlier and later testing periods and were never considered to be VOCs. Although the CoV2[US] lineage was still being detected, Wave 2 primarily comprised of non-VOCs (Figure 4B). As the Ides of March approached in 2021, so too did two VOCs begin appearing with increasing frequency: the Alpha VOC (CoV2[Alpha]) and Gamma VOCs (CoV2[Gamma]). CoV2[Alpha] and CoV2[Gamma] were widely considered at that time to be more transmissible than previous lineages[66,137]. CoV2[Alpha] and CoV2[Gamma] were the primary lineages detected during Wave 3 (Figure 4B), and continued to predominate among the few positive samples collected during May 2021. The Beta VOC (CoV2[Beta]) only appeared once in our university community (April 15 2021). Beginning June 2021 and continuing through December 2021 the new Delta VOC (CoV2[Delta]) made up the vast majority of PCR[POS] saliva samples (Figure 4B). CoV2[Delta] is more transmissible than CoV2[Alpha] and CoV2[Gamma138], and the period in which CoV2[Delta] predominated coincided with COVID-19 Wave 4 in our community (Figure 3). Wave 5, the penultimate and largest COVID-19 wave, coincided with the emergence and dominance of the Omicron VOC (CoV2[Omicron]) subvariant, BA.1 (CoV2[O-BA.1]). Wave 6, final wave before our COVID-19 monitoring program ended, was dominated by the CoV2[Omicron] subvariant BA.2 (CoV2[O-BA.2]) (Figure

29

4B). When considered alongside the C_T values and SARS-CoV-2 genome copy numbers

that characterized each wave (Figure 4C and 4D), the above data demonstrate that the

shift from CoV2^{US} to CoV2^{Alpha}/CoV2^{Gamma} to CoV2^{Delta} coincided with the virus

becoming progressively more concentrated in the saliva of asymptomatic individuals, this

trend ending after community vaccine requirements were established.

Among pre-Omicron lineages, CoV2^{Delta} elicited the highest levels of Spike-specific

IgA and IgG in unvaccinated, asymptomatic individuals

To assess whether SARS-CoV-2-specific Ig was detectable in the saliva of asymptomatic

SARS-CoV-2 PCR^{POS} individuals, as well as whether levels of the same Ig varied

depending on the SARS-CoV-2 lineage present, we used the same samples described

above (i.e. those used for lineage identification) to measure saliva levels of SARS-CoV-2

Spike-specific IgM (IgM^{Spike}), SARS-CoV-2 Spike-specific IgA (IgA^{Spike}), and SARS-

CoV-2 Spike-specific IgG (IgG^{Spike}) (Figure 5). Individuals vaccinated against COVID-

19 were excluded from this analysis (the vaccination record of each person in our

university community was closely monitored during this time period), and saliva samples

from individuals infected with CoV2^{Anc}, CoV2^{Alpha} and CoV2^{Gamma} were collected prior

to COVID-19 vaccines being widely available in our community; therefore, no vaccine-

elicited antibody responses would be expected in these samples. Among individuals

infected with CoV2^{Delta}, only unvaccinated individuals were included in the Figure 5

analysis. To eliminate viral load as a confounding variable, only PCR^{POS} saliva samples

with similar C_T range were used for Ig comparisons (C_T range = 22–26). PCR^{NEG} saliva

collected in early 2020 from healthy individuals living in the US and no COVID-19 history were used to estimate "pre-pandemic" levels of IgM^{Spike}, IgA^{Spike}, and IgG^{Spike} binding.

Saliva IgM^{Spike} (Figure 5A), IgA^{Spike} (Figure 5B), and IgG^{Spike} (Figure 5C) data are shown relative to which SARS-CoV-2 lineage was detected in the same saliva donor ($CoV2^{US}$, $CoV2^{Alpha}$, $CoV2^{Gamma}$, or $CoV2^{Delta}$) and are expressed as WHO binding antibody units, or BAUs. As shown in Figure 5A–5C, respectively, nearly all PCR^{POS} individuals had saliva IgM^{Spike}, IgA^{Spike}, and IgG^{Spike} levels that were above "pre-pandemic" levels, regardless of whether they were infected with $CoV2^{US}$, $CoV2^{Alpha}$, $CoV2^{Gamma}$, or $CoV2^{Delta}$. All PCR^{POS} individuals had similar IgM^{Spike} levels (Figure 5A). There were, however, two noteworthy differences between PCR^{POS} individuals depending on the lineage present. First, saliva IgA^{Spike} levels were similar between individuals infected with $CoV2^{US}$, $CoV2^{Alpha}$ and $CoV2^{Gamma}$; $CoV2^{Delta}$ infected individuals, on the other hand, had significantly higher IgA^{Spike} levels compared to those infected with $CoV2^{US}$, $CoV2^{Alpha}$, or $CoV2^{Gamma}$ (Figure 5B). Second and analogous to IgA^{Spike} differences (Figure 5B), $CoV2^{Delta}$-infected individuals had significantly higher IgG^{Spike} levels compared to those infected with $CoV2^{US}$, $CoV2^{Alpha}$, or $CoV2^{Gamma}$ (Figure 5C). For IgM^{Spike}, IgA^{Spike}, and IgG^{Spike} measurements, the recombinant Spike antigen used for Ig detection was identical to that of $CoV2^{Anc}$, as this enabled data transformation to WHO BAU (see chapter 2.2); the same patterns were observed, however, when the same saliva

samples were tested against recombinant $CoV2^{Alpha}$, $CoV2^{Beta}$, and $CoV2^{Gamma}$ Spike antigens (Figure 12).

Following infection of unvaccinated individuals, IgG^{Spike} and IgG^{RBD} persisted at higher levels in saliva than IgG^N

To determine the extent to which SARS-CoV-2-specific IgG in saliva was sustained over time, we performed the analysis shown in Figure 6 wherein saliva IgG^{Spike} levels, as well as Nucleocapsid (N)-specific IgG (IgG^N) levels, were compared across two groups of individuals: "New^{POS}" individuals who, at the time of saliva collection, were positive for either $CoV2^{US}$ or $CoV2^{Alpha}$; "$Prior^{POS}$" individuals who were uninfected at the time of saliva collection, but had been PCR^{POS} 14–252 days earlier. In this instance, saliva samples from $Prior^{POS}$ individuals were collected in May 2021. Most individuals in our $Prior^{POS}$ cohort were infected during the Autumn 2020 semester, before COVID-19 vaccines were available; however, since a portion of these individuals did go on to receive the COVID-19 vaccine prior to May 2021, we subdivided the data from $Prior^{POS}$ individuals into those who did not receive the vaccine (Vax^{NEG}) prior to May 2021, and those who did receive the vaccine (Vax^{POS}) prior to May 2021.

Among New^{POS} individuals, saliva IgG^N levels were similar regardless of whether they were infected with $CoV2^{US}$ or $CoV2^{Alpha}$ (Figure 6A), $CoV2^{Alpha}$ having slightly higher levels than $CoV2^{US}$), as were saliva IgG^{Spike} levels (Figure 6B). Relative to New^{POS} individuals, saliva IgG^N levels in $Prior^{POS}$ individuals were higher (Figure 6A); however,

the difference in saliva IgG^{Spike} levels between New^{POS} versus Prior^{POS} individuals was more pronounced (Figure 6B). Among Prior^{POS} individuals who did not receive a vaccine, saliva IgG^N and IgG^{Spike} levels persisted at average concentrations of 0.0212 WHO BAU/mL and 1.58 WHO BAU/mL, respectively for up to 252 days after their initial positivity date (Figure 6D and 6E). Interestingly, mean saliva IgG^{Spike} levels were only slightly higher in Prior^{POS} individuals who were Vax^{POS} compared to those who were Vax^{NEG} (Figure 6B), as were the levels of IgG^{RBD} (Figure 6C). These results indicate that although IgG^N and IgG^{Spike} both persist in saliva following natural infection, IgG^{Spike} persists at higher levels and reacts against Spike regions that are essential for ACE2 binding (i.e., the RBD).

Individuals with breakthrough CoV2^{Delta} infections had comparable saliva IgG^{Spike} levels to those of uninfected, vaccinated individuals

During the period of December 2020 to March 2021, COVID-19 vaccination was prioritized and available to the elderly and other individuals at increased risk of severe disease (e.g. healthcare workers, first responders). In Ohio, beginning on March 22 2021, individuals who were 16 years or older could receive a COVID-19 vaccine, including all college students[139]. Despite the widespread availability of vaccines by our Autumn 2021 semester, CoV2^{Delta} lineage infections occurred among unvaccinated (Vax^{NEG}) individuals and vaccinated (Vax^{POS}) individuals. The term "breakthrough infection" is older than COVID[140] but is now commonly applied to individuals who are PCR^{POS} despite their being Vax^{POS}. Since BNT162b2, mRNA-1273 and Ad26.COV2.S were each

33

designed to elicit an Ig response against SARS-CoV-2 Spike (since it is essential for SARS-CoV-2 infection of ACE2-expressing cells), we assessed whether breakthrough infections with CoV2^{Delta} were associated with lower levels of Spike-specific Ig in saliva compared to PCR (neg) vaccinees. Shown in Figure 7 are saliva levels of IgM^{Spike}, IgA^{Spike}, and IgG^{Spike} in three groups of individuals: VAX^{NEG}PCR^{POS} individuals infected with CoV2^{Delta}, VAX^{POS}PCR^{POS} individuals infected with CoV2^{Delta}, and VAX^{POS}PCR^{NEG} individuals. Saliva from VAX^{NEG}PCR^{POS} and VAX^{POS}PCR^{POS} individuals was collected during Wave 4 (Figure 3), when community viral burdens were their highest (Figure 4D). Saliva from VAX^{POS}PCR^{NEG} individuals was collected shortly after Wave 4 had passed; however, the time between vaccination to saliva sample collection for VAX^{NEG}PCR^{POS} and VAX^{POS}PCR^{POS} cohorts were comparable (Figure 13). These results demonstrate that VAX^{POS}PCR^{POS} and VAX^{POS}PCR^{NEG} groups each had significantly higher saliva IgG^{Spike} levels than VAX^{NEG}PCR^{POS} individuals (Figure 7C). Furthermore, the saliva IgG^{Spike} levels of VAX^{POS}PCR^{POS} and VAX^{POS}PCR^{NEG} groups did not significantly differ from one another (Figure 7C). Notably, saliva IgM^{Spike} levels were indistinguishable across groups (Figure 7A), as were saliva IgA^{Spike} levels (Figure 7B). Among VAX^{POS}PCR^{NEG} individuals, saliva IgG^{Spike} could be detected up to 352 days post-vaccination (Figure 7D–7F). Similar trends were observed using recombinant CoV2^{Alpha}, CoV2^{Beta}, CoV2^{Gamma}, and CoV2^{Delta} Spike as capture antigens (Figure 14). We conclude from this that COVID-19 vaccination increased saliva IgG^{Spike} levels in our university community as intended, the saliva IgG^{Spike} levels in all vaccinees being comparable (regardless of whether they

34

had a breakthrough CoV$^{\text{Delta}}$ infection) and significantly higher than the saliva IgG$^{\text{Spike}}$ levels of unvaccinated, infected individuals.

Despite comparable Spike-specific Ig levels, CoV2$^{\text{Delta}}$-infected vaccinee saliva was less capable of Spike:ACE2 inhibition, relative to uninfected vaccinees

Since the presence of CoV2-specific Ig does not equate to its having neutralization capacity[141], we next compared the ability of Vax$^{\text{NEG}}$PCR$^{\text{POS}}$, Vax$^{\text{POS}}$PCR$^{\text{POS}}$ and Vax$^{\text{POS}}$PCR$^{\text{NEG}}$ saliva samples to inhibit Spike:ACE2 interactions. We quantified inhibitory activity using an ACE2 displacement assay (Figure 8A), wherein plate-bound Spike was incubated with the same saliva samples above (i.e., those of Figure 7), followed by washing and addition of a luminescent probe-conjugated, recombinant form of human ACE2. The extent to which luminescence declined relative to non-saliva treated wells was used to derive a percent inhibition value for each individual sample (see chapter 2.2 for additional details). The results of this analysis are shown in Figure 8B and demonstrate that there were differences between cohorts, the inhibitory activity of VAX$^{\text{POS}}$PCR$^{\text{NEG}}$ saliva being significantly higher than that of Vax$^{\text{NEG}}$PCR$^{\text{POS}}$ saliva (Figure 8B). The inhibitory activity of Vax$^{\text{POS}}$PCR$^{\text{POS}}$ saliva (median = 12) was 50% higher than that of Vax$^{\text{NEG}}$PCR$^{\text{POS}}$ saliva (median = 8), but 25% lower than that of Vax$^{\text{POS}}$PCR$^{\text{NEG}}$ saliva (median = 16); as a whole, however, the inhibitory activity of Vax$^{\text{POS}}$PCR$^{\text{POS}}$ saliva did not significantly differ from that of Vax$^{\text{NEG}}$PCR$^{\text{POS}}$ saliva, nor did it significantly differ from Vax$^{\text{POS}}$PCR$^{\text{NEG}}$ saliva (Figure 8B). Within the Vax$^{\text{NEG}}$PCR$^{\text{POS}}$ cohort, there were no significant correlations between these samples'

inhibitory activity and their IgM^{Spike} (Figure 8C), IgA^{Spike} (Figure 8D), or IgG^{Spike}

concentrations (Figure 8E) within linear regression models. This was also true of the

Vax^{POS}PCR^{POS} cohort, as no significant correlations were observed between these

samples' inhibitory activity and their IgM^{Spike} (Figure 8F), IgA^{Spike} (Figure 8G), or

IgG^{Spike} concentrations (Figure 8H). Within the Vax^{POS}PCR^{NEG} cohort, although the

linear regression models were significant between samples' inhibitory activity and their

IgA^{Spike} concentration (Figure 8J), as well as their IgG^{Spike} concentration (Figure 8K), but

not their IgM^{Spike} concentration (Figure 8I), the Multiple R-squared values were too low

to suggest strong correlation. When considered alongside the data shown in Figure 7, we

conclude COVID-19 vaccination led to increases in saliva IgG^{Spike} concentrations, the

levels being similar between vaccinees who had a breakthrough CoV2^{Delta} infection

(Vax^{POS}PCR^{POS}) and vaccinees who did not (Vax^{POS}PCR^{NEG}), but that during Wave 4 the

antibodies in Vax^{POS}PCR^{POS} saliva were limited in their ability to inhibit Spike, the

inhibition values being intermediate between Vax^{POS}PCR^{NEG} saliva (which had the

highest inhibition values) and Vax^{NEG}PCR^{POS} controls (which had the lowest inhibition

values).

2.4 Discussion

The spread of SARS-CoV-2 to the US marked the beginning of an extraordinary period

wherein a novel respiratory virus transmitted and evolved in a population with no prior

immunity, our primary defenses being behavioral changes (e.g., masking and physical

distancing) until the advent of effective vaccines. The first COVID-19 case in the US

occurred in January 2020[142]. It was soon discovered that SARS-CoV-2 caused both symptomatic and asymptomatic infections (the latter being more common in young adults), that asymptomatic individuals could transmit SARS-CoV-2[143,144], and that isolation of symptomatic individuals alone would not sufficiently "flatten the curve" of COVID-19 incidence[108,145]. By April 2020, most US universities shut down on-campus activities so as to limit SARS-CoV-2 transmission among their students, staff, and faculty. Many universities established COVID-19 monitoring programs prior to campus reopening as a means of identifying symptomatic and asymptomatic individuals. These monitoring programs varied in their testing modalities (PCR- or antigen-based), cadence (weekly versus biweekly testing), and sample pooling practices (pooled versus individual testing); all monitoring programs, however, had the same goal in mind: enabling safe resumption of on-campus classes and activities. Now that mass COVID-19 testing programs have ended in US, enabling time for processing and reflection, we are sharing the results of our monitoring program which we believe are most relevant to the ongoing issues of community spread, the longevity of mucosal Ig following natural infection, breakthrough infections, and the utility of saliva for assessing Ig responses to newer Omicron subvariants and booster vaccines.

That the COVID-19 waves in our campus community mirrored those which occurred in surrounding counties, instead of preceding the surrounding county waves, touches on an important question at the time regarding campus reopening: what, if any, contribution would the influx of students have on COVID-19 incidence in surrounding communities.

In January 2021, student returns to university campuses were a contentious subject in the US due to the potential risk of contracting the virus and subsequent transmission to surrounding communities. COVID-19 vaccines were not yet widely available to young adults, and—fairly or unfairly—university students were perceived as being more cavalier in their adherence to masking protocols and social distancing. Whether or not the reopening of a given college or university contributed to higher off-campus COVID-19 transmission will depend on several variables (e.g. whether a school was in a state that mandated mask-wearing)[146], but in our case the COVID-19 wave that occurred in our university in January 2021 (Wave 1) peaked during the tail end of one which had been ongoing in surrounding counties (compare Figure 3 and Figure 10). This was also true in August 2022, when our campus reopened after summer break and experienced Wave 4, which followed the Delta wave that had already begun in surrounding counties. The timing of Wave 1 and Wave 4 in relation to those in surrounding counties is inconsistent with the argument that our university reopening contributed to COVID-19 incidence in the surrounding communities. Studies at other large universities with COVID-19 policies and monitoring programs similar to our own support this conclusion[147–149].

Early in the COVID-19 pandemic, it was unknown whether natural infection would give rise to Ig responses that were durable and protective, as those against common seasonal coronaviruses are short-lived (only 6 months in some cases)[150], or worse still whether the Ig response would actually enhance infection or disease[151–154]. Regarding the durability and protective capacity of the antibody response to natural SARS-CoV-2 infection,

38

current knowledge on this subject was recently reviewed[141]. In our study of asymptomatic individuals, at the time of initial PCR positivity we could already detect elevations in SARS-CoV-2-specific Ig (IgM, IgA, and to a lesser extent IgG) in the saliva, the degree to which varied by lineage, $CoV2^{Delta}$ being the most immunogenic of the lineages we assessed. Up to 252 days after initial PCR positivity, saliva levels of SARS-CoV-2-specific IgG were substantially higher in $Prior^{POS}$ individuals compared to New^{POS} individuals, were directed against Spike, Spike RBD, and (to a lesser extent) the N protein. Potential reasons why Spike-specific IgG (IgG^{Spike}) levels were higher than those of N-specific IgG (IgG^{N}) include Spike being more antigenic, or alternatively it may reflect an inherent inability of IgG^{N} to persist in saliva relative to IgG^{Spike}, as is the case in plasma[155]. The N protein of SARS-CoV-2 strongly resembles those of other coronaviruses that can infect humans[156]. For this reason, and because the US National Institutes of Health states that false positives in serological tests for SARS-CoV-2 may occur due to cross-reactivity from pre-existing antibodies to other coronaviruses[157], it is possible that our sample population could have nucleocapsid-binding antibodies from a previous coronavirus infection.

When COVID-19 vaccine doses were in short supply (early 2021), university students were generally not considered a vaccine priority by national public health agencies. By the time COVID-19 vaccines were widely available, non-trivial levels of vaccine hesitancy had arisen among university students in many countries for many reasons[158]. Vaccine hesitancy was reinforced by the occurrence of breakthrough infections with

CoV2[Delta159,160], the first lineage to emerge after vaccines had become more widely available in Summer 2021. If vaccines were effective, conventional logic at the time being, how then could a vaccinated individual still become PCR[POS]? Our current understanding is that a combination of three factors affects susceptibility to breakthrough infections: (1) antibody levels at the time of virus exposure, (2) the neutralizing capacity of these antibodies, and (3) the amount of virus to which a vaccinee is exposed. Our data demonstrate that saliva IgG[Spike] levels were comparable between CoV[Delta]-infected vaccinees (Vax[POS]PCR[POS]) and uninfected vaccinees (Vax[POS]PCR[NEG]), but that the collective inhibitory capacity of this IgG[Spike] and other saliva antibodies differed between groups, with Vax[POS]PCR[POS] saliva being less inhibitory than Vax[POS]PCR[NEG] saliva (Figure 8B). If the saliva Ig response is representative of that which occurs in other parts of the upper airway, then the combination of weak neutralization capacity and higher viral loads, which were typical of the Delta wave (Wave 4 of Figure 4D), created conditions that were conducive to CoV2[Delta] breakthrough infections. Our observation that CoV2[Delta] was more concentrated in saliva of asymptomatic individuals is consistent with work showing CoV2[Delta]-infected individuals were more likely to transmit virus before developing symptoms, compared to individuals infected with pre-Delta lineages[161].

The largest COVID-19 wave our university community experienced was caused by the Omicron lineage. The Omicron lineage spread rapidly after its first detection in southern Africa in November 2021[68]; the >30 amino acid substitutions in Spike enabled Omicron

to bind ACE2 with higher affinity, as well as escape the anti-Spike antibody response elicited by either natural infection or vaccination with pre-Omicron lineages or vaccines[162–164]. The immunoevasive properties of Omicron are consistent with its causing a COVID-19 wave in our community after vaccine mandates had been established. The rapidity with which Omicron took over was observed in other university settings which, like ours, were highly vaccinated at the time[165]. Compared to infections caused by the Delta lineage, those by Omicron tend to cause less severe disease[166], which may be due in whole or part to its being enriched in upper airways (including the oral cavity) as opposed to the lower airways[110–114]. Omicron subvariants BA.1 and BA.2 were the last lineages detected in our university community before our testing program ended in May 2022. At that time, which corresponded to Wave 6, saliva C_T values were again trending lower than the prior wave that began ~6 months earlier (Figure 4D). We are reluctant to conclude this reflected waning immunity, however, for two reasons: (1) First and from a virological perspective, Wave 6 was due to an Omicron VOC and—relative to pre-Omicron VOCs, which had a lower airway tropism—Omicron VOCs had a greater tropism for the upper airways, including the oral cavity[110–114]; the lower C_T values may be a reflection of this upper airway tropism. (2) Second, from a molecular diagnostic perspective, there are preprint studies demonstrating the SalivaDirect PCR assay we used amplifies the Omicron variants with modestly higher efficiency than pre-Omicron VOCs[167,168]; the lower C_T values may be a reflection of this higher amplification efficiency. Since then SARS-CoV-2 has continued to evolve, there now being additional Omicron subvariants (BA.4, BA.5, BA.2.12.1, BA.2.75, XBB) and "Scrabble"

41

subvariants (BQ.1 and BQ1.1) with Spike protein sequences that further desensitize the virus to *in vitro* neutralization by many (but not all) monoclonal therapies[70,169–171], as well as convalescent plasma[72]. Since Omicron has a higher tropism for the nasopharyngeal and oral cavities than that of pre-Omicron lineages[110–114], saliva antibodies may be more important inhibitors of Omicron transmission than plasma or lower airway antibodies, and saliva—the collection of which is far easier than blood—may be more suitable for rapid determination of whether someone has neutralizing capacity against future SARS-CoV-2 VOCs that have yet to emerge.

The limitations of our study are as follows: (1) Since participants in our monitoring program provided saliva on a weekly basis, we cannot know the exact date on which someone was infected, rather only that they were infected 0–7 days prior to their scheduled test; (2) By only measuring SARS-CoV-2-specific Ig in individuals whose C_T values fell within a narrow range (thus normalizing for viral load), we cannot make any statements regarding the relationship between lower or higher C_T values and SARS-CoV-2-specific Ig levels; (3) Although we can correlate saliva samples' Spike inhibition capacity with their corresponding IgM^{Spike}, IgA^{Spike}, and IgG^{Spike} levels, we cannot definitively state which of these isotypes most contributed to inhibition, nor did we test saliva using a neutralizing assay, which is the gold standard for evaluating the effectiveness of antibodies against SARS-CoV-2 (this would need to occur in a BSL3 laboratory); (4) We did not measure SARS-CoV-2-specific Ig levels in individuals infected with $CoV2^{O\text{-}BA.1}$ or $CoV2^{O\text{-}BA.2}$, a reason being at that stage in the pandemic (i.e.

Waves 5–6 in our community) vaccine mandates were in place, and boosters were becoming available, making it difficult if not impossible to discern what levels of IgM^{Spike}, IgA^{Spike}, and IgG^{Spike} were due to vaccination versus boosters versus Omicron infection; (5) Finally, our study was not designed to take into account temporal biases due to changing policies and behaviors, such as the closing of dormitories, closing of classrooms and shift to remote learning, closing of indoor eating areas, on-campus social distancing requirements or masking requirements, nor can we account for the effect of prior infection with common cold coronaviruses that existed prior to the COVID-19 pandemic. It is beyond the scope and ability of our study to measure the extent to which each of these changes—either individually or synergistically—affected C_T value differences across time.

2.5 Summary

Our study identified relationships between specific SARS-CoV-2 variants of concern (VOCs) and SARS-CoV-2-specific immunoglobulin (Ig) among asymptomatic young adults in our university community. Asymptomatic young adults are important source of SARS-CoV-2 transmission in the United States of America and other countries. Major findings from our study which we believe inform our understanding of SARS-CoV-2 transmission and immunity, and may potentially influence COVID-19 monitoring policies at other universities include the following: (1) SARS-CoV-2 positivity occurred in waves which mirrored those in regions surrounding our university campuses, and were driven by newly emerged VOCs. (2) Only after university vaccine requirements went into

effect did net viral loads among all community members decline. (3) Breakthrough infections among vaccinees were not due to an absence of vaccine-elicited Ig, but rather diminished inhibitory capacity during a period when community viral loads peaked. In other words, vaccination efforts achieved their intended goal of increasing SARS-CoV-2-specific Ig; in individuals with breakthrough infections, however, the capacity of this Ig to inhibit Spike function was limited and corresponded to when community viral loads were at their highest.
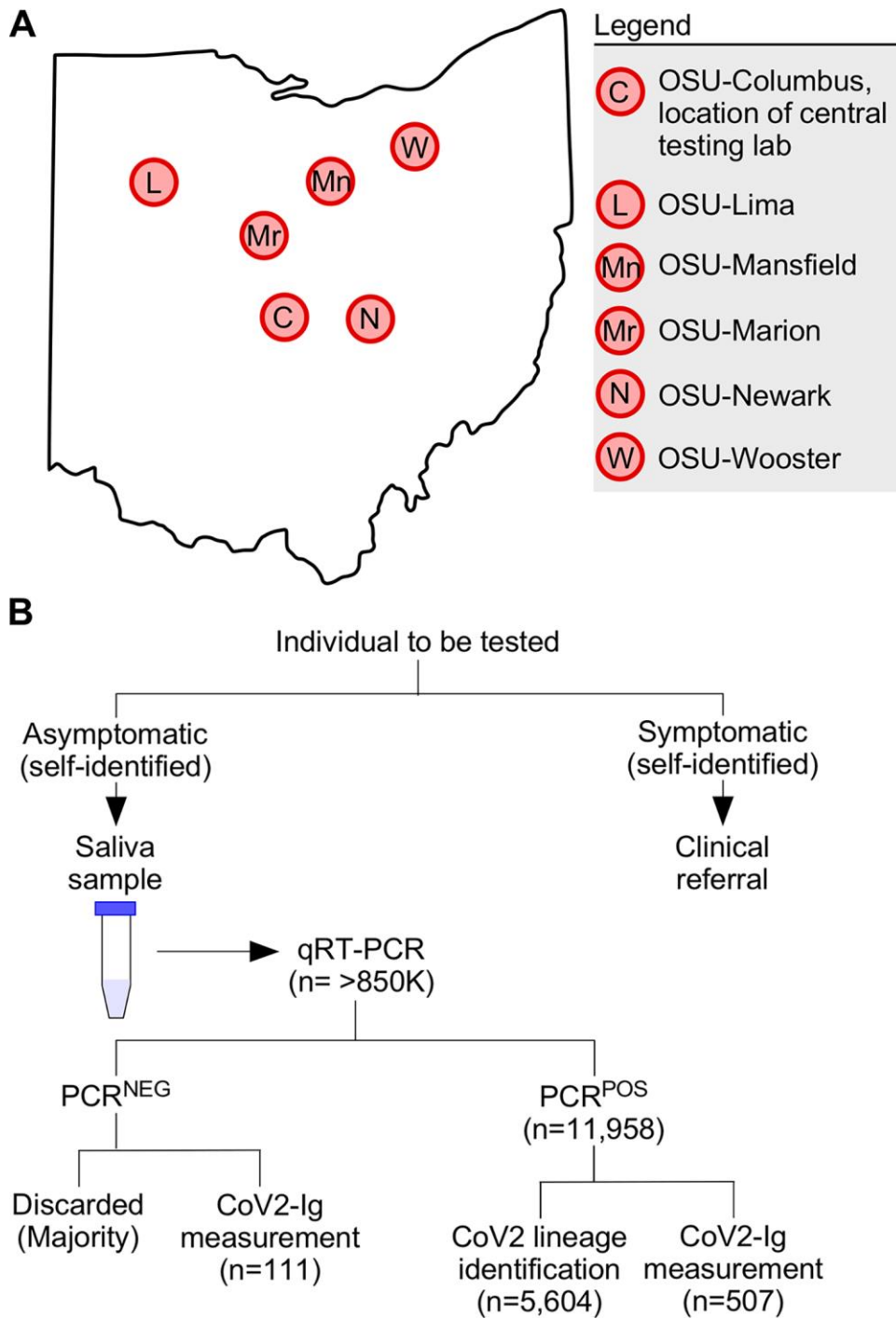
Figure 2: Overview of our university COVID monitoring program and workflow.
(**A**) Map of Ohio with locations of the six university campuses which participated in the
COVID-19 monitoring program. Original map source: Wikimedia Commons[172]. (**B**) On
and prior to the day of testing, each individual assessed themselves for one or more
COVID-19 symptoms. If symptomatic, the individual was given a clinical referral and

instructed to not go to their on-campus testing facility, to prevent contagion. If asymptomatic, the individual provided a saliva sample which was tested (typically within 24 hours of sample provision) via qRT-PCR for the presence of the SARS-CoV-2 N gene. Individuals were notified as soon as possible as to whether their sample was negative (PCR[NEG]) or positive (PCR[POS]) for the virus, a positive result being a $C_T \leq 40$. PCR[POS] samples were subsequently aliquoted and used for both SARS-CoV-2 lineage identification and measuring the concentrations of immunoglobulin against specific SARS-CoV-2 antigens (CoV2-Ig). The vast majority of PCR[NEG] samples were discarded; however, a minority were retained and used for CoV2-Ig measurements. PCR[POS] and PCR[NEG] samples were otherwise treated identically.
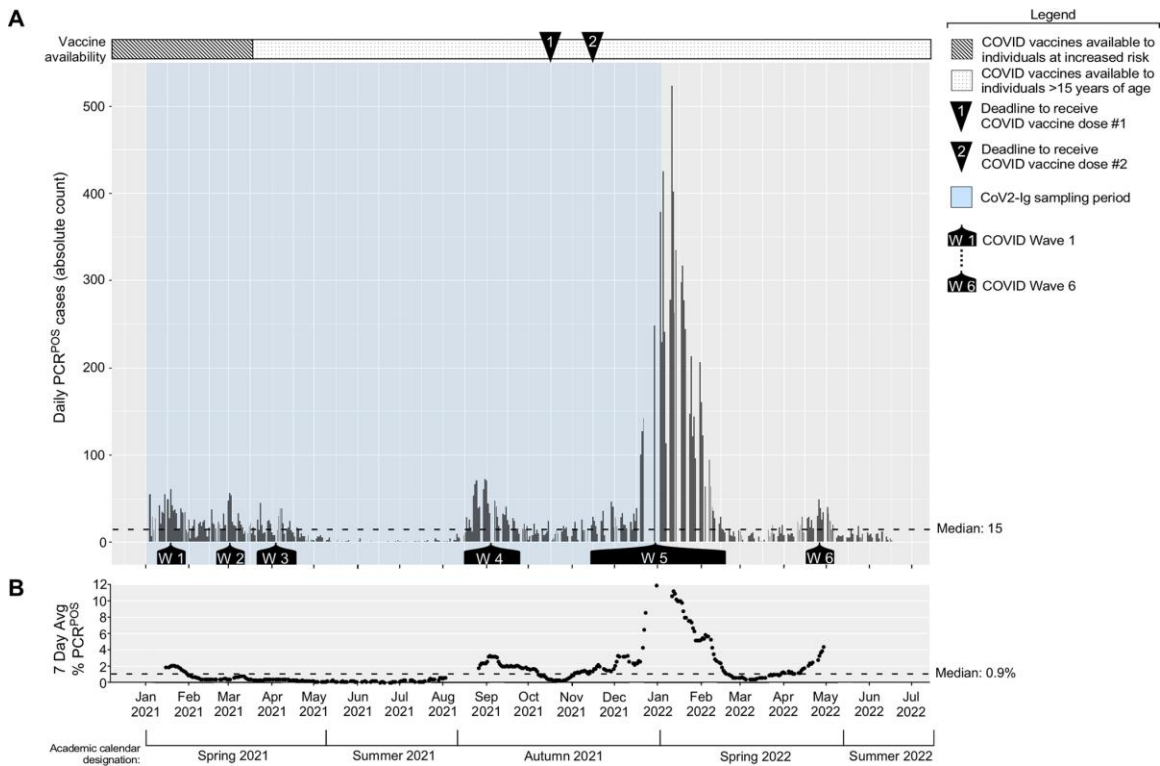

Figure 3: The incidence of PCR positivity among asymptomatic members of our university community. Saliva samples from asymptomatic individuals were collected on a daily basis and tested by qRT-PCR for the presence of the SARS-CoV-2 N gene. Shown are (**A**) the number of PCR[POS] saliva samples identified each day during the period spanning January 2021 to May 2022, with each bar representing a single day, as well as (**B**) the corresponding seven day average PCR positivity rate. Above the graph is a timeline depicting when COVID-19 vaccine availability shifted in Ohio (i.e. when the national vaccination priority expanded from vulnerable populations to encompass anyone >15 years of age), as well as indications of the deadlines by which all university community members were required to have received their first and second vaccine dose of either the BNT162b2 or mRNA-1273 vaccines. Below the graph are indications of the

periods we refer to as Waves 1–6, a wave being defined as when the daily PCR^{POS} case count exceeded the period median (15) for ≥3 weeks, as well Blue shading indicates when the samples we used for SARS-CoV-2 Ig measurements were collected.
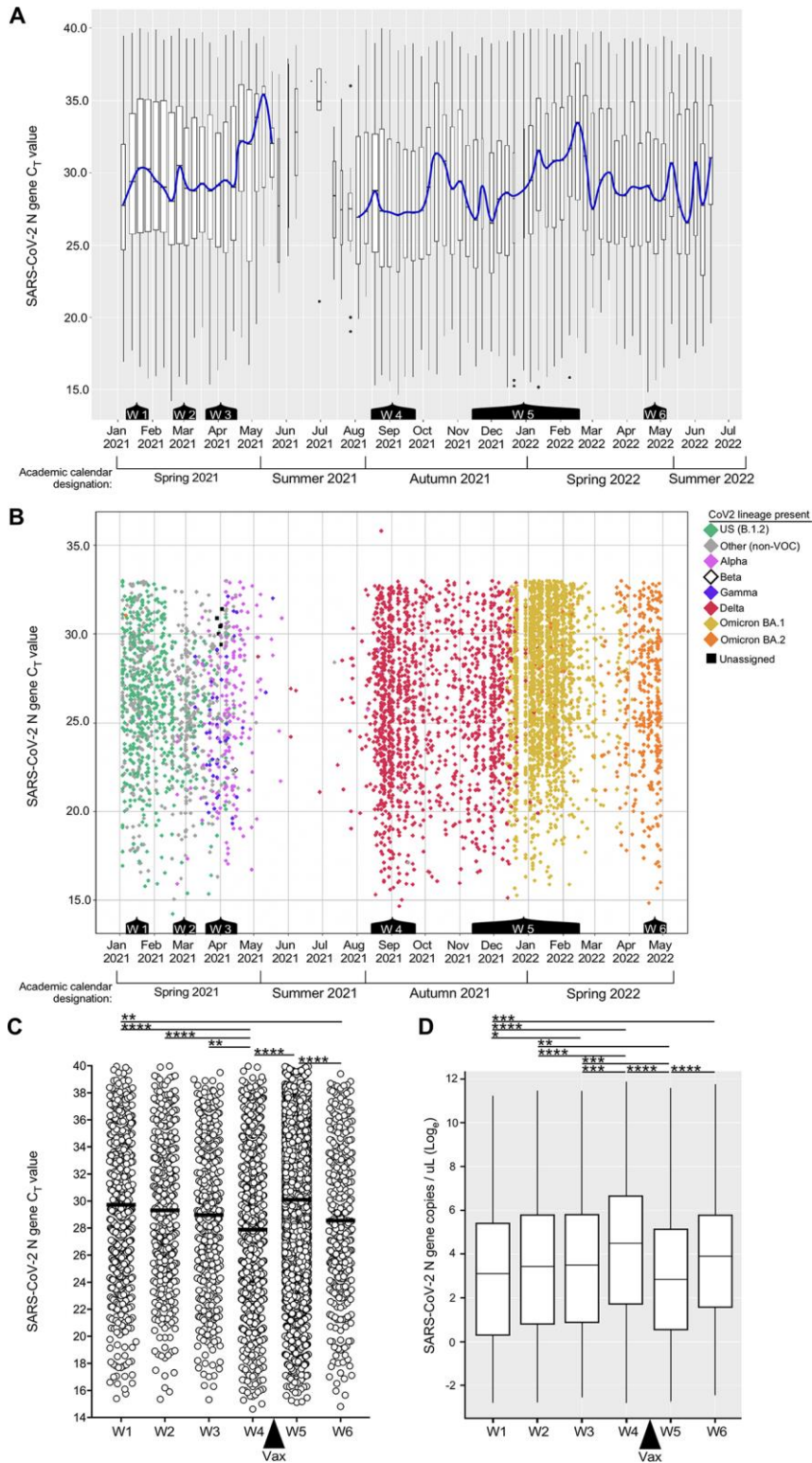
Figure 4: Saliva CoV2 viral loads among asymptomatic members of our university community. (**A**) Box plot representation of all the C_T values of all the PCR[POS] saliva samples during each week of the period spanning January 2021 to June 2022 (n = 11,958). The blue line passes through the median C_T value of each week. Below the graph are indications of the periods corresponding to Waves 1–6 of the prior figure. (**B**) Scatter plot representation of the same C_T value data as in (**A**) above, the exceptions being daily data are shown (as opposed to weekly composites) and samples with a $C_T > 33$ are omitted (with one exception in September 2021, these could not be sequenced due to insufficient amounts of genetic material). Each diamond represents an individual sample (n = 5604); the color of each diamond indicates the SARS-CoV-2 lineage present (Green, CoV2[US]; Pink, CoV2[Alpha]; White, CoV2[Beta]; Blue, CoV2[Gamma]; Red, CoV2[Delta]; Gold, CoV2[O-BA.1]; Orange, CoV2[O-BA.2]). Gray diamonds indicate samples whose lineage was not a VOC. Black squares indicate a sequence that did not align to known lineages and thus could not be assigned. Note that CoV2[Beta] only appeared once in our university community, on April 15 2021. (**C**) The C_T value and (**D**) calculated SARS-CoV-2 genome copy concentration in of each positive sample during Wave 1 (n = 638), Wave 2 (n = 442), Wave 3 (n = 453), Wave 4 (n = 1041), Wave 5 (n = 7129), and Wave 6 (n = 422). In (**C**), the mean of each Wave is indicated by a line. The "Vax" arrow indicates when community vaccine requirements went into effect (after Wave 4, before Wave 5). Asterisks indicate those inter-wave differences that were statistically significant, as determined by one way ANOVA (* $p \leq 0.05$, ** $p \leq 0.005$, *** $p \leq 0.0005$, *** $p \leq 0.00005$).

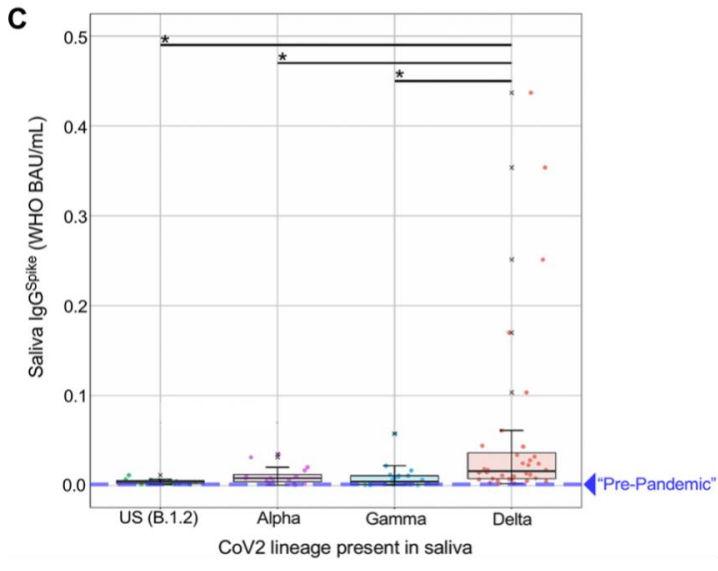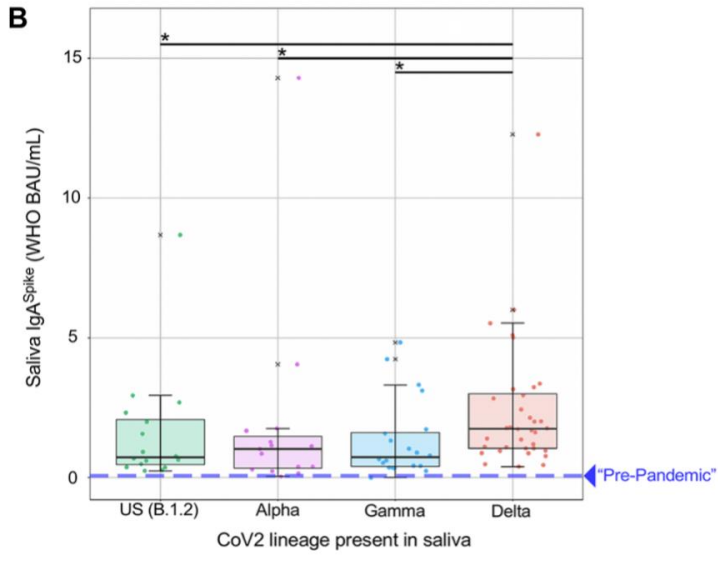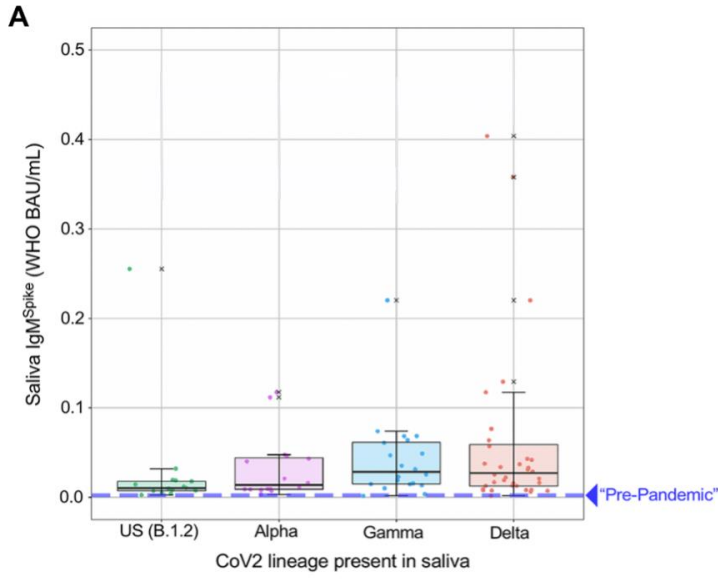**A**

Saliva IgM^{Spike} (WHO BAU/mL) vs CoV2 lineage present in saliva

B

Saliva IgA^{Spike} (WHO BAU/mL) vs CoV2 lineage present in saliva

C

Saliva IgG^{Spike} (WHO BAU/mL) vs CoV2 lineage present in saliva

Figure 5: Spike-specific Ig levels in the saliva of newly positive, asymptomatic individuals at the time of PCR testing. Saliva samples from individuals who were newly positive (New[POS], PCR positive for the first time ever) for either the CoV2[US] (n = 16), CoV2[Alpha] (n = 15), CoV2[Gamma] (n = 21), or CoV2[Delta] (n = 36) lineage were used to measure the concentrations of (**A**) IgM[Spike], (**B**) IgA[Spike] and (**C**) IgG[Spike]. The CoV2[Anc] Spike was used as the capture antigen in each case, and concentrations are expressed as World Health Organization (WHO) binding antibody units (BAU) per mL. PCR[NEG] saliva collected in early 2020, from healthy individuals living in the US with no COVID-19 history, was tested in the same manner used to estimate "pre-pandemic" levels of IgM[Spike], IgA[Spike] and IgG[Spike] binding, which are represented by the dashed lines on each graph. [X], values that were considered outliers but are nevertheless shown for completeness and are included in all statistical group comparisons. * $p \leq 0.05$, as determined by unpaired Wilcoxon tests with Benjamini-Hochberg adjustment. The dilution adjusted lower limit of quantification for each isotype were as follows (LLOQ values in WHO BAU/mL): IgM[Spike], 0.026691; IgA[Spike], 0.38378; IgG[Spike], 0.044149.
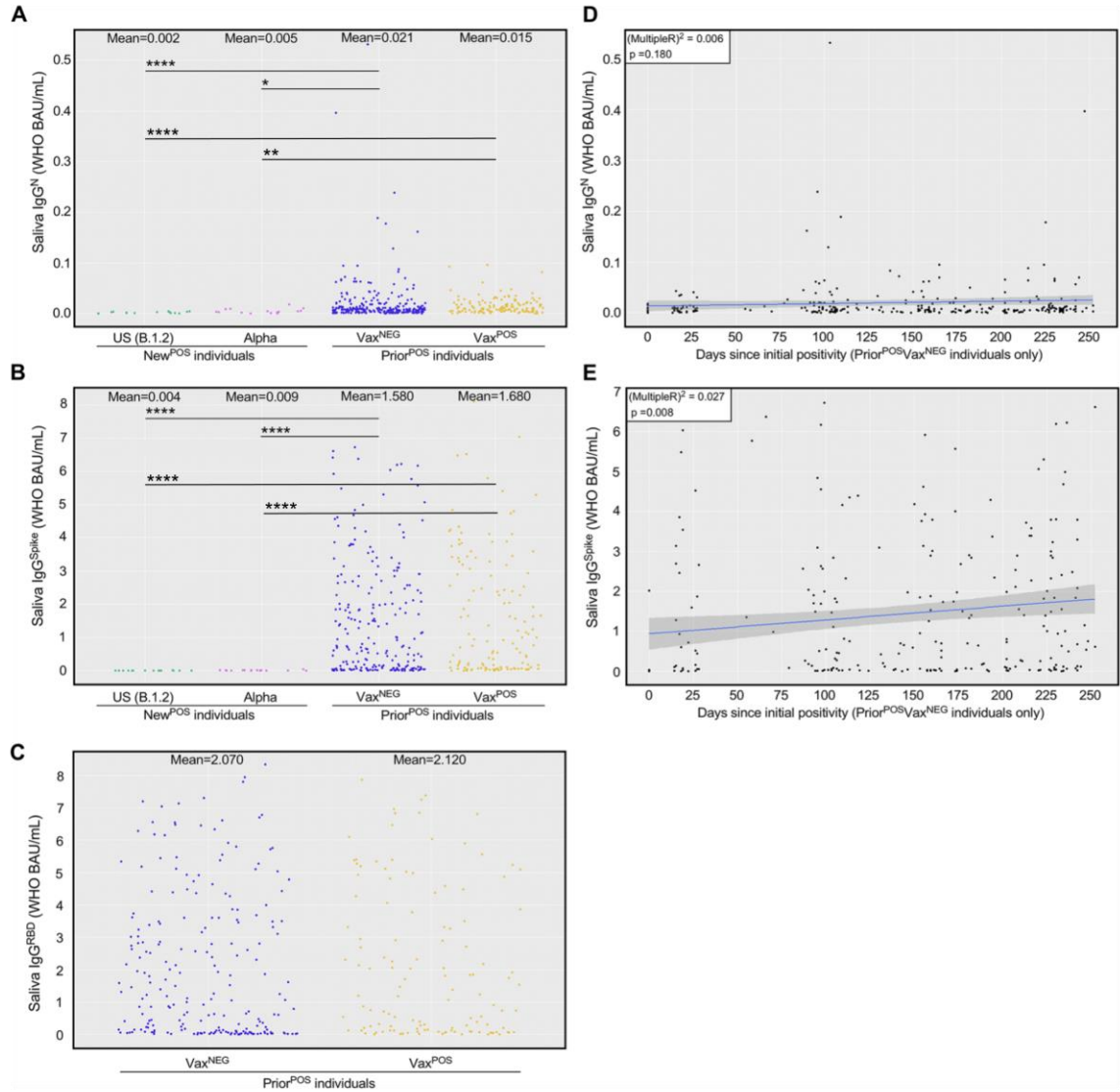
Figure 6: Nucleocapsid- and Spike-specific IgG levels in saliva of newly positive, asymptomatic individuals versus prior positive, asymptomatic individuals. Saliva from New[POS] individuals infected with either CoV2[US] (n = 16) or CoV2[Alpha] (n = 15), as well as PCR[NEG] saliva from individuals who had been infected 2–37 weeks prior (Prior[POS], n = 402) with either CoV2[US], CoV2[Alpha], or a non-VOC, were used to measure the concentrations of (**A**) Nucleocapsid-specific IgG, (**B**) Spike- specific IgG, and (**C**) Spike RBD-specific IgG. Data from Prior[POS] individuals are subdivided based on whether the individual remained unvaccinated up until the day of saliva collection (Vax[NEG], n = 257) or was vaccinated prior to the day of saliva collection (Vax[POS], n = 145). * p≤ 0.05, as determined by unpaired Wilcoxon test with Benjamini-Hochberg adjustment. (**D-E**) For those individuals who were Prior[POS]Vax[NEG], the relationship between time since original positivity (i.e. the number of days since the individual was first deemed PCR[POS]

52

by our program) and their current (**D**) saliva IgG^N level and (**E**) saliva IgG^{Spike} level at the time of sampling. Graph insets indicates the Multiple R-squared value associated with the linear regression model of the respective data set (i.e. the % variation in either saliva IgG^N or IgG^{Spike} that can be explained by the indicated time since positivity), as well as its p-value (i.e. the significance of the linear model as a whole).

Figure 7: Spike-specific Ig levels in saliva of CoV2^Delta-infected unvaccinated individuals, CoV2^Delta-infected vaccinees, and uninfected vaccinees. During and shortly after COVID-19 Wave 4 (i.e. that which was caused by CoV2^Delta), saliva from three groups of individuals were collected and used for Ig measurements: those who had not been fully vaccinated and were positive for the CoV2^Delta lineage (Vax^NEG PCR^POS, n = 36), those who had been fully vaccinated and were positive for the CoV2^Delta lineage

54

(Vax^{POS}PCR^{POS}, n = 17), and those who had been fully vaccinated and were negative for any SARS-CoV-2 lineage (Vax^{POS}PCR^{NEG}, n = 111). Shown are the (**A**) IgM^{Spike}, (**B**) IgA^{Spike}, and (**C**) IgG^{Spike} levels in each individual sample per group. ^{X}, values that were considered outliers but are nevertheless shown for completeness and are included in all statistical group comparisons. * p≤ 0.05, as determined by unpaired Wilcoxon tests with Benjamini-Hochberg adjustment. (**D-F**) For those individuals who were Vax^{POS}PCR^{NEG}, the relationship between time since being vaccinated (i.e. for those who received an mRNA-based vaccine, the number of days since their second dose) and their current (**D**) saliva IgM^{Spike}, (**E**) saliva IgA^{Spike}, and (**F**) saliva IgG^{Spike} level at time of sampling.

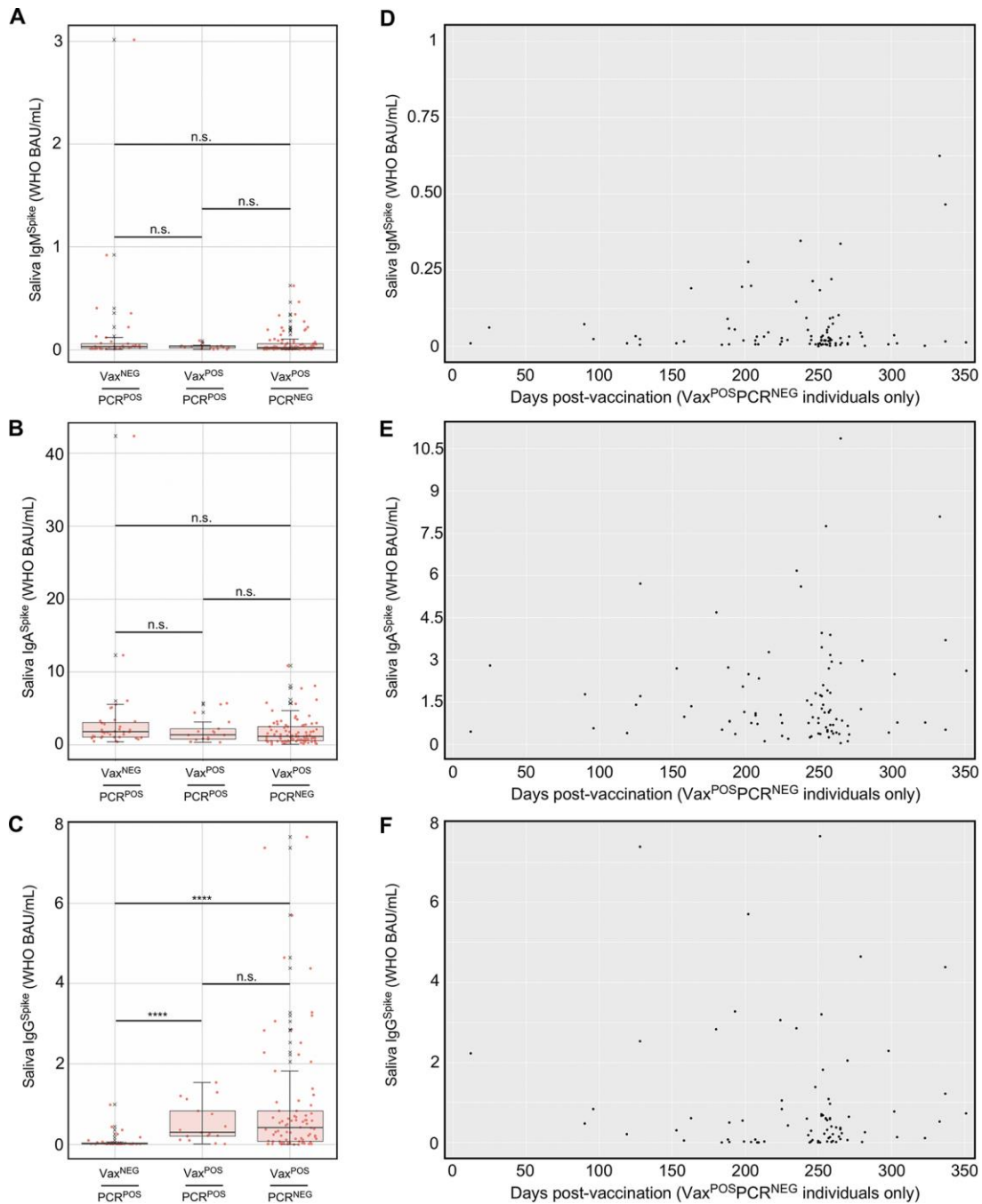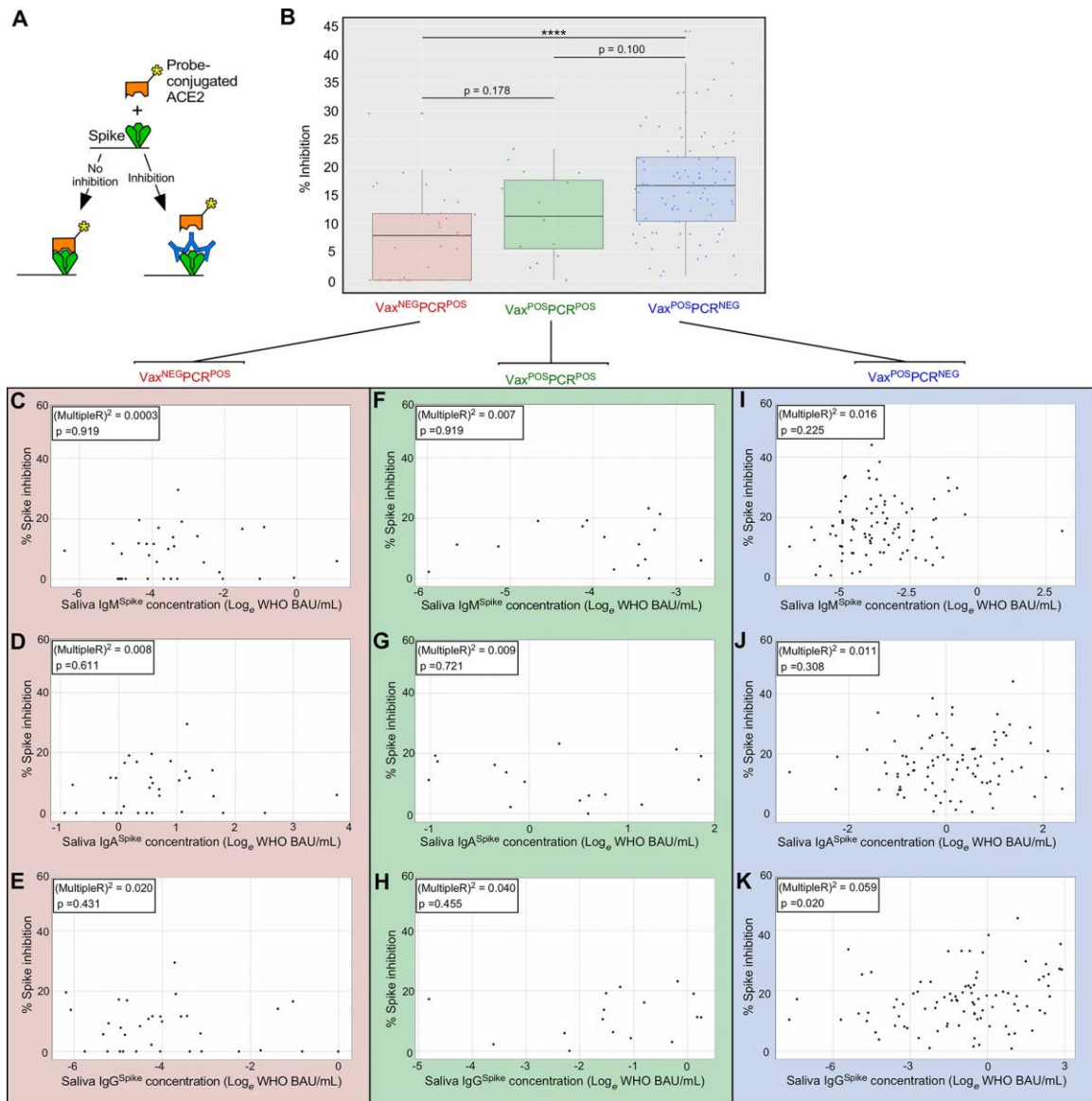**Figure 8: Inhibition of Spike function by saliva of CoV2^{Delta}-infected unvaccinated individuals, CoV2^{Delta}-infected vaccinees, and uninfected vaccinees. (A)** Depiction of the probe-conjugated ACE2 displacement assay used to measure saliva samples' ability to inhibit SARS-CoV-2 Spike binding to its human receptor, ACE2. The samples in this case were from VAX^{NEG}PCR^{POS} (n = 33), VAX^{POS}PCR^{POS} (n = 37), and VAX^{POS}PCR^{NEG} individuals (n = 91) (the same samples used for IgM^{Spike}, IgA^{Spike}, and IgG^{Spike} measurements in **Figure 7** above). **(B)** The percent inhibition value of each individual sample in each group. Within the **(C-E)** VAX^{NEG}PCR^{POS} group, **(F-H)** VAX^{POS}PCR^{POS} group, and **(I-K)** VAX^{POS}PCR^{NEG} group, the relationship between an individual samples' inhibition value and cognate **(C,F,H)** IgM^{Spike} concentration, **(D,G,I)** IgM^{Spike} concentration, and **(E,H,J)** IgG^{Spike} concentration. Graph insets indicates the Multiple R-

squared value associated with the linear regression model of the respective data set (i.e. the % variation in inhibition that can be explained by the indicated Ig concentration), as well as its p-value (i.e. the significance of the linear model as a whole).
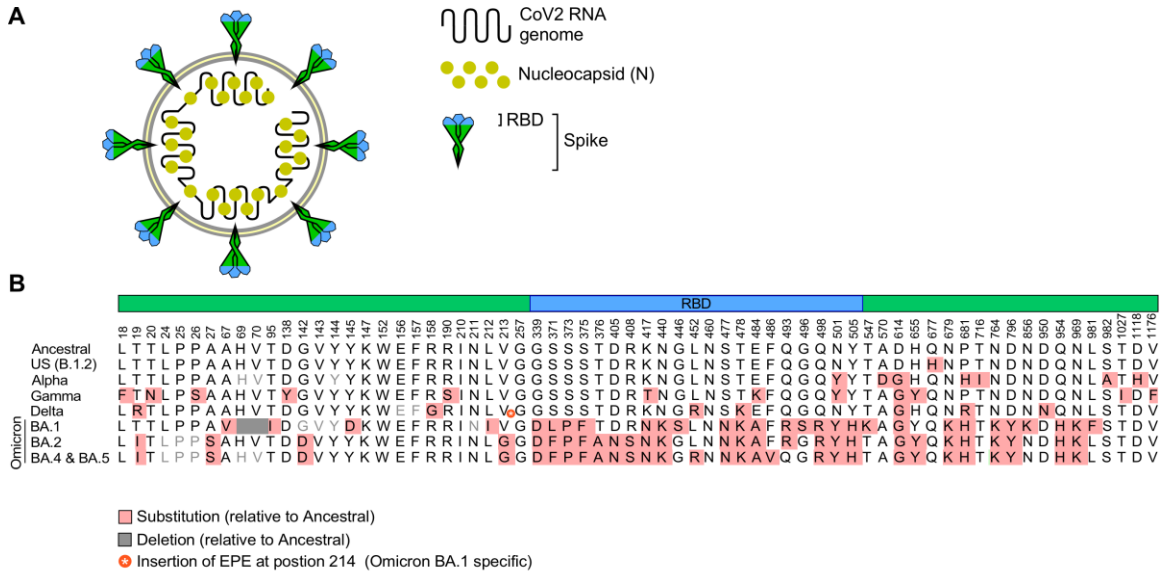
Figure 9: The CoV2 antigens and components relevant to our study. (**A**) Depiction of SARS-CoV-2 and its RNA genome, nucleocapsid (N, yellow) and Spike proteins, the latter being differentially colored to indicate the Receptor Binding Domain (RBD, blue) and non-RBD regions (green). (**B**) The amino acids which distinguish the CoV2[Anc] Spike protein from CoV2[US] (also known as B.1.2), CoV2[Alpha], CoV2[Gamma], and CoV2[Delta], as well as the Omicron lineages CoV2[O-BA.1], CoV2[O-BA.2], CoV2[O-BA.4], and CoV2[O-BA.5].
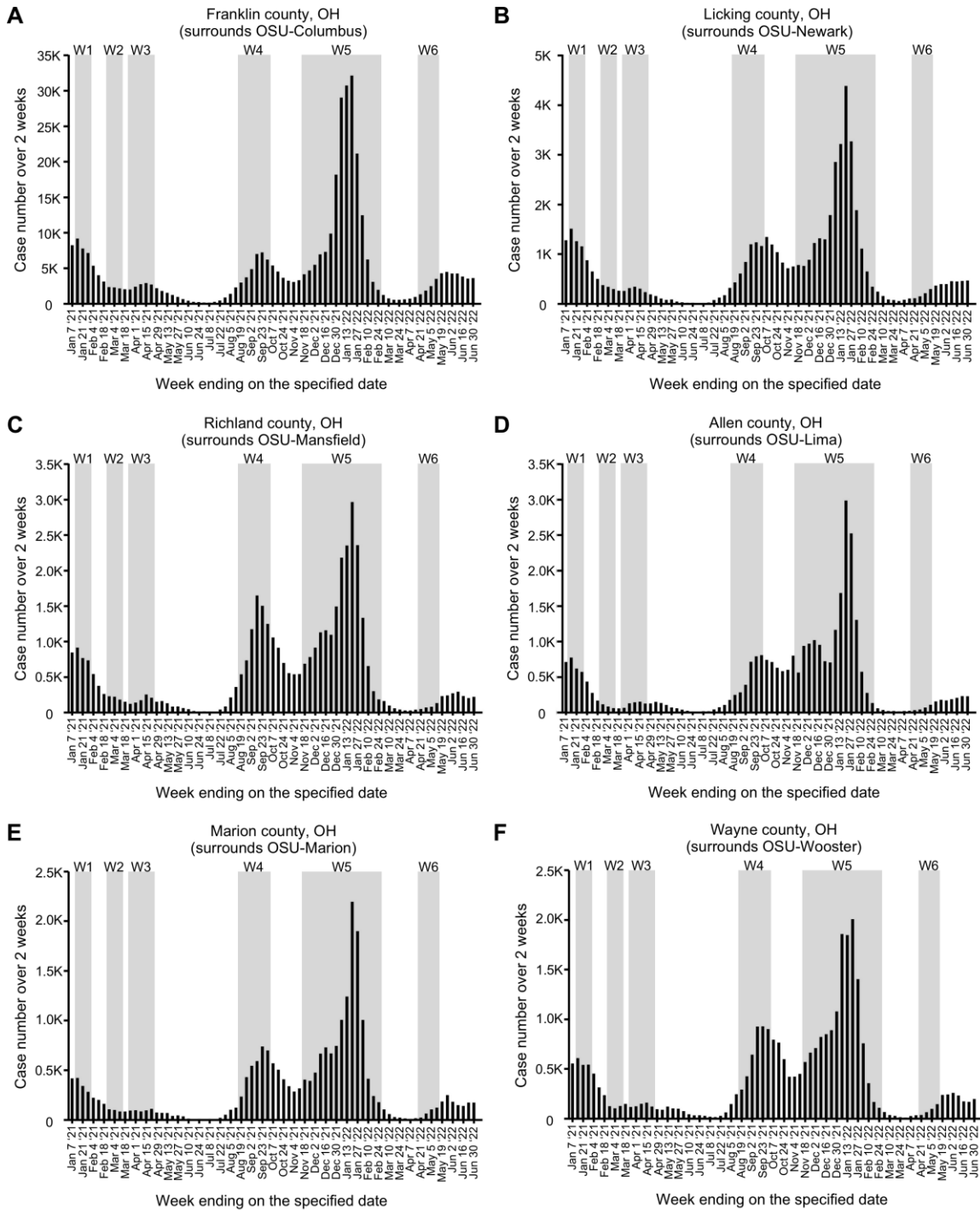
Figure 10: The waves of COVID incidence in the counties surrounding our university campuses. Daily COVID-19 cases in the counties surrounding each campus of our university, as reported by the Ohio Department of Health (ODH), for the period spanning January 2021 to May 2022. Shown are the data for (**A**) Franklin County, which

58

surrounds the OSU-Columbus campus; (**B**) Licking County, which surrounds the OSU-Newark campus; (**C**) Richland County, which surrounds the OSU-Mansfield campus; (**D**) Allen County, which surrounds the OSU-Lima campus; (**E**) Marion County, which surrounds the OSU-Marion campus; and (**F**) Wayne County, which surrounds the OSU-Wooster campus. Overlaid onto each graph are the dates which correspond to the six COVID-19 waves (W1-W6) that occurred in our campus community (see **Figure 3**).
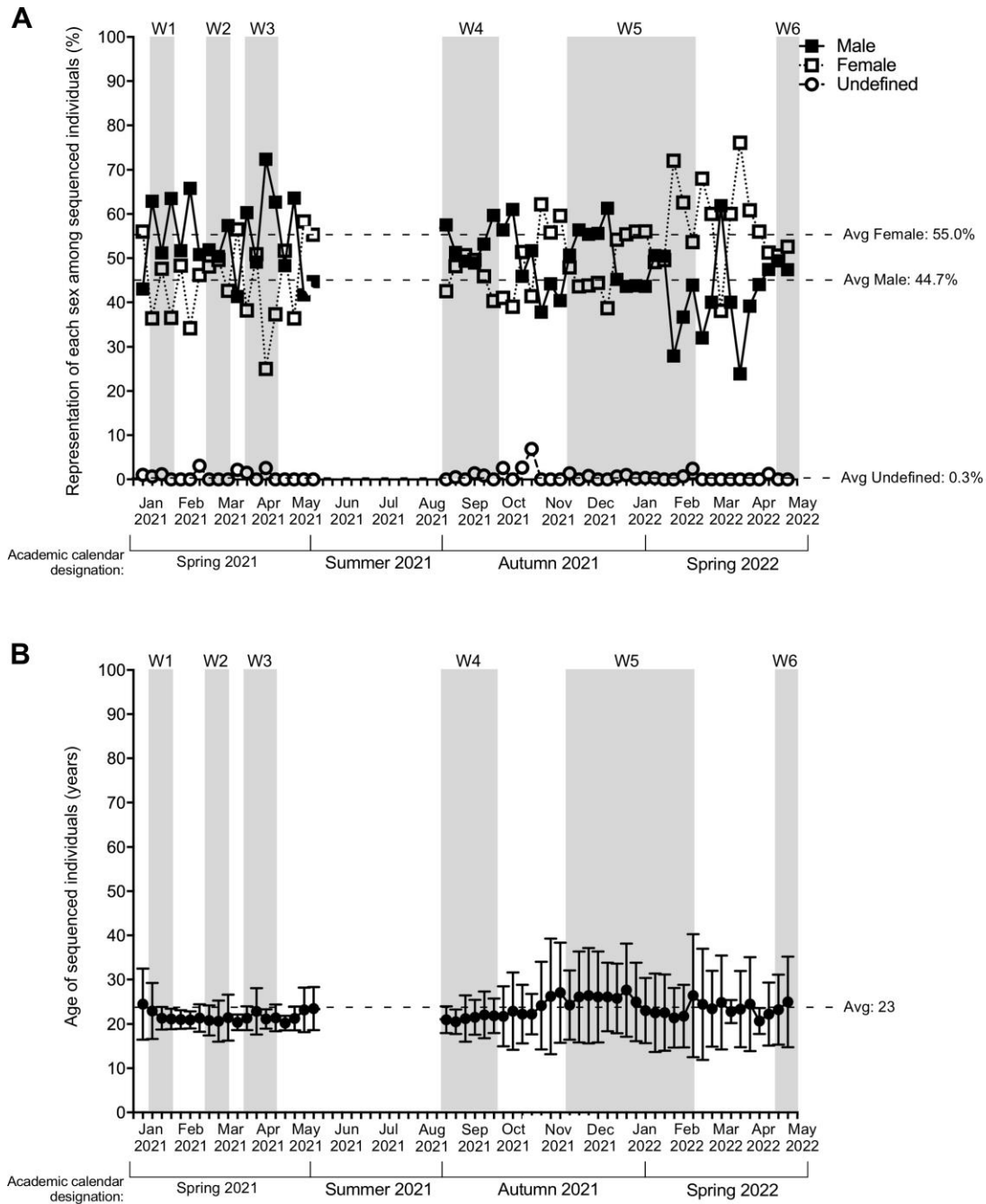
Figure 11: The representation of each sex and age of individuals whose PCR^{POS} saliva met sequencing criteria. (**A**) The percent of males, females and undefined sex among individuals whose saliva was PCR^{POS} and sequenced for lineage identification for each week of our study period, the criteria for sequencing being a $C_T \leq 33$. The average values for each sex across the entire study period are indicated by the hatched lines. (**B**) The age range of individuals whose saliva was PCR^{POS} and sequenced throughout the

monitoring period. Overlaid onto each graph in gray are the periods corresponding to Waves 1–6 in our university community along with the academic calendar beginning and end dates.

Figure 12: VOC Spike-specific Ig levels in the saliva of newly positive, asymptomatic individuals at the time of PCR testing. Saliva samples that were positive for either the CoV2^{US}, CoV2^{Alpha}, CoV2^{Gamma} or CoV2^{Delta} lineage were used to measure the concentrations of (**A**) IgM^{Spike}, (**B**) IgA^{Spike}, and (**C**) IgG^{Spike}. Varying by column were the coating antigens (Ag) used for each measurement, the Ag being recombinant forms of either the CoV^{Anc} Spike (Column 1), CoV2^{Alpha} Spike (Column 2), CoV2^{Beta} Spike (Column 3), and CoV2^{Gamma} Spike (Column 4). Antibody levels are expressed in arbitrary units of luminescence. Note that the CoV^{Anc} -specific IgM, IgA, and IgG values in (**A-C**) Column 1 were transformed into WHO Binding Antibody Units (BAUs) for **Figure 5**.
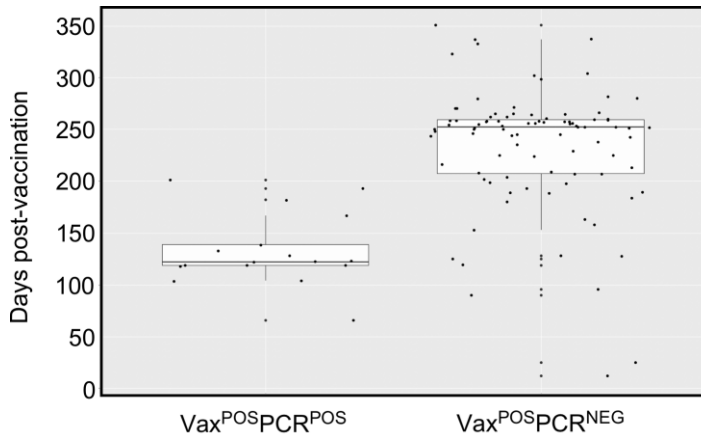
Figure 13: The time between vaccination to saliva sample collection for our Vax^{NEG}PCR^{POS} and Vax^{POS}PCR^{POS} cohorts. To generate the data shown in **Figure 7**, we analyzed saliva from individuals with a breakthrough Delta infection (Vax^{POS}PCR^{POS} individuals) and those who were vaccinated but PCR negative around the same time (Vax^{POS}PCR^{NEG} individuals). Shown for both groups are the time in days since receiving the final dose of their vaccine series, with each dot representing a single individual.

63

A

Coating antigen: CoV2^Anc Spike | CoV2^Alpha Spike | CoV2^Beta Spike | CoV2^Gamma Spike | CoV2^Delta Spike

Saliva IgM^Spike (Arbitrary Units)

Vax status: NEG POS POS
PCR status: POS NEG

B

Coating antigen: CoV2^Anc Spike | CoV2^Alpha Spike | CoV2^Beta Spike | CoV2^Gamma Spike | CoV2^Delta Spike

Saliva IgA^Spike (Arbitrary Units)

Vax status: NEG POS POS
PCR status: POS NEG

C

Coating antigen: CoV2^Anc Spike | CoV2^Alpha Spike | CoV2^Beta Spike | CoV2^Gamma Spike | CoV2^Delta Spike

Saliva IgG^Spike (Arbitrary Units)

Vax status: NEG POS POS
PCR status: POS NEG

Figure 14: VOC Spike-specific Ig levels in saliva of CoV2$^{\text{Delta}}$-infected unvaccinated individuals, CoV2$^{\text{Delta}}$-infected vaccinees, and uninfected vaccinees. During and after COVID-19 Wave 4 (i.e. that which was caused by CoV2$^{\text{Delta}}$), saliva from three groups of individuals were collected and used for Ig measurements: those who had not been fully vaccinated and were positive for CoV2$^{\text{Delta}}$ (Vax$^{\text{NEG}}$ PCR$^{\text{POS}}$), those who had been fully vaccinated and were positive for the CoV2$^{\text{Delta}}$ (Vax$^{\text{POS}}$ PCR$^{\text{POS}}$), and those who had been fully vaccinated and were negative for any SARS-CoV-2 lineage (Vax$^{\text{POS}}$ PCR$^{\text{NEG}}$). Shown for each individual in each group are the levels of (**A**) IgM$^{\text{Spike}}$, (**B**) IgA$^{\text{Spike}}$, and (**C**) IgG$^{\text{Spike}}$ which bind to four different coating antigens (Ag), the Ag being recombinant forms of either the CoV$^{\text{Anc}}$ Spike (Column 1), CoV2$^{\text{Alpha}}$ Spike (Column 2), CoV2$^{\text{Beta}}$ Spike (Column 3), CoV2$^{\text{Gamma}}$ Spike (Column 4), and CoV2$^{\text{Delta}}$ Spike (Column 5). Antibody levels are expressed in arbitrary units of luminescence. Note that for (**A**) six outliers are not shown, and that the CoV$^{\text{Anc}}$ -specific IgM, IgA, and IgG values in (**A-C**) Column 1 were transformed into WHO Binding Antibody Units (BAUs) for **Figure 7**.
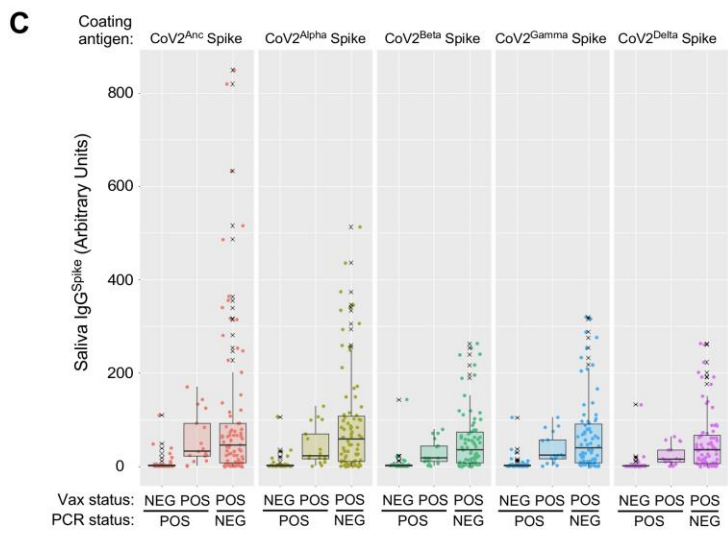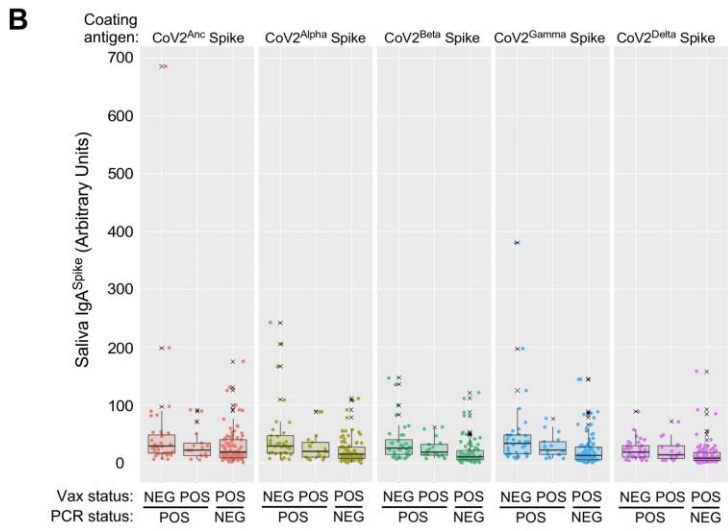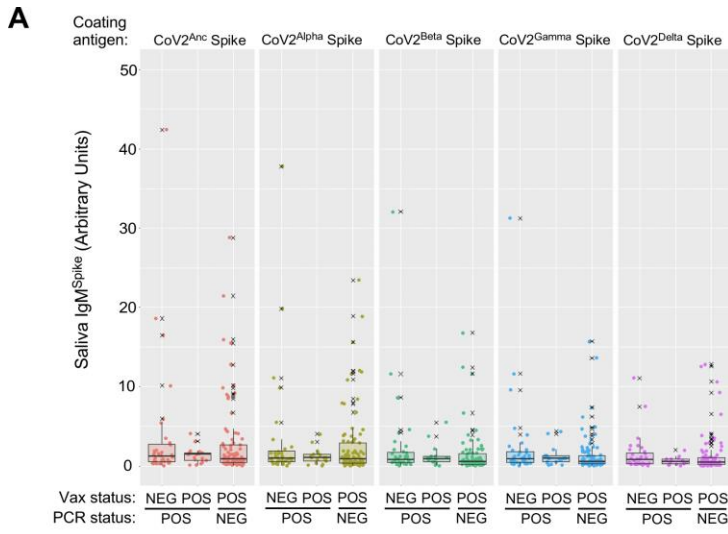
Chapter 3: Prior *Mycobacterium tuberculosis* infection primes the immune environment of the lung for subsequent viral infection

3.1 Introduction

Previous studies from both my lab and other institutions have shown that mice infected with Mtb and subsequently infected with SARS-CoV-2 had a less severe SARS-CoV-2 infection and lower viral loads than naïve mice[95–97]. However, some human studies suggest that coinfection with TB and SARS-CoV-2 is detrimental[89]. Yet, *Mycobacteria* spp express multiple proteins that are surprisingly homologous to SARS-CoV-2 antigens[173–175]. The previous Mtb and SARS-CoV-2 coinfection study from my lab showed an expansion of both T cells and B cells specific to the coinfected mice[95]. Thus, it was hypothesized that TB infected mice had cross-reactive antibodies and adaptive immune cells to SARS-CoV-2 proteins, which may explain why mice infected with Mtb had better outcomes and lower viral loads than naïve mice when subsequently infected with SARS-CoV-2. To test this, C57BL/6J mice were infected with Mtb and after forty days, challenged with human SARS-CoV-2 which does not replicate in C57BL/6J mice. In this manner, the murine immune response upon encountering SARS-CoV-2 antigens could be examined without confounding factors of having a true viral infection. By sacrificing the mice on days one, three, and seven after SARS-CoV-2 challenge, any ongoing immune responses from the TB infection could be measured early on and up to the point where the SARS-CoV-2 specific adaptive immune response would have begun.

The frequencies of activated T cells and antigen-experienced B cells in the spleen in response to SARS-CoV-2 antigens were subsequently measured to determine immune cell cross-reactivity. SARS-CoV-2-specific IgG in the lungs and serum was measured to determine if antibodies produced in response to Mtb are cross-reactive with SARS-CoV-2 proteins.

This study also measured cytokines that are involved in immune responses to Mtb or SARS-CoV-2. Interferon-gamma (IFNg) and tumor necrosis factor (TNF) have long been shown to be essential in controlling tuberculosis infection[79,80]. IL-1b, IL-6, and TNF are all inflammatory cytokines produced during the early innate immune response to both TB and SARS-CoV-2, and attract and activate other innate immune cells to the area of infection[176]. By examining cell types, antibodies, and cytokines, this study was able to gain insight into how an infection with Mtb may positively affect the immune response to a subsequent challenge with SARS-COV-2.

3.2 Methods

Mouse infection with Mtb and SARS-CoV-2 challenge

This work was reviewed and approved by the Ohio State Institutional Biosafety Committee (IBC) (ID #2018R00000051). This work was also reviewed and approved by the local Institutional Animal Care and Use Committee (IACUC) (ID # 2018A00000076-R1). Eight week old female C57BL/6J mice were purchased from Jackson Laboratories (RRID:IMSR_JAX:000664) and housed inside the Ohio State University's BSL-3

facility. There were 3 treatment groups in addition to the control group. The treatment groups included mice that were given a SARS-CoV-2 injection (i.p.), mice that were infected with Mtb but injected with media only, and mice that were infected with Mtb and given a SARS-CoV-2 injection. The control group was given an injection with Dulbecco's Modified Eagle Media (DMEM) media only. Selected mice were aerosol infected with virulent Mtb H37Rv via the Glas-Col inhalation system as described in our previous paper[177]. One day post-infection, whole lung tissue from five mice was homogenized in saline and plated on 7H11 agar media and colonies were counted after three weeks of incubation at 37°C. This verified the delivery of approximately 80 colony forming units per lung. Forty days post-infection with Mtb, selected mice were given an intraperitoneal injection of 100 uL of SARS-CoV-2 suspended in DMEM (isolate USA-WA1/2020, 25K plaque forming units), which does not replicate in mice. Mice were then sacrificed days 1, 3, and 7 post-SARS-CoV-2 challenge via carbon dioxide according to IACUC's protocols (Experiment Timeline shown in Figure 15). Days 1, 3, and 7 post-SARS-CoV-2 challenge, blood from the heart was collected for measurement of antibodies. The right upper lobe of the lungs was homogenized for RNA collection and later qPCR. The remaining lung tissue was homogenized for antibody measurements. Spleens were stimulated with SARS-CoV-2 peptides and used for flow cytometry. SARS-CoV-2 peptide libraries for the Spike, Nucleocapsid, Envelope, and Membrane proteins were obtained from BEI Resources.

Spleen Cell Stimulation and Flow cytometry

The spleens were homogenized, incubated with a red blood cell lysis, washed, and plated onto 96-well plates in media. Each well was stimulated with pooled peptides from a SARS-CoV-2 protein—Spike, Nucleocapsid, Envelope, and Membrane—with PMA and ionomycin as the positive control. The plates were incubated overnight at 37C. The plates were washed and incubated with the antibody cocktail before being fixed with 4% paraformaldehyde. The antibody cocktail consisted of the following: Live/Dead (eFluor 455UV), CD45 (clone 30-F11; PE), CD3 (clone 17A2; V450), CD4 (clone H129.19; BV750), CD8 (clone 53-8.7; NovaFluor Blue 510), CD69 (clone HI.2F3; BV711), CD62L (clone MEL-14; BV605), CD44 (clone IM7; PerCp-Cy55), B220/CD45R (clone RA3-6B2; eFluor 506), and IgD (clone 11-26c; APC-eFluor 780). With the exception of the Live/Dead stain, all antibodies were monoclonal and raised in rat. CD45 identifies immune cells, CD3 marks T cells, CD4 and CD8 identify the type of T cell, CD69 is an early activation marker, CD62L and CD44 are both T cell activation markers, B220/CD45R is a B cell marker, and IgD distinguishes naïve versus activated or memory B cells. The cells were run on a four laser Cytek Aurora flow cytometer either the same day (Day 3) or one week after fixing (Day 1 and Day 7). Samples that had a low number of events or had a pattern of events that were inconsistent with other samples beyond normal variation were excluded from data analysis. The flow gating strategy is shown in Figures 16–18.

Antibody Quantification

The collected blood was allowed to coagulate for a minimum of one hour, and then centrifuged so that sera could be collected from the supernatant and frozen. Each serum sample was filtered through a 0.2 um filter and treated with 1% Triton X 100 to remove or inactivate any Mtb or SARS-CoV-2, respectively. Lung tissue was homogenized in PBS and frozen. Lung homogenate was centrifuged at 10,000 RPM, then the supernatant was decontaminated utilizing the same methods as the sera stated above. Antibodies were quantified via a sandwich assay. The sera and lung homogenates were diluted by a factor of 10 and used in a Meso Scale Diagnostics V-Plex assay that utilized a 96-well plate coated with SARS-CoV-2 antigens—nucleocapsid, spike, and spike S1 receptor binding domain. Any antibodies specific to SARS-CoV-2 antigens would bind to the antigens coating the plate. Reporter antibodies that bind to mouse IgG bound to sample antibodies. The reporter antibody emitted a light signal which corresponded to the amount of antigen-binding IgG present in the sample. In contrast to the MSD assays used for human samples in Chapter 2, this assay did not use a standard curve so binding antibody values are reported as light signal in arbitrary units. Samples were run in duplicate, and the light signals from each sample were averaged to calculate the mean light signal. Antibodies were quantified for all samples from Day 3 and Day 7, as well as the uninfected group from Day 1.

Quantitative PCR

The upper right lung lobe was homogenized in a lysis buffer. RNA from samples collected on Day 7 were extracted from the upper right lung lobe using a Qiagen RNeasy

kit and converted to cDNA using Invitrogen Superscript IV First Strand Synthesis

System. Samples were measured on a nanodrop instrument to confirm similar amounts of

cDNA. The cDNA was then used for a qPCR assay. A qPCR assay was performed

utilizing Chmp2a, CD4, CD8a, IFNg, IL-1b, IL-6, and TNF primers with iTaq SYBR

green master mix on a Bio-Rad CFX384 instrument. The primer sequences are shown in

Table 1. CD4 and CD8a provide an estimation of the relative amounts of T cells present

within the lung that may contribute to production of cytokines. IFNg, IL-1b, IL-6, and

TNF are all inflammatory cytokines that are important for controlling TB and are

associated with COVID-19 severity. Data was normalized to Chmp2a—a chromatin-

modifying protein/charged multivesicular body protein—with relative expression within

samples calculated using the following equation:

Relative expression = 2^− (Ct of gene of interest – Ct of Chmp2a). In this manner, a gene

which is expressed the same amount as Chmp2a would have a relative expression value

of one.

IFNg Quantification

To measure amount of available IFNg, the lung homogenates from Day 3 (four mice

from each group) and Day 7 were used in a mouse IFNg enzyme-linked immunosorbent

assay (ELISA) kit from BioLegend (catalog number: 430804) following the

manufacturer's instructions. The results of the ELISA determined the amount of IFNg

present in the samples calculated from a standard curve.

Graphing and Statistics

Graphs were generated using FlowJo (version 10.10) and RStudio (version 3.6.3). Data and statistical analyses were performed in FlowJo, Microsoft Excel (2013), and RStudio. Data was tested for normality using the Kolmogorov-Smirnov test or visually using a QQ plot when there were very few data points. The data was then tested for equal variance using the Bartlett test of homogeneity of variances or Levene test. For data that did not have normal distribution, the Kruskal-Wallis rank sum test was used to determine if there were significant differences between groups in unpaired datasets, and the Friedman rank sum test was used in paired datasets. Within those datasets, the significant differences between groups were identified via an unpaired or paired Wilcoxon rank sum test as appropriate with Benjamini-Hochberg p value adjustment method. For data that had normal distribution, ANOVA was used to determine if there were significant differences between groups, followed by Tukey's HSD test to identify which groups had significant differences. Differences between groups were considered significant if $P < 0.05$ and are graphically indicated by 1 or more asterisks (*$P < 0.05$; **$P < 0.005$; ***$P < 0.0005$; ****$P < 0.00005$).

Abbreviations

The following abbreviations are used throughout this chapter: **Uninfected**, mouse group that was not infected with Mtb and received a media only injection; **CoV2 only**, mouse group that was not infected with Mtb and received an injection of human SARS-CoV-2; **TB only**, mouse group that was infected with Mtb and received a media only injection;

72

TB+CoV2, mouse group that was infected with Mtb and received an injection of human SARS-CoV-2; **Spike** and **N,** unless otherwise stated the Spike and Nucleocapsid proteins of SARS-CoV-2 (not any other coronavirus); **IgG$^{\text{Spike}}$**, IgG that recognizes Spike; **IgG$^{\text{RBD}}$**, IgG that recognizes the Spike Receptor Binding Domain; **IgG$^{\text{N}}$**, IgG that recognizes the Nucleocapsid protein.

3.3 Results

Flow Cytometry

Spleen cells suspended in media were stained with Trypan blue and counted using a hemocytometer. The total spleen counts are shown in Figure 19. For Day 1 and Day 3, both mouse groups that were infected with TB had significantly higher spleen cell counts than the uninfected and/or CoV2 only groups. On Day 7, the TB+CoV2 mouse group had significantly higher spleen cell counts than the uninfected and CoV2 only groups. This is expected of animals with an active Mtb infection.

The spleen cells were gated based on the scheme shown in Figures 16–18. The analysis focused on frequency of activated CD8 and CD4 T cells, as well as frequency of antigen-experienced B cells. T cells that were CD62L+CD44+ were labeled central memory T cells whereas CD62L−CD44+ T cells were labeled effector memory T cells. Antigen-experienced B cells were CD45+B220+IgD−. For Day 1, Day 3, and Day 7, stimulation with SARS-CoV-2 peptides showed no effect on the frequency of CD69+ T cells within the four mouse groups; only the positive controls were higher than the negative controls

and peptide stimulation groups. There was also no difference between the four groups in frequency of unstimulated CD69+ T cells, except in some cases one of the TB groups was higher than the CoV2 only group, albeit close to the cut-off of $p < 0.05$. For Day 1 and 3, there were no differences in frequencies of unstimulated effector or central CD4 T cells, effector or central CD8 T cells, or antigen-experienced B cells. For Day 7, the significant differences between frequencies of unstimulated cell types are shown in Figures 20 and 21. However, due to the low frequencies of central CD4 T cells which would more likely be found in lymphoid tissue, we are reluctant to draw any conclusions based on the data. Overall, there were not any obvious trends among the significantly different T cell populations. Notably, there were no differences in among antigen-experienced B cell populations when comparing stimulation by peptides or comparing between mouse groups (Figure 22).

Antibody Quantification

SARS-CoV-2 antigen binding antibodies were quantified in the sera and lung homogenate from Day 3 and Day 7 in all mouse groups, and from Day 1 in uninfected mice. The mean light signal in arbitrary units corresponded to amount of binding IgG in each sample. The mean light signals for each SARS-CoV-2 antigen of each mouse group is summarized in Tables 1 and 2, and as box plots in Figures 23 and 24. The mean light signals for the negative control wells which contained only the diluent were less than one thousand. The mean light signal for the uninfected group remained similar across the three time points for both sera and lung. There were no significant differences in antibody

74

levels between groups for any of the SARS-CoV-2 antigens in Day 3 sera. In Day 3 lung

homogenate, there was significantly more mouse IgG^{RBD} in the TB only group than the

uninfected group. For Day 7, there was significantly more IgG^{Spike} and IgG^{RBD} in the

CoV2 only and TB+CoV2 groups than the uninfected and TB only groups. This aligns

with expectations that mice which encounter SARS-CoV-2 via SARS-CoV-2 challenge

would develop antibodies against proteins from SARS-CoV-2. However, in Day 7 lung

homogenate, there was significantly more IgG^{N} in the TB+CoV2 group than the CoV2

only group, and significantly more IgG^{Spike} and IgG^{RBD} in the TB+CoV2 group than all

the other groups. These results demonstrate that the TB+CoV2 group generated more

SARS-CoV-2-binding IgG by Day 7 than the other groups but that it is only in the lung

that the TB+CoV2 group surpassed the CoV2 only group.

Quantitative PCR

The relative expression of the genes of interest are summarized in the boxplots in Figure

25. The groups of mice were compared to each other for each gene of interest, according

to the statistical methods outlined in 3.2. All results are from RNA collected on Day 7.

Both mouse groups infected with TB showed significantly higher expression of CD8a,

IFNg, IL-1b, and TNF than the uninfected and CoV2 only groups. For IL-1b, the TB only

group had significantly higher expression than the TB+CoV2 group. For CD4, the CoV2

only group had significantly higher expression than the uninfected group, however both

the uninfected and CoV2 only groups had significantly lower expression than the TB

only group. Although the TB+CoV2 group showed no significant differences to the other

groups, the p-values between the TB+CoV2 group and both the uninfected and CoV2 only groups were 0.0779. However, observing the boxplot in Figure 25, the presence of a single extreme outlier in the TB+CoV2 group explains the lack of statistical significance. There were no differences between groups in the amount of IL-6 expression, which was low.

IFNg Quantification

The boxplots in Figure 26 summarize the data from the IFNg ELISA performed on samples from Day 3 and Day 7. For Day 3, there were no significant differences in the amount of IFNg present in lung homogenate of the various mouse groups. There were also no significant differences in IFNg present in lung homogenate between the mouse groups for Day 7. This is in contrast to the qPCR data that showed that the mouse groups infected with TB had higher expression of IFNg in the lungs at Day 7. T cell exhaustion from chronic TB leading to a decline in cytokine production as well as protein degradation from freeze-thaw cycles or high dilution factor may have contributed to a lack of difference.

3.4 Discussion

TB has been a burden on humanity for millennia[178]. In 2020, humanity faced a global pandemic with the spread of SARS-CoV-2. Due to LTBI being widespread and SARS-CoV-2 remaining a major infectious agent, understanding the interaction of Mtb and SARS-CoV-2 is crucial in diagnosis and treatment. This study sought to examine how the

immune response to Mtb affects subsequent SARS-CoV-2 challenge. It was hypothesized that TB infected mice had cross-reactive antibodies and adaptive immune cells to SARS-CoV-2 proteins, which may explain why mice infected with Mtb had better outcomes and lower viral loads than naïve mice when subsequently infected with SARS-CoV-2. To test this, C57BL/6J mice were infected with Mtb and after forty days, challenged with human SARS-CoV-2 which does not replicate in C57BL/6J mice. In this manner, the murine immune response upon encountering SARS-CoV-2 antigens could be examined without confounding factors of having a true viral infection. By sacrificing the mice on days one, three, and seven after SARS-CoV-2 challenge, any ongoing immune responses from the TB infection could be measured early on and up to the point where the SARS-CoV-2 specific adaptive immune response would have begun. The higher spleen counts and increased inflammatory cytokines RNA from the lungs demonstrate that the TB groups had an ongoing chronic infection. However, the flow cytometry data showed that stimulation with SARS-CoV-2 peptides had no effect and that there was no consistent difference between mouse groups within the spleen, suggesting that there was no reaction to SARS-CoV-2 antigens in circulating immune cells. While there was no difference in the frequency of adaptive immune cells between mouse groups, it is possible that these cells had functional differences in cytokine production. It is also possible that due to TB being a respiratory infection, the majority of the activated immune cells would be located within the lung tissue.

Although there was no difference in the frequency of T and B cells in the spleen, it is possible that there was a difference in the lungs. The higher amounts of CD4 and CD8a RNA in the TB infected mice suggest that these mice had a higher number of T cells in the lung. Individuals with severe COVID-19 have been found to have decreased T cell counts[28,29,176], so perhaps an environment that is enriched with T cells decreases the severity of subsequent infection with SARS-CoV-2.

Next, we measured SARS-CoV-2 binding IgG. Because the mice infected with Mtb and the uninfected mice had no difference in amounts of SARS-CoV-2 binding IgG in serum or lungs, we concluded that mice with TB do not have cross-reactive antibodies to SARS-CoV-2 Nucleocapsid, Spike, or Spike S1 RBD. As expected, the mice groups that received SARS-CoV-2 antigens as an i.p. injection developed SARS-CoV-2 binding IgG in both serum and lungs. We were able to detect SARS-CoV-2 specific antibodies by Day 7 post-challenge in mice, which has not previously been well described. A point of interest among these results was that the TB+CoV2 group had significantly higher amounts of Spike-binding IgG than the CoV2 only group in the lungs by Day 7, but not in the serum. This suggests that the immune environment within mice infected with pulmonary TB accelerated the generation of new antibodies within the lungs only. An increase in SARS-CoV-2 specific antibody production within the lungs due to already having TB would be beneficial, as antibodies are a major way to combat SARS-CoV-2.

78

Severe COVID-19 cases are associated with high amounts of inflammatory cytokines, including IL-6 and IFNg[8]. Although inflammatory cytokines are necessary to contain an Mtb infection, IFNg, TNF, IL-1b, and IL-6 are markers of disease severity in pulmonary TB[179]. The RNA data from Day 7 lung homogenate do support this, as the TB mouse groups had significantly more IFNg, TNF, and IL-1b expression than the uninfected and CoV2 only groups. Interestingly, there were low amounts of IL-6 expression across all mouse groups, so this lack of IL-6 at this point in Mtb infection may be beneficial in not contributing to a cytokine storm in SARS-CoV-2 infection, as IL-6 antagonists are used as therapeutics for severe COVID-19[180]. A more complete panel of cytokines may reveal other important players, such as interferon type 3 which has been shown to be protective in SARS-CoV-2 infection[8]. Interferon type 3's role in TB has not been well studied but it is upregulated during TB infection[181,182].

Immune dysfunctions are often due to imbalance. It is possible that an overabundance of inflammatory cytokines from active TB exacerbates a subsequent SARS-CoV-2 infection, where disease severity can be caused by inflammatory dysregulation. On the other hand, if an individual's immune system is capable of suppressing an Mtb infection as in latent TB, the slightly elevated levels of inflammatory cytokines would be beneficial to having a lung environment that is prepared to fight off infection and improve outcomes of subsequent SARS-CoV-2 infection. This conclusion is supported by the recent work of NIH/NIAID researchers Katrin Mayer-Barber and Alan Sher[98].

The limitations of this study include using C57BL/6J mice as a model of TB, so our findings may not translate to humans completely accurately. However, this study would also be impossible to perform using human subjects. Future studies may involve more human-relevant models of TB, such as rhesus macaques. Additionally, IFNg, which increases antigen-presenting on macrophages and thus indirectly activates B cells, could be blocked with anti-IFNg antibodies prior to subsequent challenge with SARS-CoV-2 after TB infection in mice. Another option is to test whether exogenous IFNg could accelerate SARS-CoV-2 antibody production without TB. Parsing out what aspects of an immune response to prior Mtb infection increased the antibody response to SARS-CoV-2 may help with therapies for SARS-CoV-2 or vaccine efficacy.

3.5 Summary

TB and SARS-CoV-2 are the top causes of death by an infectious agent, but studies report conflicting results for whether coinfection with these two pathogens is beneficial or detrimental. This study examined the effects a prior tuberculosis infection had upon subsequently encountering SARS-CoV-2 antigens. Mice were infected with Mtb via aerosol and after forty days, given an i.p. injection of human SARS-CoV-2 antigens. The major findings of this study are as follows: (1) TB antibodies and spleen immune cells are not cross-reactive to SARS-CoV-2, and (2) TB accelerates the production of SARS-CoV-2 specific IgG within the lungs, with no change detected in T cell associated RNA transcripts. In summary, prior TB infection primes the lung immune environment for subsequent viral infection.
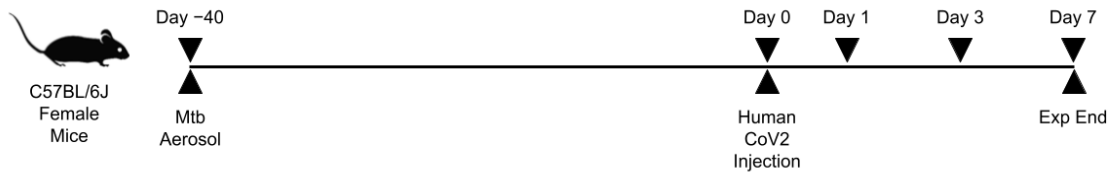
Figure 15: Experiment Timeline. The timeline of experiment showing aerosol Mtb infection and subsequent SARS-CoV-2 challenge via i.p. injection.
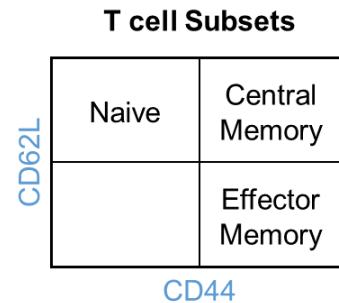
Figure 16: Flow Cytometry Gating Strategy Overview. (**A**) A text overview of the flow cytometry gating strategy, where blue text represents T cell lineages and red text represents B cell lineages. (**B**) An example of the gate used to differentiate between central and effector memory T cell subsets.

Figure 17: Representative Flow Cytometry Plots for T cell Lineages. Pseudocolor flow plots of an unstimulated sample demonstrating the gating strategy for T cell lineages and subsets. Arrows indicate the progression of gating. Analysis and flow plots performed in FlowJo.

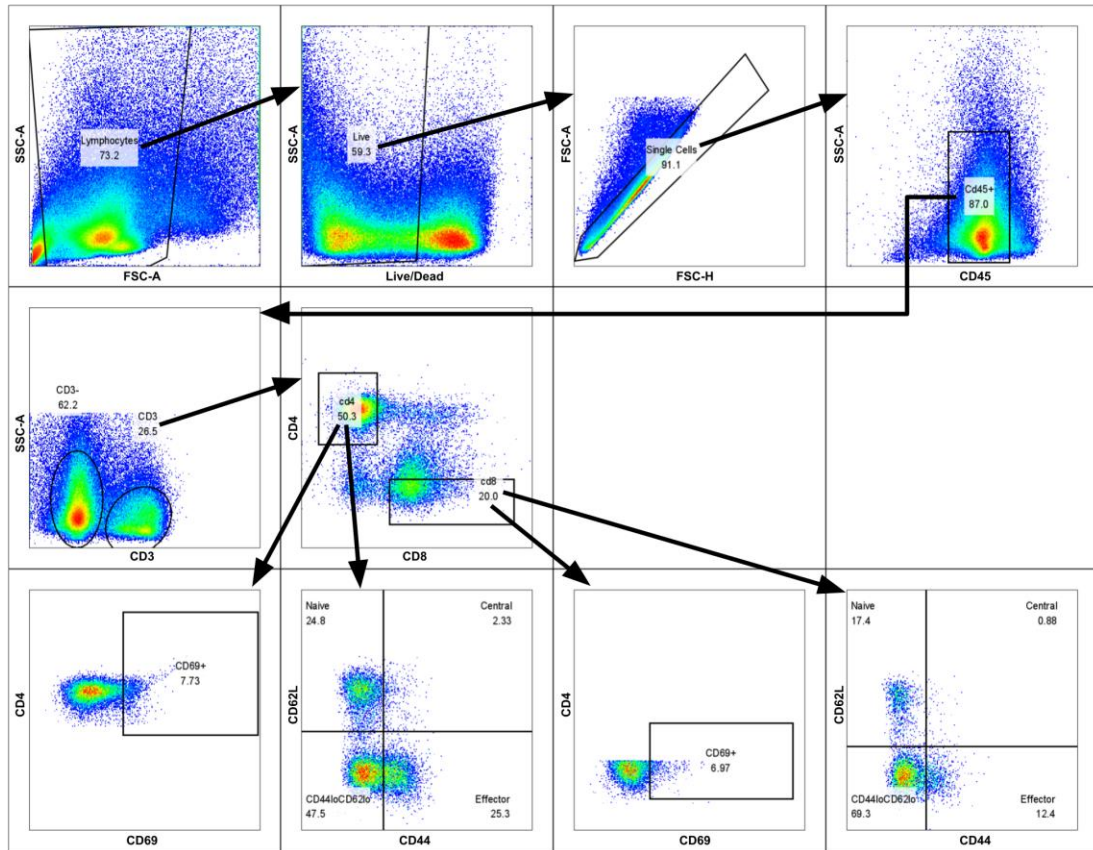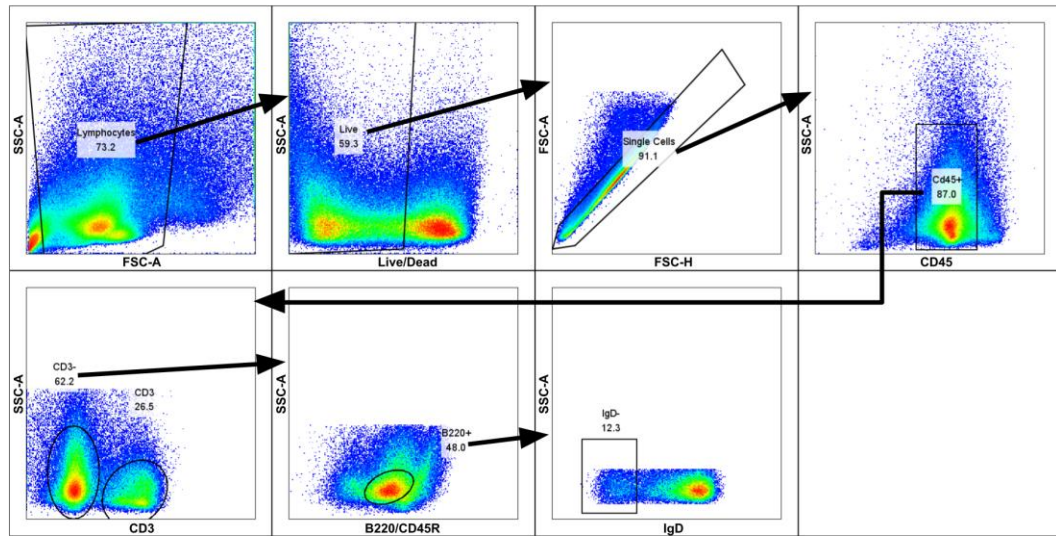**Figure 18: Representative Flow Cytometry Plots for B cell Lineages.** Pseudocolor flow plots of an unstimulated sample demonstrating the gating strategy for B cell lineages. Arrows indicate the progression of gating. Analysis and flow plots performed in FlowJo.

Chmp2a F	5'-AGACGCCAGAGGAACTACTTC-3'
Chmp2a R	5'-ACCAGGTCTTTTGCCATGATTC-3'
CD4 F	5'-GTTCAGGACAGCGACTTCTGGA-3'
CD4 R	5'-GTTCAGGACAGCGACTTCTGGA-3'
CD8a F	5'-ACTACCAAGCCAGTGCTGCGAA-3'
CD8a R	5'-ATAACAGGCGAAGTCCAATCCG-3'
IFNg F	5'-CAGCAACAGCAAGGCGAAAAAGG-3'
IFNg R	5'-TTTCCGCTTCCTGAGGCTGGAT-3'
IL-1b F	5'-CCTGAACTCAACTGTGAAATGC-3'
IL-1b R	5'-GTGCTGCTGTGAGATTTGAAG-3'
IL-6 F	5'-TAGTCCTTCCTACCCCAATTTCC-3'
IL-6 R	5'-TTGGTCCTTAGCCACTCCTTC-3'
TNF F	5'-GGTGCCTATGTCTCAGCCTCTT-3'
TNF R	5'-GCCATAGAACTGATGAGAGGGAG-3'

Table 1: Table of sequences of primers used in qPCR assays. The left column shows the gene names and the right column shows the DNA sequence of each primer in nucleic acid notation. F refers to Forward primer, R refers to Reverse primer.

A

Day 1 Spleen Cell Counts (in Millions)

B

Day 3 Spleen Cell Counts (in Millions)

C

Day 7 Spleen Cell Counts (in Millions)
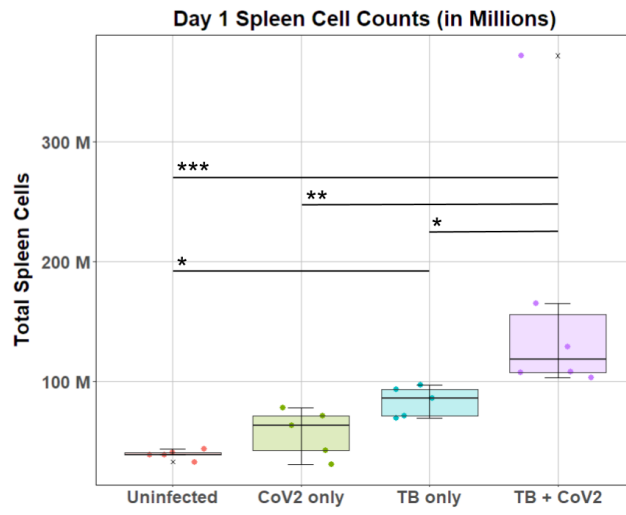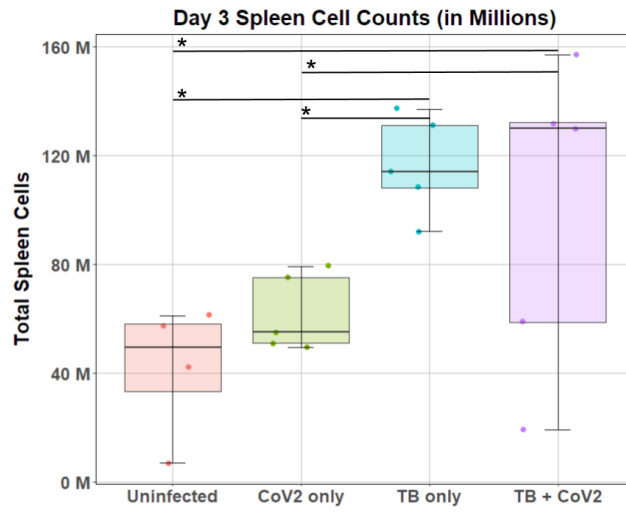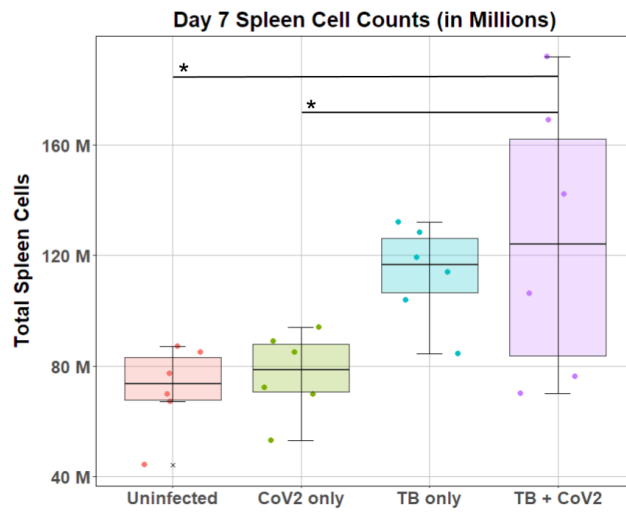
Figure 19: Spleen Cell Counts. Spleens from each mouse were homogenized and suspended in media. The total cells from the suspensions were counted using trypan blue. (**A**)–(**C**) show boxplots of total spleen cell counts in millions for each mouse group from Day 1 (**A**), Day 3 (**B**), and Day 7 (**C**), where each point represents one mouse spleen. Asterisks indicate intergroup differences as determined by Tukey's HSD test.

Figure 20: Frequency of CD4 T cell Subsets. Spleen cell suspensions were plated and stimulated overnight. The frequency of mouse spleen CD4 T cell subsets as determined

by flow cytometry is shown. Each point represents one sample. (**A**)–(**C**) show frequency of CD69+ CD4 T cells in samples stimulated with SARS-CoV-2 peptide libraries from Day 1 (**A**), Day 3 (**B**), and Day 7 (**C**) for each mouse group. The x-axis labels for (**A**)–(**C**) represent the following sample stimulation treatments: *neg*, unstimulated cells/negative control; *pos*, PMA and ionomycin/positive control; *spk*, Spike peptide library; *nuc*, Nucleocapsid peptide library; *env*, Envelope peptide library; and *mem*, Membrane peptide library. (**D**)–(**F**) show frequency of central and effector memory CD4 T cells in unstimulated samples from Day 1 (**D**), Day 3 (**E**), and Day 7 (**F**) for each mouse group.
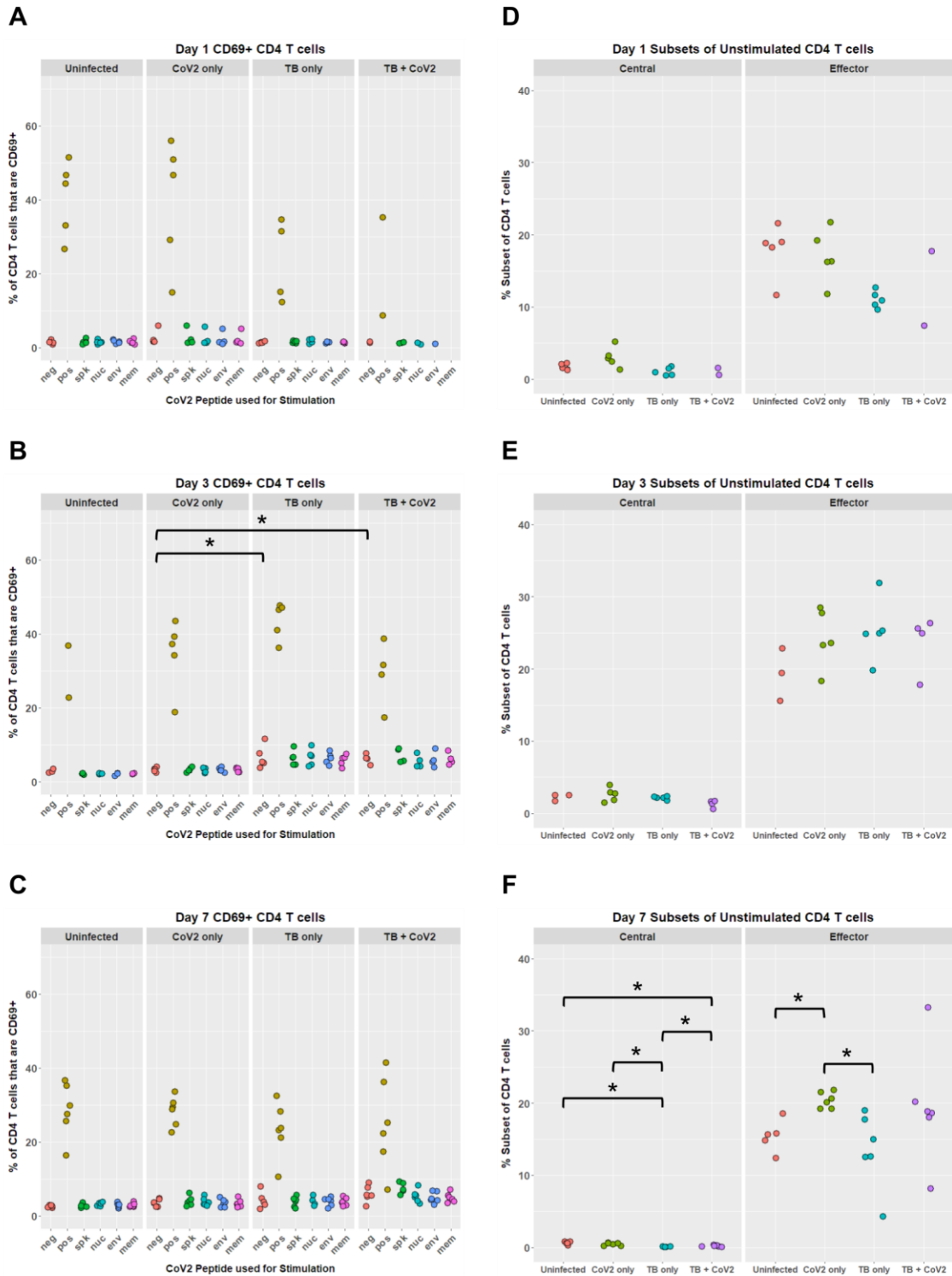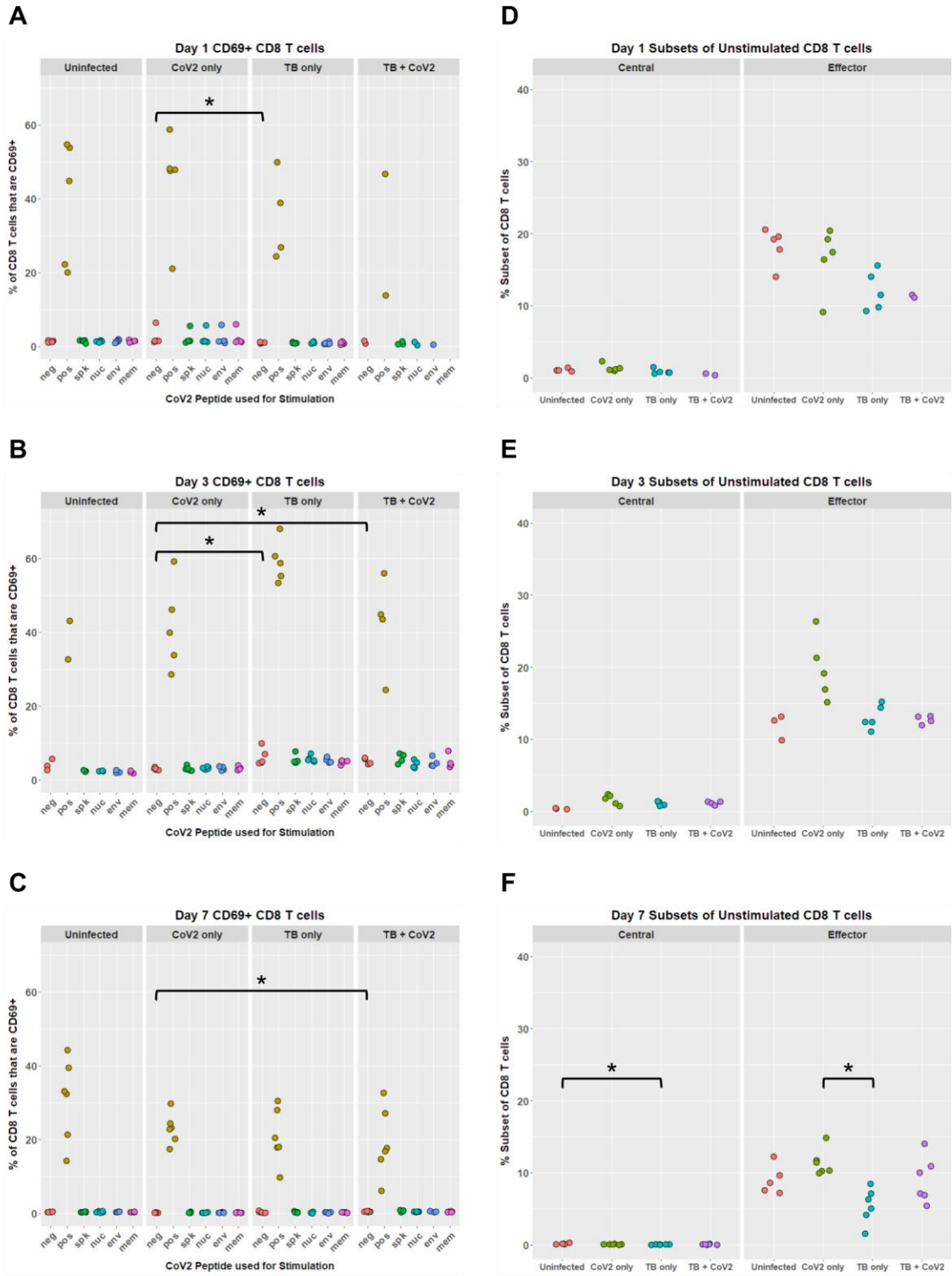
Figure 21: Frequency of CD8 T cell Subsets. Spleen cell suspensions were plated and stimulated overnight. The frequency of mouse spleen CD8 T cell subsets as determined

by flow cytometry is shown. Each point represents one sample. (**A**)–(**C**) show frequency of CD69+ CD8 T cells in samples stimulated with SARS-CoV-2 peptide libraries from Day 1 (**A**), Day 3 (**B**), and Day 7 (**C**) for each mouse group. The x-axis labels for (**A**)–(**C**) represent the following sample stimulation treatments: *neg*, unstimulated cells/negative control; *pos*, PMA and ionomycin/positive control; *spk*, Spike peptide library; *nuc*, Nucleocapsid peptide library; *env*, Envelope peptide library; and *mem*, Membrane peptide library. (**D**)–(**F**) show frequency of central and effector memory CD8 T cells in unstimulated samples from Day 1 (**D**), Day 3 (**E**), and Day 7 (**F**) for each mouse group.
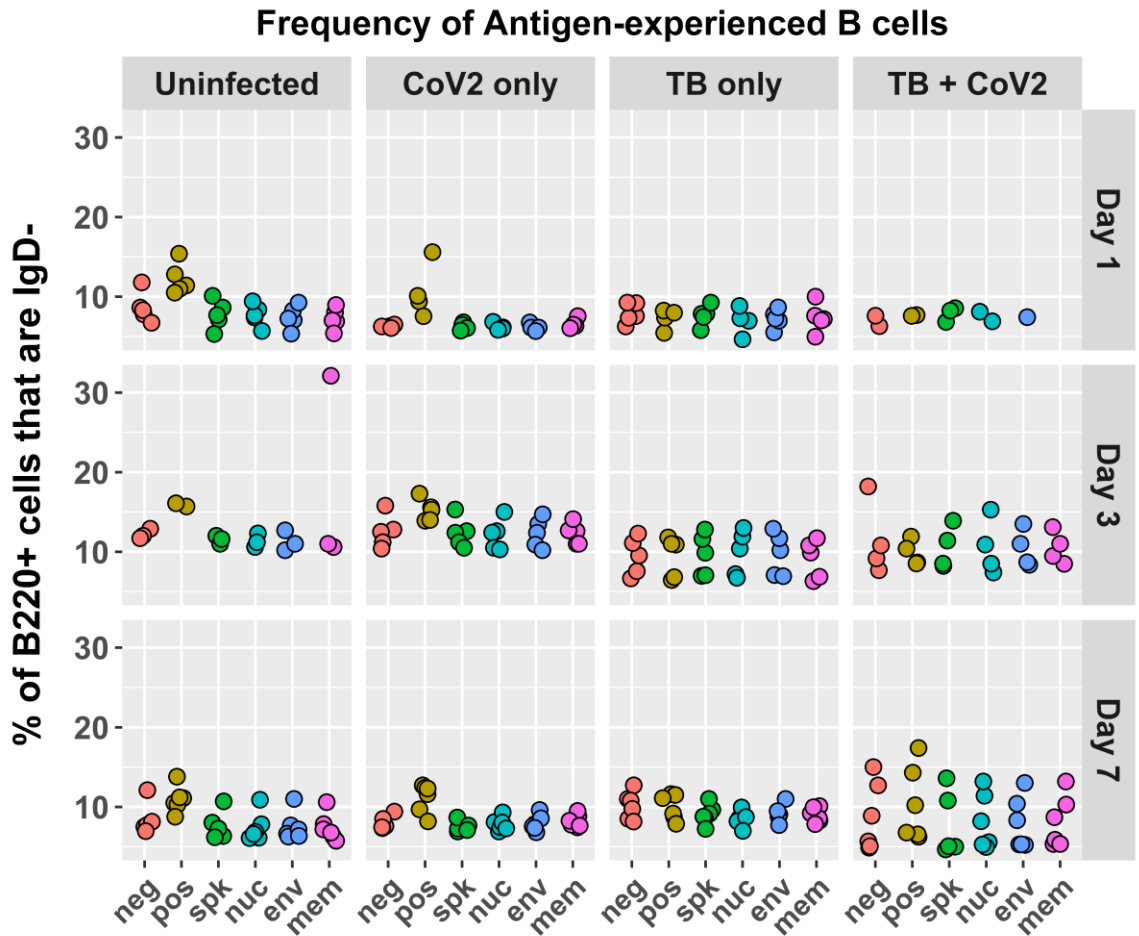
Figure 22: Frequency of Antigen-Experienced B cells. Spleen cell suspensions were plated and stimulated overnight. The frequency of mouse spleen antigen-experienced B cells as determined by flow cytometry is shown. Each point represents one sample. Each column represents the mouse group and each row represents the day post-SARS-CoV-2 challenge. The bottom x-axis labels represent the following sample stimulation treatments: *neg*, unstimulated cells/negative control; *pos*, PMA and ionomycin/positive

control; *spk*, Spike peptide library; *nuc*, Nucleocapsid peptide library; *env*, Envelope peptide library; and *mem*, Membrane peptide library.

Day	CoV2 Antigen	Mouse Group	Median Light Signal	Mean Light Signal	Minimum Value	Maximum Value
1	SARS-CoV-2 Nucleocapsid	Uninfected	9,513.00	9,709.83	4,914.00	14,348.00
1	SARS-CoV-2 Spike	Uninfected	4,585.00	4,514.00	2,228.00	7,218.00
1	SARS-CoV-2 Spike S1 RBD	Uninfected	4,247.50	4,738.00	2,467.00	8,433.00
3	SARS-CoV-2 Nucleocapsid	Uninfected	5,954.50	5,512.67	3,049.00	7,454.00
3	SARS-CoV-2 Nucleocapsid	CoV2 only	4,870.00	14,078.83	3,282.00	57,446.00
3	SARS-CoV-2 Nucleocapsid	TB only	14,740.00	14,498.67	9,081.00	21,575.00
3	SARS-CoV-2 Nucleocapsid	TB + CoV2	6,980.50	10,070.00	3,812.00	20,331.00
3	SARS-CoV-2 Spike	Uninfected	3,306.00	3,061.00	1,553.00	4,661.00
3	SARS-CoV-2 Spike	CoV2 only	2,343.00	5,925.00	1,664.00	23,157.00
3	SARS-CoV-2 Spike	TB only	5,365.50	5,716.00	3,480.00	9,117.00
3	SARS-CoV-2 Spike	TB + CoV2	3,157.00	4,781.33	1,282.00	12,356.00
3	SARS-CoV-2 Spike S1 RBD	Uninfected	2,611.00	2,443.67	1,231.00	3,629.00
3	SARS-CoV-2 Spike S1 RBD	CoV2 only	2,066.00	6,693.33	1,602.00	29,339.00
3	SARS-CoV-2 Spike S1 RBD	TB only	7,786.00	7,338.00	4,803.00	10,463.00
3	SARS-CoV-2 Spike S1 RBD	TB + CoV2	2,948.00	4,527.83	1,346.00	14,205.00
7	SARS-CoV-2 Nucleocapsid	Uninfected	9,667.00	9,939.83	5,782.00	14,968.00
7	SARS-CoV-2 Nucleocapsid	CoV2 only	6,527.50	6,906.83	5,295.00	9,438.00
7	SARS-CoV-2 Nucleocapsid	TB only	14,276.00	17,273.67	5,198.00	39,279.00
7	SARS-CoV-2 Nucleocapsid	TB + CoV2	22,087.50	20,890.00	12,642.00	26,111.00
7	SARS-CoV-2 Spike	Uninfected	4,779.50	4,441.50	2,969.00	5,076.00
7	SARS-CoV-2 Spike	CoV2 only	140,478.00	137,278.67	10,483.00	264,871.00
7	SARS-CoV-2 Spike	TB only	5,350.50	5,368.83	2,147.00	9,298.00
7	SARS-CoV-2 Spike	TB + CoV2	858,161.00	761,645.00	179,302.00	1,265,574.00
7	SARS-CoV-2 Spike S1 RBD	Uninfected	4,907.50	4,893.50	3,550.00	6,367.00
7	SARS-CoV-2 Spike S1 RBD	CoV2 only	29,059.50	34,146.33	4,764.00	89,376.00
7	SARS-CoV-2 Spike S1 RBD	TB only	8,215.00	9,027.00	2,733.00	17,615.00
7	SARS-CoV-2 Spike S1 RBD	TB + CoV2	360,236.00	354,817.00	60,625.00	782,521.00

Table 2: Lung SARS-CoV-2 Specific IgG Values. A table of summary statistics for SARS-CoV-2 specific IgG measured in mouse lung homogenate.

Day	CoV2 Antigen	Mouse Group	Median Light Signal	Mean Light Signal	Minimum Value	Maximum Value
1	SARS-CoV-2 Nucleocapsid	Uninfected	2,825.00	2,510.40	1,487.00	3,213.00
1	SARS-CoV-2 Spike	Uninfected	2,531.00	2,267.00	1,230.00	3,212.00
1	SARS-CoV-2 Spike S1 RBD	Uninfected	1,628.00	1,445.60	385.00	2,313.00
3	SARS-CoV-2 Nucleocapsid	Uninfected	9,469.00	27,140.33	3,434.00	110,128.00
3	SARS-CoV-2 Nucleocapsid	CoV2 only	8,278.50	8,316.00	3,098.00	14,665.00
3	SARS-CoV-2 Nucleocapsid	TB only	10,053.50	38,221.67	4,664.00	167,091.00
3	SARS-CoV-2 Nucleocapsid	TB + CoV2	5,271.50	39,651.00	2,700.00	210,407.00
3	SARS-CoV-2 Spike	Uninfected	4,032.50	8,694.00	1,626.00	26,878.00
3	SARS-CoV-2 Spike	CoV2 only	5,988.50	5,626.67	3,133.00	6,698.00
3	SARS-CoV-2 Spike	TB only	6,496.50	6,605.33	4,543.00	8,783.00
3	SARS-CoV-2 Spike	TB + CoV2	7,501.00	8,927.33	2,984.00	17,235.00
3	SARS-CoV-2 Spike S1 RBD	Uninfected	1,951.50	2,149.33	1,291.00	3,220.00
3	SARS-CoV-2 Spike S1 RBD	CoV2 only	4,380.00	4,329.50	2,988.00	5,101.00
3	SARS-CoV-2 Spike S1 RBD	TB only	3,058.50	3,241.67	1,882.00	4,889.00
3	SARS-CoV-2 Spike S1 RBD	TB + CoV2	3,477.50	4,311.33	2,438.00	9,050.00
7	SARS-CoV-2 Nucleocapsid	Uninfected	7,960.00	26,653.50	6,266.00	115,766.00
7	SARS-CoV-2 Nucleocapsid	CoV2 only	4,823.50	41,749.00	4,176.00	226,118.00
7	SARS-CoV-2 Nucleocapsid	TB only	7,992.50	22,597.00	3,026.00	63,189.00
7	SARS-CoV-2 Nucleocapsid	TB + CoV2	10,087.00	28,624.17	2,464.00	113,863.00
7	SARS-CoV-2 Spike	Uninfected	7,591.50	6,581.33	3,194.00	8,281.00
7	SARS-CoV-2 Spike	CoV2 only	1,638,849.00	1,409,992.17	217,432.00	1,881,658.00
7	SARS-CoV-2 Spike	TB only	2,869.00	3,729.33	1,805.00	8,601.00
7	SARS-CoV-2 Spike	TB + CoV2	1,801,289.00	1,447,307.67	594,273.00	1,965,432.00
7	SARS-CoV-2 Spike S1 RBD	Uninfected	2,780.50	2,989.83	2,492.00	4,024.00
7	SARS-CoV-2 Spike S1 RBD	CoV2 only	597,063.00	773,179.00	263,585.00	1,345,559.00
7	SARS-CoV-2 Spike S1 RBD	TB only	2,415.00	2,442.67	1,645.00	3,213.00
7	SARS-CoV-2 Spike S1 RBD	TB + CoV2	948,511.00	986,808.67	217,077.00	1,848,010.00

Table 3: Serum SARS-CoV-2 Specific IgG Values. A table of summary statistics for SARS-CoV-2 specific IgG measured in mouse serum.

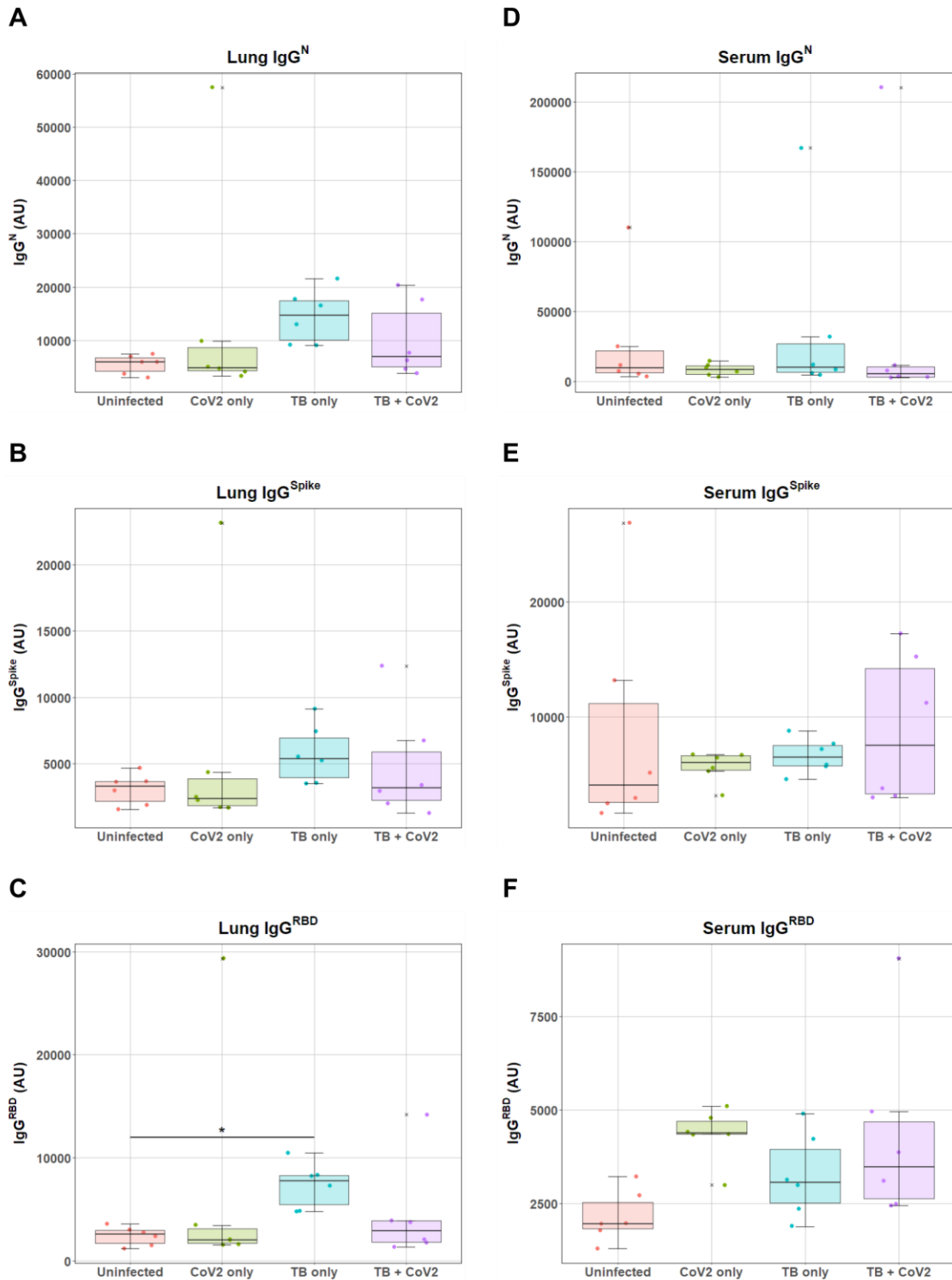**Figure 23: CoV2 Specific IgG from Day 3.** SARS-CoV-2 specific IgG was measured in lung homogenate (**A**)–(**C**) and serum (**D**)–(**F**) diluted at 1:10. Each point represents one sample run in duplicate. There were a total of six samples per mouse group from Day 3.

IgG^N (**A**) and (**D**), IgG^{Spike} (**B**) and (**E**), and IgG^{RBD} (**C**) and (**F**) are presented in arbitrary units. Asterisks indicate intergroup differences as determined by Wilcoxon test with Benjamini-Hochberg adjustment or Tukey's HSD test.

Figure 24: CoV2 Specific IgG from Day 7. SARS-CoV-2 specific IgG was measured in lung homogenate (**A**)–(**C**) and serum (**D**)–(**F**) diluted at 1:10. Each point represents one sample run in duplicate. There were a total of six samples per mouse group from Day 7.

IgG^N (**A**) and (**D**), IgG^{Spike} (**B**) and (**E**), and IgG^{RBD} (**C**) and (**F**) are presented in arbitrary units. Asterisks indicate intergroup differences as determined by Wilcoxon test with Benjamini-Hochberg adjustment or Tukey's HSD test.
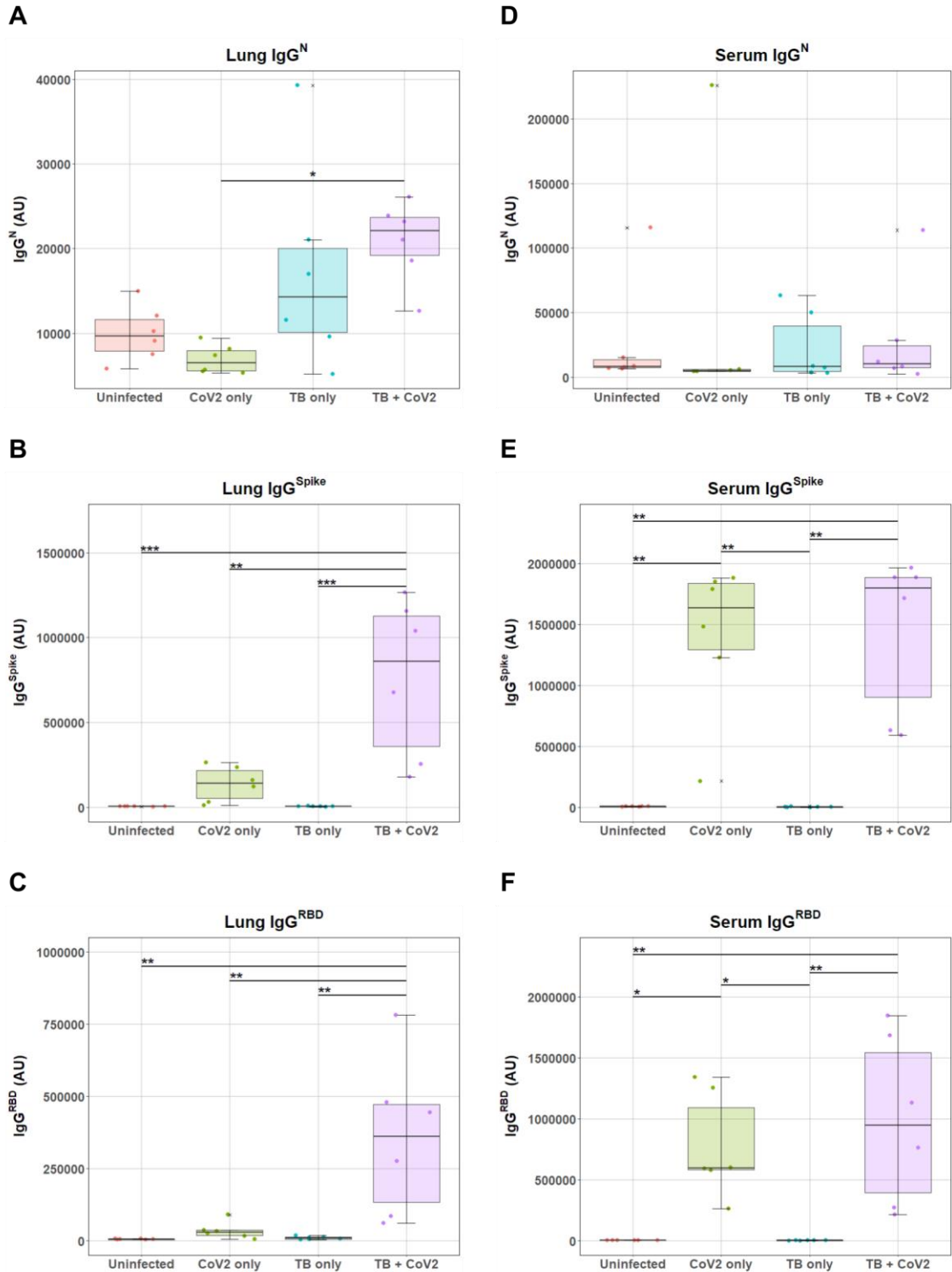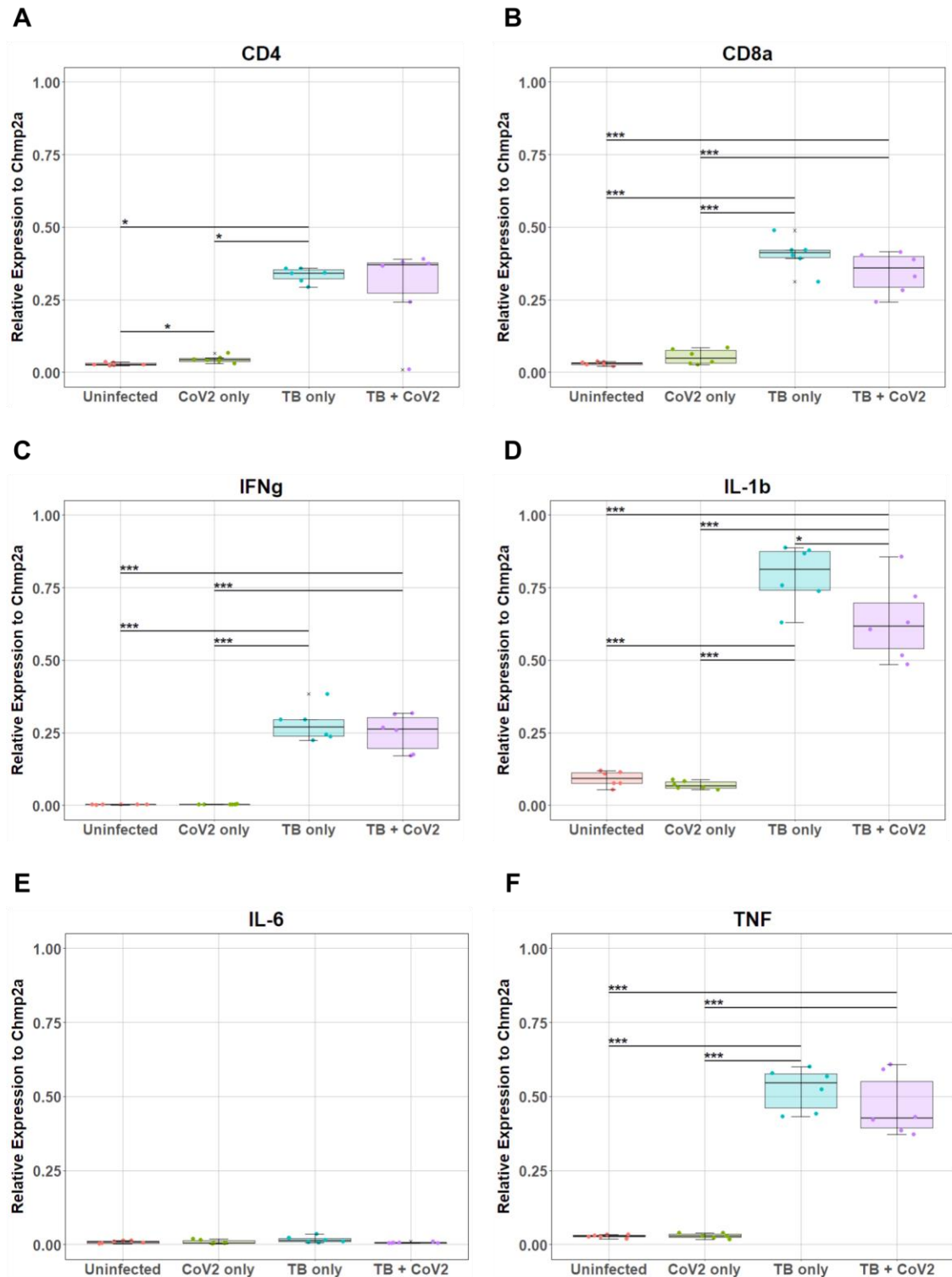
Figure 25: Relative Expression of Day 7 Lung RNA. RNA was extracted from the right upper lobe of lungs from Day 7, converted to cDNA, and run on RT-PCR to

96

quantify relative expression to Chmp2a. The genes shown are as follows: (**A**) CD4; (**B**) CD8a; (**C**) IFNg; (**D**) IL-1b; (**E**) IL-6; and (**F**) TNF. Each point represents one sample run in either triplicate in (**A**) and (**B**), or duplicate in (**C**)–(**F**). There were a total of six samples per mouse group. Asterisks indicate intergroup differences as determined by Wilcoxon test with Benjamini-Hochberg adjustment or Tukey's HSD test.

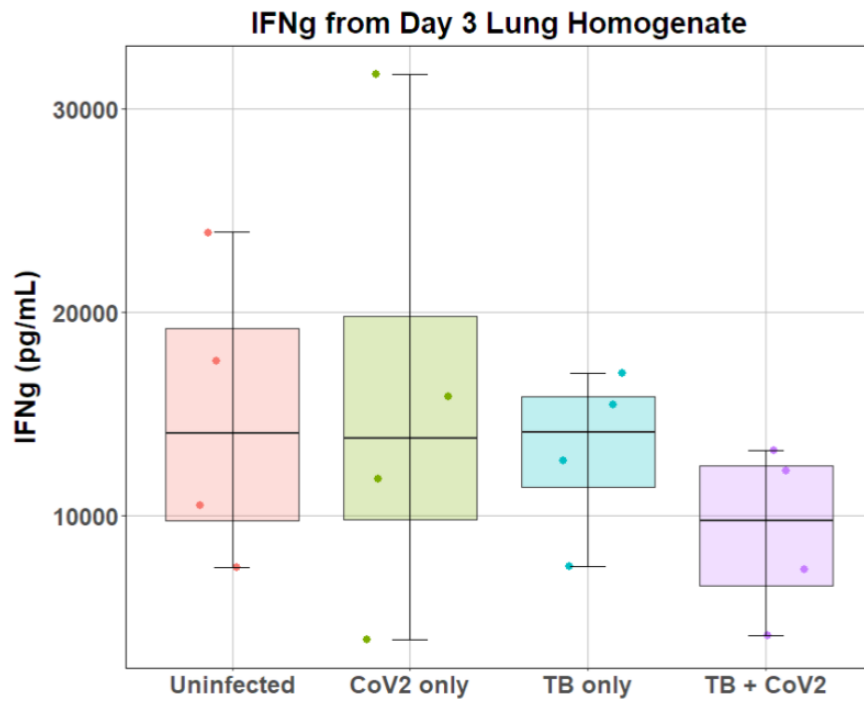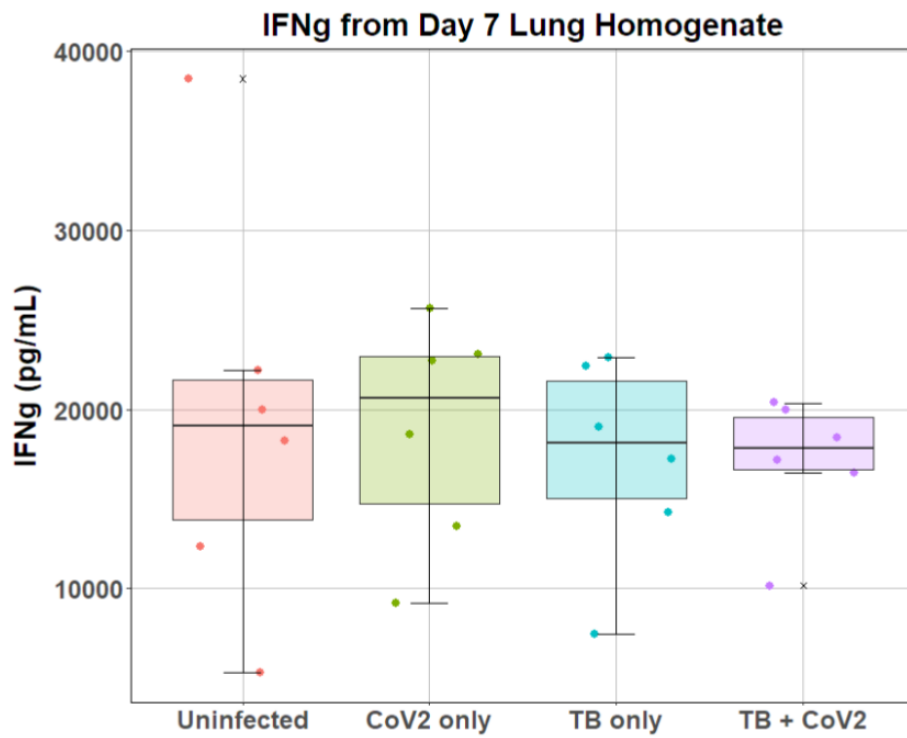**A** IFNg from Day 3 Lung Homogenate

B IFNg from Day 7 Lung Homogenate

Figure 26: Interferon gamma from Day 3 and 7 Lung Homogenate. IFNg was measured via ELISA on lung homogenate diluted at 1:100. Four samples from each mouse group were used from Day 3 (**A**); six samples from each mouse group were used from Day 7 (**B**). IFNg is presented as pg/mL and was adjusted for dilution.

Chapter 4: Final Discussion

At the beginning of my graduate school journey, I rotated in labs that studied topics ranging from more basic science researching the role of macrophages in pulmonary fibrosis to translational science analyzing factors affecting patient abdominal infections. The majority of my research, as described in this document, likewise ranges from a broader perspective in Chapter 2 where I show SARS-CoV-2 variants emerging over time across Ohio State's campus and examined antibody responses in human saliva to a narrower focus in Chapter 3 where I found that Mtb accelerates antibody production against SARS-CoV-2 in mice.

The COVID-19 pandemic tragically cost millions of people their lives and affected the entire world, but it also provided a unique opportunity to study an infectious disease as it spread. My research in chapter 2 represents a snapshot in time during a global pandemic. These experiments would be impossible to replicate going forward due to too many confounding factors as nearly everybody has had exposure to SARS-CoV-2 in some form. Thus, I found it rewarding to seize the opportunity to use data and samples from the university's existing monitoring program at that time and learn from it. My research provides validation for the use of saliva as a way to measure SARS-CoV-2 specific antibody, as I was able to measure three isotypes of Ig, and show that it has neutralizing

capabilities. Saliva collection not only spares the individual pain or discomfort from blood collection, but it also eliminates the need for a second person to get into close contact with the individual. Additionally, antibodies measured in saliva, which is collected from a mucosal site, indicate protection at one of the main entry points of the virus into the human body. Many findings from my research provide hope as SARS-CoV-2 persists and continues to mutate. Antibodies generated in response to one variant are cross-reactive with other variants, Spike specific antibodies remain in the body for months after infection, and vaccinations do elicit Spike specific IgG. I also found that individuals with Delta breakthrough infections had antibodies that were less capable of inhibiting Spike:ACE2 interaction than uninfected vaccinees. A remaining question is why do some individuals produce these less functional antibodies, and how can vaccinations be changed to elicit a more protective humoral response. As humanity continues to be exposed to SARS-CoV-2 and develop immunity against it, I believe that the future of COVID-19 will be similar to influenza: a common viral infection that can be fatal in elderly or immunocompromised individuals, but manageable with vaccinations.

Due to its rarity in the United States as well as being a BSL3 (biosafety level 3) pathogen, Mtb is underfunded in the United States, despite being a global burden. Fortunately, Ohio State has a BSL3 facility that allowed me to research Mtb and SARS-CoV-2 which are both BSL3 pathogens. Working in a BSL3 facility honed my abilities to plan experiments long in advance and thoroughly prepare materials and protocols. Aside from the skills that working in a BSL3 facility has taught me, my research investigated the complex

immune response between the world's two deadliest infectious agents. TB diagnosis and treatment decreased in the first two years following the onset of the COVID-19 pandemic, which led to an increase in deaths due to TB and new TB infections[75]. Many patients in countries with high TB burden present symptoms of a respiratory infection, which may be TB, SARS-CoV-2, or both in coinfection. Although there are limitations to the applicability of utilizing mice in my experiments, coinfection is especially challenging to study in humans as there are many confounding factors such as malnutrition and pre-existing health conditions that makes parsing out effects of coinfection difficult. Nonetheless, I was able to answer a few questions regarding TB and SARS-CoV-2 coinfection. The main findings were that antibodies generated in response to TB do not cross-react with SARS-CoV-2 antigens, but the mice with TB were able to produce more SARS-CoV-2 specific antibodies by day seven post-SARS-CoV-2 challenge than mice given SARS-CoV-2 only. Although human studies of TB and SARS-CoV-2 have some conflicting conclusions, it is clear that TB and SARS-CoV-2 are not mutually antagonist to the same degree as TB and HIV. My research suggests that the immune environment of TB accelerates the generation of SARS-CoV-2 specific antibodies which are protective against SARS-CoV-2 infection. This continues to fill the gap in knowledge of specifically how TB can be beneficial to subsequent infection with SARS-CoV-2. Further research to parse out what specific aspects of the TB lung environment accelerates antibody production upon exposure to SARS-CoV-2 and whether it is TB specific could lead to discovery of adjuvants that improve SARS-CoV-2 vaccination efficacy and provide protection sooner. Continuing to explore the interaction

of TB/SARS-CoV-2 coinfection, given its unique relationship that appears beneficial, is important for public health and would inform better care of both TB and SARS-CoV-2 patients.

In my breadth of research, which included both human samples and mouse samples, I have found that human immune responses are quite variable. There were many more outliers and increased data variance in the human saliva Ig measurements than in the mouse Ig measurements. This logically makes sense because the mice were genetically identical and housed in the same place, so much of the variation is removed. Although this helps in scientific reproducibility and reduction in confounding factors, the reality of humanity includes those confounding factors of genetic variation and differences in diet and environment. The increase of recorded health data and its availability has made meta-analyses possible where now thousands of patients and numerous factors can be included. Yet, it is important to find ways to confirm findings from mouse or other animal model studies in humans. Animal models and *in vitro* assays can inform researchers about the human immune response to confirm in human studies whereas observations found in clinical data can be examined in detail within a laboratory setting. However, more prospective human studies that aim to validate conclusions of basic science and animal studies are needed. The ultimate goal of biomedical research is to positively impact human health, so maintaining human relevancy in research is crucial.

Bibliography

1. Keusch, G.T., Amuasi, J.H., Anderson, D.E., Daszak, P., Eckerle, I., Field, H., Koopmans, M., Lam, S.K., Das Neves, C.G., Peiris, M., et al. (2022). Pandemic origins and a One Health approach to preparedness and prevention: Solutions based on SARS-CoV-2 and other RNA viruses. Proc Natl Acad Sci U S A *119*, e2202871119. 10.1073/pnas.2202871119.

2. Worobey, M. (2021). Dissecting the early COVID-19 cases in Wuhan. Science *374*, 1202–1204. 10.1126/science.abm4454.

3. Zhu, N., Zhang, D., Wang, W., Li, X., Yang, B., Song, J., Zhao, X., Huang, B., Shi, W., Lu, R., et al. (2020). A Novel Coronavirus from Patients with Pneumonia in China, 2019. N Engl J Med *382*, 727–733. 10.1056/NEJMoa2001017.

4. Wu, Y., Ho, W., Huang, Y., Jin, D.-Y., Li, S., Liu, S.-L., Liu, X., Qiu, J., Sang, Y., Wang, Q., et al. (2020). SARS-CoV-2 is an appropriate name for the new coronavirus. Lancet *395*, 949–950. 10.1016/S0140-6736(20)30557-2.

5. World Health Organization (2024). COVID-19 cases | WHO COVID-19 dashboard. WHO COVID-19 dashboard. https://data.who.int/dashboards/covid19/cases.

6. Johns Hopkins University (2023). Mortality Analyses. Johns Hopkins Coronavirus Resource Center. https://coronavirus.jhu.edu/data/mortality.

7. Tellier, R. (2022). COVID-19: the case for aerosol transmission. Interface Focus *12*, 20210072. 10.1098/rsfs.2021.0072.

8. Wang, Y., and Perlman, S. (2022). COVID-19: Inflammatory Profile. Annual Review of Medicine *73*, 65–80. 10.1146/annurev-med-042220-012417.

9. Centers for Disease Control and Prevention (2020). Coronavirus Disease 2019 (COVID-19) – Symptoms. Centers for Disease Control and Prevention. https://www.cdc.gov/coronavirus/2019-ncov/symptoms-testing/symptoms.html.

10. Sanyaolu, A., Okorie, C., Marinkovic, A., Patidar, R., Younis, K., Desai, P., Hosein, Z., Padda, I., Mangat, J., and Altaf, M. (2020). Comorbidity and its Impact on Patients with COVID-19. SN Compr Clin Med, 1–8. 10.1007/s42399-020-00363-4.

11. Bai, C., Zhong, Q., and Gao, G.F. (2022). Overview of SARS-CoV-2 genome-encoded proteins. Sci. China Life Sci. *65*, 280–294. 10.1007/s11427-021-1964-4.

12. Evans, J.P., and Liu, S.-L. (2021). Role of host factors in SARS-CoV-2 entry. J Biol Chem *297*, 100847. 10.1016/j.jbc.2021.100847.

13. Zhou, P., Yang, X.-L., Wang, X.-G., Hu, B., Zhang, L., Zhang, W., Si, H.-R., Zhu, Y., Li, B., Huang, C.-L., et al. (2020). A pneumonia outbreak associated with a new coronavirus of probable bat origin. Nature *579*, 270–273. 10.1038/s41586-020-2012-7.

14. Shang, J., Wan, Y., Luo, C., Ye, G., Geng, Q., Auerbach, A., and Li, F. (2020). Cell entry mechanisms of SARS-CoV-2. PNAS *117*, 11727–11734. 10.1073/pnas.2003138117.

15. Hikmet, F., Méar, L., Edvinsson, Å., Micke, P., Uhlén, M., and Lindskog, C. (2020). The protein expression profile of ACE2 in human tissues. Mol Syst Biol *16*, e9610. 10.15252/msb.20209610.

16. Puelles Victor G., Lütgehetmann Marc, Lindenmeyer Maja T., Sperhake Jan P., Wong Milagros N., Allweiss Lena, Chilla Silvia, Heinemann Axel, Wanner Nicola, Liu Shuya, et al. (2020). Multiorgan and Renal Tropism of SARS-CoV-2. New England Journal of Medicine *383*, 590–592. 10.1056/NEJMc2011400.

17. Hartard, C., Chaqroun, A., Settembre, N., Gauchotte, G., Lefevre, B., Marchand, E., Mazeaud, C., Nguyen, D.T., Martrille, L., Koscinski, I., et al. (2022). Multiorgan and Vascular Tropism of SARS-CoV-2. Viruses *14*, 515. 10.3390/v14030515.

18. Yang, H., and Rao, Z. (2021). Structural biology of SARS-CoV-2 and implications for therapeutic development. Nat Rev Microbiol *19*, 685–700. 10.1038/s41579-021-00630-8.

19. Gorkhali, R., Koirala, P., Rijal, S., Mainali, A., Baral, A., and Bhattarai, H.K. (2021). Structure and Function of Major SARS-CoV-2 and SARS-CoV Proteins. Bioinform Biol Insights *15*, 11779322211025876. 10.1177/11779322211025876.

20. Hoffmann, M., Kleine-Weber, H., Schroeder, S., Krüger, N., Herrler, T., Erichsen, S., Schiergens, T.S., Herrler, G., Wu, N.-H., Nitsche, A., et al. (2020). SARS-CoV-2 Cell Entry Depends on ACE2 and TMPRSS2 and Is Blocked by a Clinically Proven Protease Inhibitor. Cell *181*, 271-280.e8. 10.1016/j.cell.2020.02.052.

21. Brant, A.C., Tian, W., Majerciak, V., Yang, W., and Zheng, Z.-M. (2021). SARS-CoV-2: from its discovery to genome structure, transcription, and replication. Cell Biosci *11*, 136. 10.1186/s13578-021-00643-z.

22. Aiello, A., Grossi, A., Meschi, S., Meledandri, M., Vanini, V., Petrone, L., Casetti, R., Cuzzi, G., Salmi, A., Altera, A.M., et al. (2022). Coordinated innate and T-cell immune responses in mild COVID-19 patients from household contacts of COVID-19 cases during the first pandemic wave. Front Immunol *13*, 920227. 10.3389/fimmu.2022.920227.

23. Chandran, A., Rosenheim, J., Nageswaran, G., Swadling, L., Pollara, G., Gupta, R.K., Burton, A.R., Guerra-Assunção, J.A., Woolston, A., Ronel, T., et al. (2022). Rapid synchronous type 1 IFN and virus-specific T cell responses characterize first wave non-severe SARS-CoV-2 infections. Cell Rep Med *3*, 100557. 10.1016/j.xcrm.2022.100557.

24. Kim, Y.-M., and Shin, E.-C. (2021). Type I and III interferon responses in SARS-CoV-2 infection. Exp Mol Med *53*, 750–760. 10.1038/s12276-021-00592-0.

25. Schoggins, J.W. (2014). Interferon-stimulated genes: roles in viral pathogenesis. Curr Opin Virol *6*, 40–46. 10.1016/j.coviro.2014.03.006.

26. Sette, A., and Crotty, S. (2021). Adaptive immunity to SARS-CoV-2 and COVID-19. Cell *184*, 861–880. 10.1016/j.cell.2021.01.007.

27. Galani, I.-E., Rovina, N., Lampropoulou, V., Triantafyllia, V., Manioudaki, M., Pavlos, E., Koukaki, E., Fragkou, P.C., Panou, V., Rapti, V., et al. (2021). Untuned antiviral immunity in COVID-19 revealed by temporal type I/III interferon patterns and flu comparison. Nat Immunol *22*, 32–40. 10.1038/s41590-020-00840-x.

28. Liu, J., Li, S., Liu, J., Liang, B., Wang, X., Wang, H., Li, W., Tong, Q., Yi, J., Zhao, L., et al. (2020). Longitudinal characteristics of lymphocyte responses and cytokine profiles in the peripheral blood of SARS-CoV-2 infected patients. EBioMedicine *55*, 102763. 10.1016/j.ebiom.2020.102763.

29. Huang, C., Wang, Y., Li, X., Ren, L., Zhao, J., Hu, Y., Zhang, L., Fan, G., Xu, J., Gu, X., et al. (2020). Clinical features of patients infected with 2019 novel coronavirus in Wuhan, China. The Lancet *395*, 497–506. 10.1016/S0140-6736(20)30183-5.

30. Yang, L., Liu, S., Liu, J., Zhang, Z., Wan, X., Huang, B., Chen, Y., and Zhang, Y. (2020). COVID-19: immunopathogenesis and Immunotherapeutics. Signal Transduction and Targeted Therapy *5*, 1–8. 10.1038/s41392-020-00243-2.

31. Zhao, J., Li, K., Wohlford-Lenane, C., Agnihothram, S.S., Fett, C., Zhao, J., Gale, M.J., Baric, R.S., Enjuanes, L., Gallagher, T., et al. (2014). Rapid generation of a mouse model for Middle East respiratory syndrome. Proc Natl Acad Sci U S A *111*, 4970–4975. 10.1073/pnas.1323279111.

32. Yao, Y., Bao, L., Deng, W., Xu, L., Li, F., Lv, Q., Yu, P., Chen, T., Xu, Y., Zhu, H., et al. (2014). An animal model of MERS produced by infection of rhesus macaques with MERS coronavirus. J Infect Dis *209*, 236–242. 10.1093/infdis/jit590.

33. Jang, T.-H., Park, W.-J., Lee, H., Woo, H.-M., Lee, S.-Y., Kim, K.-C., Kim, S.S., Hong, E., Song, J., and Lee, J.-Y. (2022). The structure of a novel antibody against the spike protein inhibits Middle East respiratory syndrome coronavirus infections. Sci Rep *12*, 1260. 10.1038/s41598-022-05318-4.

34. Du, L., Zhao, G., Yang, Y., Qiu, H., Wang, L., Kou, Z., Tao, X., Yu, H., Sun, S., Tseng, C.-T.K., et al. (2014). A conformation-dependent neutralizing monoclonal antibody specifically targeting receptor-binding domain in Middle East respiratory syndrome coronavirus spike protein. J Virol *88*, 7045–7053. 10.1128/JVI.00433-14.

35. Ma, C., Li, Y., Wang, L., Zhao, G., Tao, X., Tseng, C.-T.K., Zhou, Y., Du, L., and Jiang, S. (2014). Intranasal vaccination with recombinant receptor-binding domain of MERS-CoV spike protein induces much stronger local mucosal immune responses than subcutaneous immunization: Implication for designing novel mucosal MERS vaccines. Vaccine *32*, 2100–2108. 10.1016/j.vaccine.2014.02.004.

36. Song, F., Fux, R., Provacia, L.B., Volz, A., Eickmann, M., Becker, S., Osterhaus, A.D.M.E., Haagmans, B.L., and Sutter, G. (2013). Middle East respiratory syndrome coronavirus spike protein delivered by modified vaccinia virus Ankara efficiently induces virus-neutralizing antibodies. J Virol *87*, 11950–11954. 10.1128/JVI.01672-13.

37. Du, L., Zhao, G., Kou, Z., Ma, C., Sun, S., Poon, V.K.M., Lu, L., Wang, L., Debnath, A.K., Zheng, B.-J., et al. (2013). Identification of a receptor-binding domain in the S protein of the novel human coronavirus Middle East respiratory syndrome coronavirus as an essential target for vaccine development. J Virol *87*, 9939–9942. 10.1128/JVI.01048-13.

38. Mou, H., Raj, V.S., van Kuppeveld, F.J.M., Rottier, P.J.M., Haagmans, B.L., and Bosch, B.J. (2013). The receptor binding domain of the new Middle East respiratory syndrome coronavirus maps to a 231-residue region in the spike protein that efficiently elicits neutralizing antibodies. J Virol *87*, 9379–9383. 10.1128/JVI.01277-13.

39. Ptasiewicz, M., Bębnowska, D., Małkowska, P., Sierawska, O., Poniewierska-Baran, A., Hrynkiewicz, R., Niedźwiedzka-Rystwej, P., Grywalska, E., and Chałas, R. (2022). Immunoglobulin Disorders and the Oral Cavity: A Narrative Review. J Clin Med *11*, 4873. 10.3390/jcm11164873.

40. Brandtzaeg, P. (2013). Secretory immunity with special reference to the oral cavity. J Oral Microbiol *5*, 10.3402/jom.v5i0.20401. 10.3402/jom.v5i0.20401.

41. Sterlin, D., Mathian, A., Miyara, M., Mohr, A., Anna, F., Claër, L., Quentric, P., Fadlallah, J., Devilliers, H., Ghillani, P., et al. (2021). IgA dominates the early neutralizing antibody response to SARS-CoV-2. Science Translational Medicine *13*. 10.1126/scitranslmed.abd2223.

42. Bahnan, W., Wrighton, S., Sundwall, M., Bläckberg, A., Larsson, O., Höglund, U., Khakzad, H., Godzwon, M., Walle, M., Elder, E., et al. (2021). Spike-Dependent Opsonization Indicates Both Dose-Dependent Inhibition of Phagocytosis and That Non-Neutralizing Antibodies Can Confer Protection to SARS-CoV-2. Frontiers in Immunology *12*. 10.3389/fimmu.2021.808932.

43. Kline, D., Li, Z., Chu, Y., Wakefield, J., Miller, W.C., Norris Turner, A., and Clark, S.J. (2021). Estimating seroprevalence of SARS-CoV-2 in Ohio: A Bayesian multilevel poststratification approach with multiple diagnostic tests. Proc Natl Acad Sci U S A *118*, e2023947118. 10.1073/pnas.2023947118.

44. Robbiani, D.F., Gaebler, C., Muecksch, F., Lorenzi, J.C.C., Wang, Z., Cho, A., Agudelo, M., Barnes, C.O., Gazumyan, A., Finkin, S., et al. (2020). Convergent antibody responses to SARS-CoV-2 in convalescent individuals. Nature *584*, 437–442. 10.1038/s41586-020-2456-9.

45. Bloch, E.M., Shoham, S., Casadevall, A., Sachais, B.S., Shaz, B., Winters, J.L., van Buskirk, C., Grossman, B.J., Joyner, M., Henderson, J.P., et al. (2020). Deployment of convalescent plasma for the prevention and treatment of COVID-19. J Clin Invest *130*, 2757–2765. 10.1172/JCI138745.

46. Commissioner, O. of the (2020). FDA Takes Key Action in Fight Against COVID-19 By Issuing Emergency Use Authorization for First COVID-19 Vaccine. FDA. https://www.fda.gov/news-events/press-announcements/fda-takes-key-action-fight-against-covid-19-issuing-emergency-use-authorization-first-covid-19.

47. Commissioner, O. of the (2020). FDA Takes Additional Action in Fight Against COVID-19 By Issuing Emergency Use Authorization for Second COVID-19 Vaccine. FDA. https://www.fda.gov/news-events/press-announcements/fda-takes-additional-action-fight-against-covid-19-issuing-emergency-use-authorization-second-covid.

48. Commissioner, O. of the (2021). FDA Issues Emergency Use Authorization for Third COVID-19 Vaccine. FDA. https://www.fda.gov/news-events/press-announcements/fda-issues-emergency-use-authorization-third-covid-19-vaccine.

49. Barouch, D.H. (2022). Covid-19 Vaccines - Immunity, Variants, Boosters. N Engl J Med *387*, 1011–1020. 10.1056/NEJMra2206573.

50. Johnson, A.G., Amin, A.B., Ali, A.R., Hoots, B., Cadwell, B.L., Arora, S., Avoundjian, T., Awofeso, A.O., Barnes, J., Bayoumi, N.S., et al. (2022). COVID-19 Incidence and Death Rates Among Unvaccinated and Fully Vaccinated Adults with and Without Booster Doses During Periods of Delta and Omicron Variant Emergence - 25 U.S. Jurisdictions, April 4-December 25, 2021. MMWR Morb Mortal Wkly Rep *71*, 132–138. 10.15585/mmwr.mm7104e2.

51. Banerjee, A.K., Blanco, M.R., Bruce, E.A., Honson, D.D., Chen, L.M., Chow, A., Bhat, P., Ollikainen, N., Quinodoz, S.A., Loney, C., et al. (2020). SARS-CoV-2 Disrupts Splicing, Translation, and Protein Trafficking to Suppress Host Defenses. Cell *183*, 1325-1339.e21. 10.1016/j.cell.2020.10.004.

52. Vora, S.M., Fontana, P., Mao, T., Leger, V., Zhang, Y., Fu, T.-M., Lieberman, J., Gehrke, L., Shi, M., Wang, L., et al. (2022). Targeting stem-loop 1 of the SARS-CoV-2 5' UTR to suppress viral translation and Nsp1 evasion. Proc Natl Acad Sci U S A *119*, e2117198119. 10.1073/pnas.2117198119.

53. Xia, H., Cao, Z., Xie, X., Zhang, X., Chen, J.Y.-C., Wang, H., Menachery, V.D., Rajsbaum, R., and Shi, P.-Y. (2020). Evasion of Type I Interferon by SARS-CoV-2. Cell Rep *33*, 108234. 10.1016/j.celrep.2020.108234.

54. Wu, Y., Ma, L., Zhuang, Z., Cai, S., Zhao, Z., Zhou, L., Zhang, J., Wang, P.-H., Zhao, J., and Cui, J. (2020). Main protease of SARS-CoV-2 serves as a bifunctional molecule in restricting type I interferon antiviral signaling. Signal Transduct Target Ther *5*, 221. 10.1038/s41392-020-00332-2.

55. Zhang, Y., Chen, Y., Li, Y., Huang, F., Luo, B., Yuan, Y., Xia, B., Ma, X., Yang, T., Yu, F., et al. (2021). The ORF8 protein of SARS-CoV-2 mediates immune evasion through down-regulating MHC-I. Proc Natl Acad Sci U S A *118*, e2024202118. 10.1073/pnas.2024202118.

56. Rubio-Casillas, A., Redwan, E.M., and Uversky, V.N. (2022). SARS-CoV-2: A Master of Immune Evasion. Biomedicines *10*, 1339. 10.3390/biomedicines10061339.

57. Domingo, E., and Holland, J.J. (1997). Rna Virus Mutations and Fitness for Survival. Annual Review of Microbiology *51*, 151–178. 10.1146/annurev.micro.51.1.151.

58. Moeller, N.H., Shi, K., Demir, Ö., Belica, C., Banerjee, S., Yin, L., Durfee, C., Amaro, R.E., and Aihara, H. (2022). Structure and dynamics of SARS-CoV-2 proofreading exoribonuclease ExoN. Proceedings of the National Academy of Sciences *119*, e2106379119. 10.1073/pnas.2106379119.

59. Galloway, S.E., Paul, P., MacCannell, D.R., Johansson, M.A., Brooks, J.T., MacNeil, A., Slayton, R.B., Tong, S., Silk, B.J., Armstrong, G.L., et al. (2021). Emergence of SARS-CoV-2 B.1.1.7 Lineage - United States, December 29, 2020-January 12, 2021. MMWR Morb Mortal Wkly Rep *70*, 95–99. 10.15585/mmwr.mm7003e2.

60. Tegally, H., Wilkinson, E., Giovanetti, M., Iranzadeh, A., Fonseca, V., Giandhari, J., Doolabh, D., Pillay, S., San, E.J., Msomi, N., et al. (2021). Detection of a SARS-CoV-2 variant of concern in South Africa. Nature *592*, 438–443. 10.1038/s41586-021-03402-9.

61. Zhou, D., Dejnirattisai, W., Supasa, P., Liu, C., Mentzer, A.J., Ginn, H.M., Zhao, Y., Duyvesteyn, H.M.E., Tuekprakhon, A., Nutalai, R., et al. (2021). Evidence of escape of SARS-CoV-2 variant B.1.351 from natural and vaccine-induced sera. Cell *184*, 2348-2361.e6. 10.1016/j.cell.2021.02.037.

62. Harvey, W.T., Carabelli, A.M., Jackson, B., Gupta, R.K., Thomson, E.C., Harrison, E.M., Ludden, C., Reeve, R., Rambaut, A., Peacock, S.J., et al. (2021). SARS-CoV-2 variants, spike mutations and immune escape. Nat Rev Microbiol *19*, 409–424. 10.1038/s41579-021-00573-0.

63. Volz, E., Mishra, S., Chand, M., Barrett, J.C., Johnson, R., Geidelberg, L., Hinsley, W.R., Laydon, D.J., Dabrera, G., O'Toole, Á., et al. (2021). Assessing transmissibility of SARS-CoV-2 lineage B.1.1.7 in England. Nature *593*, 266–269. 10.1038/s41586-021-03470-x.

64. Davies, N.G., Jarvis, C.I., CMMID COVID-19 Working Group, Edmunds, W.J., Jewell, N.P., Diaz-Ordaz, K., and Keogh, R.H. (2021). Increased mortality in community-tested cases of SARS-CoV-2 lineage B.1.1.7. Nature *593*, 270–274. 10.1038/s41586-021-03426-1.

65. Liu, Y., Liu, J., Plante, K.S., Plante, J.A., Xie, X., Zhang, X., Ku, Z., An, Z., Scharton, D., Schindewolf, C., et al. (2022). The N501Y spike substitution enhances SARS-CoV-2 infection and transmission. Nature *602*, 294–299. 10.1038/s41586-021-04245-0.

66. Faria, N.R., Mellan, T.A., Whittaker, C., Claro, I.M., Candido, D. da S., Mishra, S., Crispim, M.A.E., Sales, F.C.S., Hawryluk, I., McCrone, J.T., et al. (2021). Genomics and epidemiology of the P.1 SARS-CoV-2 lineage in Manaus, Brazil. Science *372*, 815–821. 10.1126/science.abh2644.

67. Mlcochova, P., Kemp, S.A., Dhar, M.S., Papa, G., Meng, B., Ferreira, I.A.T.M., Datir, R., Collier, D.A., Albecka, A., Singh, S., et al. (2021). SARS-CoV-2 B.1.617.2 Delta variant replication and immune evasion. Nature *599*, 114–119. 10.1038/s41586-021-03944-y.

68. Viana, R., Moyo, S., Amoako, D.G., Tegally, H., Scheepers, C., Althaus, C.L., Anyaneji, U.J., Bester, P.A., Boni, M.F., Chand, M., et al. (2022). Rapid epidemic expansion of the SARS-CoV-2 Omicron variant in southern Africa. Nature *603*, 679–686. 10.1038/s41586-022-04411-y.

69. Liu, Y., Liu, J., Johnson, B.A., Xia, H., Ku, Z., Schindewolf, C., Widen, S.G., An, Z., Weaver, S.C., Menachery, V.D., et al. (2022). Delta spike P681R mutation enhances SARS-CoV-2 fitness over Alpha variant. Cell Rep *39*, 110829. 10.1016/j.celrep.2022.110829.

70. Hoffmann, M., Krüger, N., Schulz, S., Cossmann, A., Rocha, C., Kempf, A., Nehlmeier, I., Graichen, L., Moldenhauer, A.-S., Winkler, M.S., et al. (2022). The Omicron variant is highly resistant against antibody-mediated neutralization: Implications for control of the COVID-19 pandemic. Cell *185*, 447-456.e11. 10.1016/j.cell.2021.12.032.

71. Carabelli, A.M., Peacock, T.P., Thorne, L.G., Harvey, W.T., Hughes, J., Peacock, S.J., Barclay, W.S., de Silva, T.I., Towers, G.J., and Robertson, D.L. (2023). SARS-CoV-2 variant biology: immune escape, transmission and fitness. Nat Rev Microbiol *21*, 162–177. 10.1038/s41579-022-00841-7.

72. Qu, P., Evans, J.P., Zheng, Y.-M., Carlin, C., Saif, L.J., Oltz, E.M., Xu, K., Gumina, R.J., and Liu, S.-L. (2022). Evasion of neutralizing antibody responses by the SARS-CoV-2 BA.2.75 variant. Cell Host Microbe *30*, 1518-1526.e4. 10.1016/j.chom.2022.09.015.

73. Schöley, J., Aburto, J.M., Kashnitsky, I., Kniffka, M.S., Zhang, L., Jaadla, H., Dowd, J.B., and Kashyap, R. (2022). Life expectancy changes since COVID-19. Nat Hum Behav *6*, 1649–1659. 10.1038/s41562-022-01450-3.

74. Xu, J., Murphy, S., Kochanek, K., and Arias, E. (2022). Mortality in the United States, 2021 (National Center for Health Statistics (U.S.)) 10.15620/cdc:122516.

75. World Health Organization (2023). Global tuberculosis report 2023.

76. Vynnycky, E., and Fine, P.E.M. (2000). Lifetime Risks, Incubation Period, and Serial Interval of Tuberculosis. American Journal of Epidemiology *152*, 247–263. 10.1093/aje/152.3.247.

77. Pai, M., Behr, M.A., Dowdy, D., Dheda, K., Divangahi, M., Boehme, C.C., Ginsberg, A., Swaminathan, S., Spigelman, M., Getahun, H., et al. (2016). Tuberculosis. Nat Rev Dis Primers *2*, 1–23. 10.1038/nrdp.2016.76.

78. Flynn, J.L., and Chan, J. (2022). Immune cell interactions in tuberculosis. Cell *185*, 4682–4702. 10.1016/j.cell.2022.10.025.

79. Flynn, J.L., Chan, J., Triebold, K., Dalton, D., Stewart, T., and Bloom, B. (1993). An essential role for interferon gamma in resistance to Mycobacterium tuberculosis infection. J Exp Med *178*, 2249–2254. https://doi.org/10.1084/jem.178.6.2249.

80. Flynn, J.L., Goldstein, M.M., Chan, J., Triebold, K.J., Pfeffer, K., Lowenstein, C.J., Schreiber, R., Mak, T.W., and Bloom, B.R. (1995). Tumor necrosis factor-alpha is required in the protective immune response against Mycobacterium tuberculosis in mice. Immunity *2*, 561–572. 10.1016/1074-7613(95)90001-2.

81. Resende Co, T., Hirsch, C.S., Toossi, Z., Dietze, R., and Ribeiro-Rodrigues, R. (2007). Intestinal helminth co-infection has a negative impact on both anti-Mycobacterium tuberculosis immunity and clinical response to tuberculosis therapy. Clin Exp Immunol *147*, 45–52. 10.1111/j.1365-2249.2006.03247.x.

82. Babu, S., and Nutman, T.B. (2016). Helminth-Tuberculosis Co-Infection: an Immunologic Perspective. Trends Immunol *37*, 597–607. 10.1016/j.it.2016.07.005.

83. Walaza, S., Cohen, C., Tempia, S., Moyes, J., Nguweneza, A., Madhi, S.A., McMorrow, M., and Cohen, A.L. (2020). Influenza and tuberculosis co-infection: A systematic review. Influenza Other Respir Viruses *14*, 77–91. 10.1111/irv.12670.

84. Bell, L.C.K., and Noursadeghi, M. (2018). Pathogenesis of HIV-1 and Mycobacterium tuberculosis co-infection. Nat Rev Microbiol *16*, 80–90. 10.1038/nrmicro.2017.128.

85. Campbell, J.H., Hearps, A.C., Martin, G.E., Williams, K.C., and Crowe, S.M. (2014). The importance of monocytes and macrophages in HIV pathogenesis, treatment, and cure. AIDS *28*, 2175–2187. 10.1097/QAD.0000000000000408.

86. Stochino, C., Villa, S., Zucchi, P., Parravicini, P., Gori, A., and Raviglione, M.C. (2020). Clinical characteristics of COVID-19 and active tuberculosis co-infection in an Italian reference hospital. Eur Respir J *56*, 2001708. 10.1183/13993003.01708-2020.

87. Motta, I., Centis, R., D'Ambrosio, L., García-García, J.-M., Goletti, D., Gualano, G., Lipani, F., Palmieri, F., Sánchez-Montalvá, A., Pontali, E., et al. (2020). Tuberculosis, COVID-19 and migrants: Preliminary analysis of deaths occurring in 69 patients from two cohorts. Pulmonology *26*, 233–240. 10.1016/j.pulmoe.2020.05.002.

88. Jassat, W., Cohen, C., Tempia, S., Masha, M., Goldstein, S., Kufa, T., Murangandi, P., Savulescu, D., Walaza, S., Bam, J.-L., et al. (2021). Risk factors for COVID-19-related in-hospital mortality in a high HIV and tuberculosis prevalence setting in South Africa: a cohort study. Lancet HIV *8*, e554–e567. 10.1016/S2352-3018(21)00151-X.

89. Booysen, P., Wilkinson, K.A., Sheerin, D., Waters, R., Coussens, A.K., and Wilkinson, R.J. (2023). Immune interaction between SARS-CoV-2 and Mycobacterium tuberculosis. Front Immunol *14*, 1254206. 10.3389/fimmu.2023.1254206.

90. Wang, Y., Feng, R., Xu, J., Hou, H., Feng, H., and Yang, H. (2021). An updated meta-analysis on the association between tuberculosis and COVID-19 severity and mortality. J Med Virol *93*, 5682–5686. 10.1002/jmv.27119.

91. Rajamanickam, A., Pavan Kumar, N., Chandrasekaran, P., Nancy, A., Bhavani, P.K., Selvaraj, N., Karunanithi, K., Munisankar, S., Srinivasan, R., Mariam Renji, R., et al. (2022). Effect of SARS-CoV-2 seropositivity on antigen – specific cytokine and chemokine responses in latent tuberculosis. Cytokine *150*, 155785. 10.1016/j.cyto.2021.155785.

92. Hilligan, K.L., Namasivayam, S., Clancy, C.S., O'Mard, D., Oland, S.D., Robertson, S.J., Baker, P.J., Castro, E., Garza, N.L., Lafont, B.A.P., et al. (2022). Intravenous administration of BCG protects mice against lethal SARS-CoV-2 challenge. J Exp Med *219*, e20211862. 10.1084/jem.20211862.

93. Zhang, B.-Z., Shuai, H., Gong, H.-R., Hu, J.-C., Yan, B., Yuen, T.T.-T., Hu, Y.-F., Yoon, C., Wang, X.-L., Hou, Y., et al. (2022). Bacillus Calmette-Guérin-induced trained immunity protects against SARS-CoV-2 challenge in K18-hACE2 mice. JCI Insight *7*, e157393. 10.1172/jci.insight.157393.

94. Singh, A.K., Wang, R., Lombardo, K.A., Praharaj, M., Bullen, C.K., Um, P., Davis, S., Komm, O., Illei, P.B., Ordonez, A.A., et al. (2022). Dynamic single-cell RNA sequencing reveals BCG vaccination curtails SARS-CoV-2 induced disease severity and lung inflammation. Preprint at bioRxiv, 10.1101/2022.03.15.484018 10.1101/2022.03.15.484018.

95. Mejia, O.R., Gloag, E.S., Li, J., Ruane-Foster, M., Claeys, T.A., Farkas, D., Wang, S.-H., Farkas, L., Xin, G., and Robinson, R.T. (2022). Mice infected with Mycobacterium tuberculosis are resistant to acute disease caused by secondary infection with SARS-CoV-2. PLOS Pathogens *18*, e1010093. 10.1371/journal.ppat.1010093.

96. Baker, P.J., Amaral, E.P., Castro, E., Bohrer, A.C., Torres-Juárez, F., Jordan, C.M., Nelson, C.E., Barber, D.L., Johnson, R.F., Hilligan, K.L., et al. (2023). Co-infection of mice with SARS-CoV-2 and Mycobacterium tuberculosis limits early viral replication but does not affect mycobacterial loads. Front Immunol *14*, 1240419. 10.3389/fimmu.2023.1240419.

97. Hildebrand, R.E., Chandrasekar, S.S., Riel, M., Touray, B.J.B., Aschenbroich, S.A., and Talaat, A.M. Superinfection with SARS-CoV-2 Has Deleterious Effects on

Mycobacterium bovis BCG Immunity and Promotes Dissemination of Mycobacterium tuberculosis. Microbiol Spectr *10*, e03075-22. 10.1128/spectrum.03075-22.

98. Hilligan, K.L., Namasivayam, S., Clancy, C.S., Baker, P.J., Old, S.I., Peluf, V., Amaral, E.P., Oland, S.D., O'Mard, D., Laux, J., et al. (2023). Bacterial-induced or passively administered interferon gamma conditions the lung for early control of SARS-CoV-2. Nat Commun *14*, 8229. 10.1038/s41467-023-43447-0.

99. Gupta, A., Sural, S., Gupta, A., Rousa, S., Koner, B.C., Bhalotra, A., and Chawla, R. (2021). Positive QuantiFERON test and the severity of COVID-19 disease: A prospective study. Indian Journal of Tuberculosis *68*, 474–480. 10.1016/j.ijtb.2020.12.013.

100. Solanich, X., Fernández-Huerta, M., Basaez, C., Antolí, A., Rocamora-Blanch, G., Corbella, X., Santin, M., and Alcaide, F. (2021). Clinical Significance of Indeterminate QuantiFERON-TB Gold Plus Assay Results in Hospitalized COVID-19 Patients with Severe Hyperinflammatory Syndrome. Journal of Clinical Medicine *10*, 918. 10.3390/jcm10050918.

101. Ward, J.D., Cornaby, C., and Schmitz, J.L. (2021). Indeterminate QuantiFERON Gold Plus Results Reveal Deficient Interferon Gamma Responses in Severely Ill COVID-19 Patients. Journal of Clinical Microbiology *59*, 10.1128/jcm.00811-21. 10.1128/jcm.00811-21.

102. Merling, M.R., Williams, A., Mahfooz, N.S., Ruane-Foster, M., Smith, J., Jahnes, J., Ayers, L.W., Bazan, J.A., Norris, A., Norris Turner, A., et al. (2023). The emergence of SARS-CoV-2 lineages and associated saliva antibody responses among asymptomatic individuals in a large university community. PLoS Pathog *19*, e1011596. 10.1371/journal.ppat.1011596.

103. Baden, L.R., El Sahly, H.M., Essink, B., Kotloff, K., Frey, S., Novak, R., Diemert, D., Spector, S.A., Rouphael, N., Creech, C.B., et al. (2021). Efficacy and Safety of the mRNA-1273 SARS-CoV-2 Vaccine. N Engl J Med *384*, 403–416. 10.1056/NEJMoa2035389.

104. Polack, F.P., Thomas, S.J., Kitchin, N., Absalon, J., Gurtman, A., Lockhart, S., Perez, J.L., Pérez Marc, G., Moreira, E.D., Zerbini, C., et al. (2020). Safety and Efficacy of the BNT162b2 mRNA Covid-19 Vaccine. N Engl J Med *383*, 2603–2615. 10.1056/NEJMoa2034577.

105. Bojadzic, D., Alcazar, O., Chen, J., Chuang, S.-T., Condor Capcha, J.M., Shehadeh, L.A., and Buchwald, P. (2021). Small-Molecule Inhibitors of the Coronavirus Spike: ACE2 Protein-Protein Interaction as Blockers of Viral Attachment and Entry for SARS-CoV-2. ACS Infect Dis *7*, 1519–1534. 10.1021/acsinfecdis.1c00070.

106. Huang, Y., Yang, C., Xu, X.-F., Xu, W., and Liu, S.-W. (2020). Structural and functional properties of SARS-CoV-2 spike protein: potential antivirus drug development for COVID-19. Acta Pharmacol Sin *41*, 1141–1149. 10.1038/s41401-020-0485-4.

107. Hart, W.S., Maini, P.K., and Thompson, R.N. (2021). High infectiousness immediately before COVID-19 symptom onset highlights the importance of continued contact tracing. Elife *10*, e65534. 10.7554/eLife.65534.

108. Johansson, M.A., Quandelacy, T.M., Kada, S., Prasad, P.V., Steele, M., Brooks, J.T., Slayton, R.B., Biggerstaff, M., and Butler, J.C. (2021). SARS-CoV-2 Transmission From People Without COVID-19 Symptoms. JAMA Netw Open *4*, e2035057. 10.1001/jamanetworkopen.2020.35057.

109. Huang, N., Pérez, P., Kato, T., Mikami, Y., Okuda, K., Gilmore, R.C., Conde, C.D., Gasmi, B., Stein, S., Beach, M., et al. (2021). SARS-CoV-2 infection of the oral cavity and saliva. Nat Med *27*, 892–903. 10.1038/s41591-021-01296-8.

110. Migueres, M., Mansuy, J.-M., Vasseur, S., Claverie, N., Lougarre, C., Soulier, F., Trémeaux, P., and Izopet, J. (2022). Omicron Wave SARS-CoV-2 Diagnosis: Evaluation of Saliva, Anterior Nasal, and Nasopharyngeal Swab Samples. Microbiol Spectr *10*, e0252122. 10.1128/spectrum.02521-22.

111. Marais, G., Hsiao, N.-Y., Iranzadeh, A., Doolabh, D., Joseph, R., Enoch, A., Chu, C.-Y., Williamson, C., Brink, A., and Hardie, D. (2022). Improved oral detection is a characteristic of Omicron infection and has implications for clinical sampling and tissue tropism. J Clin Virol *152*, 105170. 10.1016/j.jcv.2022.105170.

112. Suzuki, R., Yamasoba, D., Kimura, I., Wang, L., Kishimoto, M., Ito, J., Morioka, Y., Nao, N., Nasser, H., Uriu, K., et al. (2022). Attenuated fusogenicity and pathogenicity of SARS-CoV-2 Omicron variant. Nature *603*, 700–705. 10.1038/s41586-022-04462-1.

113. Hui, K.P.Y., Ng, K.-C., Ho, J.C.W., Yeung, H.-W., Ching, R.H.H., Gu, H., Chung, J.C.K., Chow, V.L.Y., Sit, K.-Y., Hsin, M.K.Y., et al. (2022). Replication of SARS-CoV-2 Omicron BA.2 variant in ex vivo cultures of the human upper and lower respiratory tract. EBioMedicine *83*, 104232. 10.1016/j.ebiom.2022.104232.

114. Meng, B., Abdullahi, A., Ferreira, I.A.T.M., Goonawardane, N., Saito, A., Kimura, I., Yamasoba, D., Gerber, P.P., Fatihi, S., Rathore, S., et al. (2022). Altered TMPRSS2 usage by SARS-CoV-2 Omicron impacts infectivity and fusogenicity. Nature *603*, 706–714. 10.1038/s41586-022-04474-x.

115. Yale School of Public Health (2023). SalivaDirect Assay Emergency Use Authorization (EUA) Summary SARS-CoV-2 RT-PCR Assay.

116. Vogels, C.B.F., Watkins, A.E., Harden, C.A., Brackney, D.E., Shafer, J., Wang, J., Caraballo, C., Kalinich, C.C., Ott, I.M., Fauver, J.R., et al. (2021). SalivaDirect: A simplified and flexible platform to enhance SARS-CoV-2 testing capacity. Med *2*, 263-280.e6. 10.1016/j.medj.2020.12.010.

117. Hale, V.L., Dennis, P.M., McBride, D.S., Nolting, J.M., Madden, C., Huey, D., Ehrlich, M., Grieser, J., Winston, J., Lombardi, D., et al. (2022). SARS-CoV-2 infection in free-ranging white-tailed deer. Nature *602*, 481–486. 10.1038/s41586-021-04353-x.

118. Rambaut, A., Holmes, E.C., O'Toole, Á., Hill, V., McCrone, J.T., Ruis, C., du Plessis, L., and Pybus, O.G. (2020). A dynamic nomenclature proposal for SARS-CoV-2 lineages to assist genomic epidemiology. Nat Microbiol *5*, 1403–1407. 10.1038/s41564-020-0770-5.

119. Hodcroft, E.B., Domman, D.B., Snyder, D.J., Oguntuyo, K.Y., Van Diest, M., Densmore, K.H., Schwalm, K.C., Femling, J., Carroll, J.L., Scott, R.S., et al. (2021). Emergence in late 2020 of multiple lineages of SARS-CoV-2 Spike protein variants affecting amino acid position 677. medRxiv, 2021.02.12.21251658. 10.1101/2021.02.12.21251658.

120. Patterson, E.I., Prince, T., Anderson, E.R., Casas-Sanchez, A., Smith, S.L., Cansado-Utrilla, C., Solomon, T., Griffiths, M.J., Acosta-Serrano, Á., Turtle, L., et al. (2020). Methods of Inactivation of SARS-CoV-2 for Downstream Biological Assays. J Infect Dis *222*, 1462–1467. 10.1093/infdis/jiaa507.

121. Filby, M. 3 Ohioans test positive for coronavirus. The Columbus Dispatch. https://www.dispatch.com/story/news/2020/03/09/3-ohioans-test-positive-for/1553817007/.

122. Milnes, O., Garrison, M., and Raudins, S. (2020). Ohio State suspends classes until March 30 due to coronavirus outbreak. The Lantern. https://www.thelantern.com/2020/03/ohio-state-suspends-classes-until-march-30-due-to-coronavirus-outbreak/.

123. Long, J. (2020). Ohio State announces proactive COVID-19 testing measures, no specific guidance on when to close campus. The Lantern. https://www.thelantern.com/2020/07/ohio-state-announces-proactive-covid-19-testing-measures-no-specific-guidance-on-when-to-close-campus/.

124. Johnson, K. (2021). Ohio State announces vaccination requirement. Ohio State announces vaccination requirement. https://news.osu.edu/ohio-state-announces-vaccination-requirement/.

125. Ohio Department of Health Ohio Department of Health COVID-19 Dashboard. Archived COVID-19 Reporting | DataOhio. https://data.ohio.gov/wps/portal/gov/data/view/archived-covid-19-reporting.

126. World Health Organization (2021). Statement on the sixth meeting of the International Health Regulations (2005) Emergency Committee regarding the coronavirus disease (COVID-19) pandemic. https://www.who.int/news/item/15-01-2021-statement-on-the-sixth-meeting-of-the-international-health-regulations-(2005)-emergency-committee-regarding-the-coronavirus-disease-(covid-19)-pandemic.

127. Spicker, K. (2021). Delta variant in Ohio: What you should know. dayton-daily-news. https://www.daytondailynews.com/local/delta-variant-in-ohio-what-you-should-know/WQ3EI57ZPNA67OC346RKSDCKAU/.

128. Ohio Department of Health (2021). COVID-19 Update: Vaccinations Increasing, Delta Variant, Local Efforts Encouraged | Governor Mike DeWine. https://governor.ohio.gov/media/news-and-media/COVID-19-Update-Vaccinations-Increasing-Delta-Variant-Local-Efforts-Encouraged-08062021.

129. Bounds, B., and Ugino, O. (2021). Ohio Department of Health launches COVID variant dashboard. 10tv.com. https://www.10tv.com/article/news/health/coronavirus/covid-variant-dashboard/530-0a10581c-cf0b-4255-b2f0-46984b0cbd30.

130. Ohio Department of Health (2021). Omicron Variant Detected in Ohio | Ohio Department of Health. https://odh.ohio.gov/media-center/odh-news-releases/odh-news-release-12-11-21.

131. Orozco, J. (2021). First cases of omicron COVID-19 variant detected in Ohio. The Lantern. https://www.thelantern.com/2021/12/first-cases-of-omicron-covid-19-variant-detected-in-ohio/.

132. Woodbridge, Y., Amit, S., Huppert, A., and Kopelman, N.M. (2022). Viral load dynamics of SARS-CoV-2 Delta and Omicron variants following multiple vaccine doses and previous infection. Nat Commun *13*, 6706. 10.1038/s41467-022-33096-0.

133. Trunfio, M., Richiardi, L., Alladio, F., Staffilano, E., Longo, B., Venuti, F., Ghisetti, V., Burdino, E., Bonora, S., Vineis, P., et al. (2022). Determinants of SARS-CoV-2 Contagiousness in Household Contacts of Symptomatic Adult Index Cases. Front Microbiol *13*, 829393. 10.3389/fmicb.2022.829393.

134. Levine-Tiefenbrun, M., Yelin, I., Alapi, H., Katz, R., Herzel, E., Kuint, J., Chodick, G., Gazit, S., Patalon, T., and Kishony, R. (2021). Viral loads of Delta-variant SARS-CoV-2 breakthrough infections after vaccination and booster with BNT162b2. Nat Med *27*, 2108–2110. 10.1038/s41591-021-01575-4.

135. Al Bayat, S., Mundodan, J., Hasnain, S., Sallam, M., Khogali, H., Ali, D., Alateeg, S., Osama, M., Elberdiny, A., Al-Romaihi, H., et al. (2021). Can the cycle threshold (Ct) value of RT-PCR test for SARS CoV2 predict infectivity among close contacts? J Infect Public Health *14*, 1201–1205. 10.1016/j.jiph.2021.08.013.

136. Kawasuji, H., Takegoshi, Y., Kaneda, M., Ueno, A., Miyajima, Y., Kawago, K., Fukui, Y., Yoshida, Y., Kimura, M., Yamada, H., et al. (2020). Transmissibility of COVID-19 depends on the viral load around onset in adult and symptomatic patients. PLoS One *15*, e0243597. 10.1371/journal.pone.0243597.

137. Davies, N.G., Abbott, S., Barnard, R.C., Jarvis, C.I., Kucharski, A.J., Munday, J.D., Pearson, C.A.B., Russell, T.W., Tully, D.C., Washburne, A.D., et al. (2021). Estimated transmissibility and impact of SARS-CoV-2 lineage B.1.1.7 in England. Science *372*, eabg3055. 10.1126/science.abg3055.

138. Hart, W.S., Miller, E., Andrews, N.J., Waight, P., Maini, P.K., Funk, S., and Thompson, R.N. (2022). Generation time of the alpha and delta SARS-CoV-2 variants: an epidemiological analysis. Lancet Infect Dis *22*, 603–610. 10.1016/S1473-3099(22)00001-9.

139. Garrison, M. (2021). DeWine: All Ohio college students will have access to single-dose COVID vaccine. The Lantern. https://www.thelantern.com/2021/04/dewine-all-ohio-college-students-will-have-access-to-single-dose-covid-vaccine/.

140. Mahoney, J.L. (1981). Malaria "breakthroughs" and resistance to chloroquine in Africa. Case reports. S Afr Med J *60*, 786–788.

141. Sette, A., and Crotty, S. (2022). Immunological memory to SARS-CoV-2 infection and COVID-19 vaccines. Immunol Rev *310*, 27–46. 10.1111/imr.13089.

142. Holshue, M.L., DeBolt, C., Lindquist, S., Lofy, K.H., Wiesman, J., Bruce, H., Spitters, C., Ericson, K., Wilkerson, S., Tural, A., et al. (2020). First Case of 2019 Novel Coronavirus in the United States. N Engl J Med *382*, 929–936. 10.1056/NEJMoa2001191.

143. Bai, Y., Yao, L., Wei, T., Tian, F., Jin, D.-Y., Chen, L., and Wang, M. (2020). Presumed Asymptomatic Carrier Transmission of COVID-19. JAMA *323*, 1406–1407. 10.1001/jama.2020.2565.

144. Rothe, C., Schunk, M., Sothmann, P., Bretzel, G., Froeschl, G., Wallrauch, C., Zimmer, T., Thiel, V., Janke, C., Guggemos, W., et al. (2020). Transmission of 2019-nCoV Infection from an Asymptomatic Contact in Germany. N Engl J Med *382*, 970–971. 10.1056/NEJMc2001468.

145. Nussbaumer-Streit, B., Mayr, V., Dobrescu, A.I., Chapman, A., Persad, E., Klerings, I., Wagner, G., Siebert, U., Ledinger, D., Zachariah, C., et al. (2020). Quarantine alone or in combination with other public health measures to control COVID-19: a rapid review. Cochrane Database Syst Rev *9*, CD013574. 10.1002/14651858.CD013574.pub2.

146. Chang, C.-N., Chien, H.-Y., and Malagon-Palacios, L. (2022). College reopening and community spread of COVID-19 in the United States. Public Health *204*, 70–75. 10.1016/j.puhe.2022.01.001.

147. Arnold, C.R.K., Srinivasan, S., Rodriguez, S., Rydzak, N., Herzog, C.M., Gontu, A., Bharti, N., Small, M., Rogers, C.J., Schade, M.M., et al. (2022). A longitudinal study of the impact of university student return to campus on the SARS-CoV-2 seroprevalence among the community members. Sci Rep *12*, 8586. 10.1038/s41598-022-12499-5.

148. Bharti, N., Lambert, B., Exten, C., Faust, C., Ferrari, M., and Robinson, A. (2022). Large university with high COVID-19 incidence is not associated with excess cases in non-student population. Sci Rep *12*, 3313. 10.1038/s41598-022-07155-x.

149. Pollock, B.H., Kilpatrick, A.M., Eisenman, D.P., Elton, K.L., Rutherford, G.W., Boden-Albala, B.M., Souleles, D.M., Polito, L.E., Martin, N.K., and Byington, C.L. (2021). Safe reopening of college campuses during COVID-19: The University of California experience in Fall 2020. PLoS One *16*, e0258738. 10.1371/journal.pone.0258738.

150. Edridge, A.W.D., Kaczorowska, J., Hoste, A.C.R., Bakker, M., Klein, M., Loens, K., Jebbink, M.F., Matser, A., Kinsella, C.M., Rueda, P., et al. (2020). Seasonal coronavirus protective immunity is short-lasting. Nat Med *26*, 1691–1693. 10.1038/s41591-020-1083-1.

151. Lee, W.S., Wheatley, A.K., Kent, S.J., and DeKosky, B.J. (2020). Antibody-dependent enhancement and SARS-CoV-2 vaccines and therapies. Nat Microbiol *5*, 1185–1191. 10.1038/s41564-020-00789-5.

152. Arvin, A.M., Fink, K., Schmid, M.A., Cathcart, A., Spreafico, R., Havenar-Daughton, C., Lanzavecchia, A., Corti, D., and Virgin, H.W. (2020). A perspective on potential antibody-dependent enhancement of SARS-CoV-2. Nature *584*, 353–363. 10.1038/s41586-020-2538-8.

153. Graham, B.S. (2020). Rapid COVID-19 vaccine development. Science *368*, 945–946. 10.1126/science.abb8923.

154. Iwasaki, A., and Yang, Y. (2020). The potential danger of suboptimal antibody responses in COVID-19. Nat Rev Immunol *20*, 339–341. 10.1038/s41577-020-0321-6.

155. Van Elslande, J., Oyaert, M., Lorent, N., Vande Weygaerde, Y., Van Pottelbergh, G., Godderis, L., Van Ranst, M., André, E., Padalko, E., Lagrou, K., et al. (2022). Lower persistence of anti-nucleocapsid compared to anti-spike antibodies up to one year after SARS-CoV-2 infection. Diagn Microbiol Infect Dis *103*, 115659. 10.1016/j.diagmicrobio.2022.115659.

156. Peng, Y., Du, N., Lei, Y., Dorje, S., Qi, J., Luo, T., Gao, G.F., and Song, H. (2020). Structures of the SARS-CoV-2 nucleocapsid and their perspectives for drug design. EMBO J *39*, e105938. 10.15252/embj.2020105938.

157. National Institutes of Health (2023). SARS-CoV-2 Testing. COVID-19 Treatment Guidelines. https://www.covid19treatmentguidelines.nih.gov/overview/sars-cov-2-testing/.

158. Schäfer, M., Stark, B., Werner, A.M., Mülder, L.M., Heller, S., Reichel, J.L., Schwab, L., Rigotti, T., Beutel, M.E., Simon, P., et al. (2022). Determinants of university students' COVID-19 vaccination intentions and behavior. Sci Rep *12*, 18067. 10.1038/s41598-022-23044-9.

159. Dzinamarira, T., Tungwarara, N., Chitungo, I., Chimene, M., Iradukunda, P.G., Mashora, M., Murewanhema, G., Rwibasira, G.N., and Musuka, G. (2022). Unpacking the Implications of SARS-CoV-2 Breakthrough Infections on COVID-19 Vaccination Programs. Vaccines (Basel) *10*, 252. 10.3390/vaccines10020252.

160. Haque, A., and Pant, A.B. (2022). Mitigating Covid-19 in the face of emerging virus variants, breakthrough infections and vaccine hesitancy. J Autoimmun *127*, 102792. 10.1016/j.jaut.2021.102792.

161. Kang, M., Xin, H., Yuan, J., Ali, S.T., Liang, Z., Zhang, J., Hu, T., Lau, E.H., Zhang, Y., Zhang, M., et al. (2022). Transmission dynamics and epidemiological characteristics of SARS-CoV-2 Delta variant infections in Guangdong, China, May to June 2021. Euro Surveill *27*, 2100815. 10.2807/1560-7917.ES.2022.27.10.2100815.

162. Nutalai, R., Zhou, D., Tuekprakhon, A., Ginn, H.M., Supasa, P., Liu, C., Huo, J., Mentzer, A.J., Duyvesteyn, H.M.E., Dijokaite-Guraliuc, A., et al. (2022). Potent cross-reactive antibodies following Omicron breakthrough in vaccinees. Cell *185*, 2116-2131.e18. 10.1016/j.cell.2022.05.014.

163. Liu, L., Iketani, S., Guo, Y., Chan, J.F.-W., Wang, M., Liu, L., Luo, Y., Chu, H., Huang, Y., Nair, M.S., et al. (2022). Striking antibody evasion manifested by the

Omicron variant of SARS-CoV-2. Nature *602*, 676–681. 10.1038/s41586-021-04388-0.

164. Cameroni, E., Bowen, J.E., Rosen, L.E., Saliba, C., Zepeda, S.K., Culap, K., Pinto, D., VanBlargan, L.A., De Marco, A., di Iulio, J., et al. (2022). Broadly neutralizing antibodies overcome SARS-CoV-2 Omicron antigenic shift. Nature *602*, 664–670. 10.1038/s41586-021-04386-2.

165. Petros, B.A., Turcinovic, J., Welch, N.L., White, L.F., Kolaczyk, E.D., Bauer, M.R., Cleary, M., Dobbins, S.T., Doucette-Stamm, L., Gore, M., et al. (2023). Early Introduction and Rise of the Omicron Severe Acute Respiratory Syndrome Coronavirus 2 (SARS-CoV-2) Variant in Highly Vaccinated University Populations. Clin Infect Dis *76*, e400–e408. 10.1093/cid/ciac413.

166. van Doremalen, N., Singh, M., Saturday, T.A., Yinda, C.K., Perez-Perez, L., Bohler, W.F., Weishampel, Z.A., Lewis, M., Schulz, J.E., Williamson, B.N., et al. (2022). SARS-CoV-2 Omicron BA.1 and BA.2 are attenuated in rhesus macaques as compared to Delta. Sci Adv *8*, eade1860. 10.1126/sciadv.ade1860.

167. Bei, Y., Vrtis, K.B., Borgaro, J.G., Langhorst, B.W., and Nichols, N.M. (2021). The Omicron variant mutation at position 28,311 in the SARS-CoV-2 N gene does not perturb CDC N1 target detection. Preprint at medRxiv, 10.1101/2021.12.16.21267734 10.1101/2021.12.16.21267734.

168. Tan, Y.P., Al-Halbouni, M., Chen, C.-H., Hirst, D.B., and Pickering, P.J. (2022). Analytical Sensitivity of the SalivaDirect^TM Assay on the Liberty16 for detecting SARS-CoV-2 B.1.1.529 ("Omicron"). Preprint at medRxiv, 10.1101/2022.02.16.22271096 10.1101/2022.02.16.22271096.

169. Takashita, E., Yamayoshi, S., Halfmann, P., Wilson, N., Ries, H., Richardson, A., Bobholz, M., Vuyk, W., Maddox, R., Baker, D.A., et al. (2022). In Vitro Efficacy of Antiviral Agents against Omicron Subvariant BA.4.6. N Engl J Med *387*, 2094–2097. 10.1056/NEJMc2211845.

170. Cox, M., Peacock, T.P., Harvey, W.T., Hughes, J., Wright, D.W., COVID-19 Genomics UK (COG-UK) Consortium, Willett, B.J., Thomson, E., Gupta, R.K., Peacock, S.J., et al. (2023). SARS-CoV-2 variant evasion of monoclonal antibodies based on in vitro studies. Nat Rev Microbiol *21*, 112–124. 10.1038/s41579-022-00809-7.

171. Park, Y.-J., Pinto, D., Walls, A.C., Liu, Z., De Marco, A., Benigni, F., Zatta, F., Silacci-Fregni, C., Bassi, J., Sprouse, K.R., et al. (2022). Imprinted antibody responses against SARS-CoV-2 Omicron sublineages. Science *378*, 619–627. 10.1126/science.adc9127.

172. Benbennick, D. (2006). English: This is a locator map showing Delaware County in Ohio. For more information, see Commons:United States county locator maps.

173. Dakal, T.C. (2021). Antigenic sites in SARS-CoV-2 spike RBD show molecular similarity with pathogenic antigenic determinants and harbors peptides for vaccine development. Immunobiology *226*, 152091. 10.1016/j.imbio.2021.152091.

174. Eggenhuizen, P.J., Ng, B.H., Chang, J., Fell, A.L., Cheong, R.M.Y., Wong, W.Y., Gan, P.-Y., Holdsworth, S.R., and Ooi, J.D. (2021). BCG Vaccine Derived Peptides Induce SARS-CoV-2 T Cell Cross-Reactivity. Front Immunol *12*, 692729. 10.3389/fimmu.2021.692729.

175. Nuovo, G., Tili, E., Suster, D., Matys, E., Hupp, L., and Magro, C. (2020). Strong homology between SARS-CoV-2 envelope protein and a Mycobacterium sp. antigen allows rapid diagnosis of Mycobacterial infections and may provide specific anti-SARS-CoV-2 immunity via the BCG vaccine. Ann Diagn Pathol *48*, 151600. 10.1016/j.anndiagpath.2020.151600.

176. Aiello, A., Najafi-Fard, S., and Goletti, D. (2023). Initial immune response after exposure to Mycobacterium tuberculosis or to SARS-COV-2: similarities and differences. Front Immunol *14*, 1244556. 10.3389/fimmu.2023.1244556.

177. Miller, H.E., and Robinson, R.T. (2012). Early Control of Mycobacterium tuberculosis Infection Requires il12rb1 Expression by rag1-Dependent Lineages. Infect Immun *80*, 3828–3841. 10.1128/IAI.00426-12.

178. BUZIC, I., and GIUFFRA, V. (2020). The paleopathological evidence on the origins of human tuberculosis: a review. J Prev Med Hyg *61*, E3–E8. 10.15167/2421-4248/jpmh2020.61.1s1.1379.

179. Kumar, N.P., Moideen, K., Banurekha, V.V., Nair, D., and Babu, S. (2019). Plasma Proinflammatory Cytokines Are Markers of Disease Severity and Bacterial Burden in Pulmonary Tuberculosis. Open Forum Infect Dis *6*, ofz257. 10.1093/ofid/ofz257.

180. Haddad, F., Dokmak, G., and Karaman, R. (2022). A Comprehensive Review on the Efficacy of Several Pharmacologic Agents for the Treatment of COVID-19. Life *12*, 1758. 10.3390/life12111758.

181. Bierne, H., Travier, L., Mahlakõiv, T., Tailleux, L., Subtil, A., Lebreton, A., Paliwal, A., Gicquel, B., Staeheli, P., Lecuit, M., et al. (2012). Activation of type III interferon genes by pathogenic bacteria in infected epithelial cells and mouse placenta. PLoS One *7*, e39080. 10.1371/journal.pone.0039080.

182. Travar, M., Vucic, M., and Petkovic, M. (2014). Interferon lambda-2 levels in sputum of patients with pulmonary Mycobacterium tuberculosis infection. Scand J Immunol *80*, 43–49. 10.1111/sji.12178.